

**UCSF**

**UC San Francisco Electronic Theses and Dissertations**

**Title**

Synapse Stabilization, De-stabilization, and Re-stabilization: Genetic analysis of neuroprotective Fos signaling at the Drosophila neuromuscular junction

**Permalink**

<https://escholarship.org/uc/item/3sm2c831>

**Author**

Massaro, Catherine Marie

**Publication Date**

2009

Peer reviewed|Thesis/dissertation

Synapse Stabilization, De-stabilization, and Re-stabilization: Genetic analysis of  
neuroprotective Fos signaling at the *Drosophila* neuromuscular junction

by

Catherine Marie Massaro

DISSERTATION

Submitted in partial satisfaction of the requirements for the degree of

DOCTOR OF PHILOSOPHY

in

Neuroscience

in the

GRADUATE DIVISION

of the

UNIVERSITY OF CALIFORNIA, SAN FRANCISCO

Copyright (2009)

by

Catherine Marie Massaro

*A man should look for what is, and not for what he thinks should be.*

**- Albert Einstein**

## ACKNOWLEDGEMENTS

I have been very fortunate throughout my time in graduate school, in that I have been surrounded by supportive friends and colleagues. My time at UCSF has flown by; something I feel is a testament to those with whom I have spent this time. While my scientific journey has not always been a smooth one, I have thoroughly enjoyed it.

Grae Davis has been a phenomenal mentor, and I certainly would not have survived graduate school without his guidance and support. I knew soon after starting graduate school that I wanted to join the Davis Lab, but it is only now, as I am leaving, that I fully appreciate the scientific environment Grae has created. Throughout the years, Grae has gone out of his way to mentor me and help guide me through the trials and tribulations that come with science. Grae also has a knack for reminding everyone how exciting and amazing scientific discovery can be, something that comes in handy on the long journey that is graduate school. I am sincerely grateful to Grae for everything he has done for me.

I am also grateful to the entire Davis Lab for all of their support along the way. It is not always easy to find people whom you respect and with whom you enjoy working. Furthermore, to find people with whom you also enjoy spending your day is invaluable. From commiseration to celebration, the members of the Davis Lab have always been there. I feel a special sense of gratitude to my fellow graduate students Kira, Sharon, Ervin, and Meg, and to my baymates, Martin and Ed. They have all made each day in the Davis Lab unique and unpredictable, and I will certainly miss them.

Thank you also to Pat, Carrie, and the entire UCSF Neuroscience Graduate Program. This includes my professors and both my orals and thesis committees, for invaluable input and guidance: Ulrike Heberlein, Steve Finkbeiner, Hilary Beggs, Antonello Bonci, Robert Edwards, Louis Reichardt, and Cynthia Kenyon.

Lastly, I want to thank all my family and friends for their love and unflinching support. My parents instilled in me the ability to pursue anything and the knowledge that they would always be there if I needed them. Thank you, Dad, for the gift of scientific curiosity. Thank you, Mom, for the confidence to persevere. Thank you, John and Donald, for sharing the journey with me. Thank you, Kieran, for your patience and for being on my team.

## PREFACE

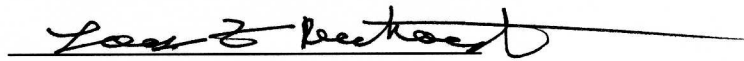
Chapter 1 contains general background information as well as an unpublished electron micrograph which was taken by Richard Fetter.

Chapter 2 is based on a paper published in the *Journal of Cell Biology*. All data in this chapter, except for that shown in Figure 2-3, was recently published in *J Cell Biol.* (2009) 187(1):101-17 (Massaro et al., 2009). Additionally, some data in Chapter 3 (part of Figure 3-1E and all of Figure 3-3) was also published in the same *J Cell Biol* paper (Massaro et al., 2009). This publication has multiple authors, including Jan Pielage and Graeme Davis. Jan Pielage developed assays that were used in this publication and he performed many experiments that provided the intellectual basis for my thesis work. He also provided guidance, advice, and support along the way. Graeme Davis performed the electrophysiological experiments and collected the data presented in Figure 2-2. He also supervised my research and provided guidance and support throughout my thesis work. I performed all other experiments and collected all other data presented in this thesis.

**Synapse Stabilization, De-stabilization, and Re-stabilization: Genetic analysis of  
neuroprotective Fos signaling at the Drosophila neuromuscular junction**

**By**

**Catherine Marie Massaro**



**Louis Reichardt**

**Committee Chair**

**ABSTRACT**

**Work in the lab of Graeme Davis has shown that genetic disruption of the presynaptic Spectrin-Ankyrin skeleton results in catastrophic degeneration of the presynaptic motoneuron terminal at the Drosophila neuromuscular junction (NMJ). My dissertation work has focused on identifying genes that protect against presynaptic neuromuscular degeneration following disruption of this presynaptic Spectrin-Ankyrin skeleton. The following chapters identify and describe presynaptic neuroprotective signaling, which can significantly slow the progression of NMJ degeneration and dysfunction.**



**In Chapter 2, I demonstrate that NMJ disassembly following loss of  $\alpha$ -Spectrin can be suppressed by a *Wld<sup>S</sup>* (*Wallerian degeneration slow*) transgene, providing evidence for a Wallerian-type degenerative mechanism. I subsequently describe a second neuroprotective signaling system, and show that enhanced MAPK-JNK-Fos signaling suppresses NMJ disassembly. Importantly, Fos over-expression does not restore  $\alpha$ -Spectrin protein levels at the NMJ, nor does it rescue defects in the underlying microtubule cytoskeleton, demonstrating that Fos has a neuroprotective activity that is separable from cytoskeletal disruption. This signaling pathway is activated following an acute cytoskeletal disruption, suggesting an endogenous role during neurological stress, and includes delayed, negative feedback via the JNK phosphatase *puckered*. This negative feedback of JNK-Fos allows NMJ disassembly in the presence of persistent cytoskeletal stress. I present a model in which signaling via JNK-Fos functions as a stress response that is transiently activated following cytoskeletal disruption to enhance NMJ stability, and is then shut off through *puckered* to allow NMJ disassembly during persistent cytoskeletal disruption.**

**In Chapter 3, I present evidence that the transcription factor Fos may also be required for maintaining baseline stability, as well as overall motoneuron health and function. Neuronal expression of a dominant-negative Fos construct results in significant degeneration of the NMJ terminal, as well as motor dysfunction and premature death. Interestingly, this impairment of NMJ stability occurs without any obvious preceding disruption of the underlying synaptic microtubule**

**cytoskeleton, further confirming the placement of this stabilizing Fos activity downstream of the microtubule cytoskeleton. Lastly, in Chapter 4, I present evidence that this neuroprotective pathway may also play a role in regulating axonal transport and subsequent signaling within the axonal compartment.**

## TABLE OF CONTENTS

<b>ACKNOWLEDGEMENTS</b> -----	iv
<b>PREFACE</b> -----	vi
<b>ABSTRACT</b> -----	vii
<b>TABLE OF CONTENTS</b> -----	x
<b>LIST OF FIGURES</b> -----	xi
<b>Chapter 1: General Background</b> -----	1
<i>Mechanisms of synapse stabilization</i> -----	2
<i>Assaying stability at the Drosophila NMJ</i> -----	3
<i>MAP Kinase Signaling and Fos</i> -----	5
<b>Chapter 2: Neuroprotective Fos Signaling Enhances Synapse Stability Despite Persistant Disruption of the Spectrin/Ankyrin/Microtubule Cytoskeleton</b> -----	10
<i>Introduction</i> -----	11
<i>Results</i> -----	12
<i>Discussion</i> -----	26
<i>Figures</i> -----	31
<b>Chapter 3: Fos is Required to Maintain Synaptic Stability at the Drosophila Neuromuscular Junction</b> -----	58
<i>Introduction</i> -----	59
<i>Results</i> -----	60
<i>Discussion</i> -----	65
<i>Figures</i> -----	67
<b>Chapter 4: MAPK-Fos Signaling and Axonal Transport</b> -----	75
<i>Introduction</i> -----	76
<i>Results</i> -----	77
<i>Discussion</i> -----	77
<i>Figures</i> -----	80
<b>CONCLUSIONS</b> -----	83
<i>A model for the neuroprotective actions of Fos</i> -----	85
<b>EXPERIMENTAL PROCEDURES</b> -----	88
<b>REFERENCES</b> -----	97

**LIST OF FIGURES**

**Figure 1-1. NMJ morphology and stability analysis----- 8**

**Figure 2-1. Overexpression of Fos, but not Jun, suppresses synaptic instability at the NMJ -----31**

**Figure 2-2. Overexpression of Fos rescues synaptic function following loss of presynaptic  $\alpha$ -Spectrin-----34**

**Figure 2-3. Increased Fos expression improves adult motor behavior following  $\alpha$ -Spectrin knockdown -----36**

**Figure 2-4. Overexpression of Fos suppresses instability despite persistent microtubule disruption -----38**

**Figure 2-5. Wld<sup>S</sup> expression and potentiation of trophic signaling suppress instability at the NMJ in animals lacking presynaptic  $\alpha$ -Spectrin-----40**

**Figure 2-6. Fos-MAPK signaling is induced following cytoskeletal disruption -----42**

**Figure 2-7. Loss of Puckered suppresses synaptic stability at the NMJ -----45**

**Figure 2-8. Highwire mutation suppresses synaptic instability at the NMJ -----47**

**Figure 2-9. Model for synapse stabilizing effects of MAPK signaling-----50**

**Supplemental Figure 2-1. Overexpression of Fos does not increase presynaptic  $\alpha$ -Spectrin levels -----52**

**Supplemental Figure 2-2. Overexpression of Fos suppresses synaptic instability due to ank2 mutation-----54**

**Supplemental Figure 2-3. Overexpression of Fos does not upregulate cell adhesion proteins at the NMJ -----56**

**Figure 3-1. Fos is critical for synaptic stability downstream of the NMJ cytoskeleton -----67**

**Figure 3-2. Fos signaling regulates motor function and viability in adult flies-----69**

**Figure 3-3. Upstream Wnd/JNK signaling is not required for stability-----71**

**Supplemental Figure 3-1. Dominant-negative Fos and Jun constructs both impair synaptic growth at the NMJ -----73**

**Figure 4-1. MAPK-Fos signaling regulates accumulation of protein within axons--80**

# Chapter 1:

General Background

Proper functioning of the nervous system is dependent on reliable, high-fidelity communication between pre- and postsynaptic neurons. This communication is made possible by the successful completion of numerous complex developmental processes. During development, a neuron must extend an axonal growth cone, which must navigate across a distance to locate its proper postsynaptic target. Once this process of axonal pathfinding has completed, the growth cone must differentiate into a presynaptic terminal and form a functional connection with its target neuron. If any one of these processes fails to occur properly, the functioning of an individual circuit or of the nervous system as a whole may be compromised. Following the successful execution of axonal pathfinding, terminal differentiation, and synapse formation, the connections that have formed must be stabilized to insure proper functioning of neuronal circuits for the lifespan of the animal. Furthermore, these stable synaptic connections must retain the ability to undergo both functional and anatomical changes necessary for memory formation and other forms of plasticity. Thus, stabilization of anatomical connections represents a crucial undertaking with implications for both the function and dysfunction of the developing and adult nervous system.

### **Mechanisms of synapse stabilization**

There is increasing evidence that mutations exist which either delay or block the progression of developmental pruning and/or neurodegeneration. For example, pharmacological or genetic inhibition of the ubiquitin proteasome system (UPS) has been shown to block pruning of mushroom body axons in *Drosophila* (Watts et al., 2003) and

to slow Wallerian axonal degeneration in both vertebrates and invertebrates (Hoopfer et al., 2006; Watts et al., 2003; Zhai et al., 2003). The identification and characterization of the Wallerian degeneration slow (*Wld<sup>S</sup>*) mutation in mice provides a second example of a genetic perturbation that can slow the process of Wallerian degeneration in multiple species (Ludwin and Bisby, 1992; Lunn et al., 1989; Perry et al., 1991). The *Wld<sup>S</sup>* mutation results in a fusion protein combining the N-terminal 70 amino acids of Ube4b with the entire coding sequence of nicotinamide mononucleotide adenylyltransferase (NMNAT), an enzyme involved in the biosynthesis of nicotinamide adenine dinucleotide (NAD) (Mack et al., 2001). Remarkably, a single copy of the *Wld<sup>S</sup>* mutation can also suppress neurodegeneration caused by pharmacological disruption of microtubules (Wang et al., 2001; Wang et al., 2002), neurotrophin deprivation (Zhai et al., 2003), or genetic perturbations such as those seen in mouse models of spinal muscular atrophy (Bommel et al., 2002; Ferri et al., 2003; Martin et al., 2002) and Parkinson's disease (Sajadi et al., 2004). Together, these studies suggest the existence of conserved signaling systems that actively participate in the elimination of neuronal structure during both development and disease. It is likely that similar types of signaling participate in the mechanisms that control synapse stability versus disassembly, either during development or neurodegenerative disease.

### **Assaying stability at the *Drosophila* NMJ**

The Davis Lab previously published an assay for synapse integrity at the *Drosophila* NMJ (Eaton and Davis, 2005; Eaton et al., 2002; Koch et al., 2008; Pielage et al., 2008;

Pielage et al., 2005) that is similar to assays of synapse stability used at the vertebrate NMJ (Pun et al., 2006). In this assay we use neural specific antibodies to label the presynaptic motoneuron terminal and simultaneously label the postsynaptic muscle membrane folds (termed the subsynaptic reticulum or SSR) with antibodies to the scaffolding protein Discs-large (Eaton and Davis, 2005; Eaton et al., 2002; Pielage et al., 2008; Pielage et al., 2005). In wild type animals, there is a precise alignment of pre- and postsynaptic markers throughout the *Drosophila* larval NMJ. However, mutations that disrupt synaptic integrity result in sites where the presynaptic nerve terminal retracts, leaving behind well-organized postsynaptic muscle membrane folds with clusters of postsynaptic glutamate receptors. Since this type of highly organized postsynaptic apparatus only forms in apposition to a functional presynaptic nerve terminal (Guan et al., 1996; Saitoe et al., 2001; Thomas et al., 2000), these represent sites where the nerve terminal once resided and has since retracted. This conclusion is supported by recent developmental and live imaging studies of motoneuron retraction at the *Drosophila* NMJ (Koch et al., 2008; Pielage et al., 2008). This assay has now been verified in *Drosophila* at multiple developmental stages using diverse pre- and postsynaptic markers, including antibodies that label the presynaptic motoneuron membrane (anti-HRP), endocytic proteins (anti-Dap160), vesicle associated proteins (anti-Synapsin or anti-Synaptotagmin), cytoskeletal markers (anti-Futsch), and trans-synaptic cell adhesion molecules (Pielage et al., 2005). This assay has been further verified by serial section electron microscopy and synaptic electrophysiology (Pielage et al., 2005). Finally,



similar conclusions have been made using this assay at the vertebrate NMJ (Pun et al., 2006).

### **Map Kinase Signaling and Fos Regulation**

Mitogen-Activated-Protein-Kinase (MAPK) pathways respond to stimuli that result from stress to the cell or its environment, thereby converting extracellular stimuli into an appropriate intracellular response (Lau and Nathans, 1987; Morgan et al., 1987). MAPK proteins have been implicated in various processes including cell growth, cell differentiation, and the decision between cell survival and cell death (i.e. apoptosis) (reviewed in (Herdegen and Waetzig, 2001)). MAPK signaling activates downstream transcription factors, including c-fos and c-jun, which interact to form the Activator Protein-1 (AP-1). In *Drosophila*, Fos is encoded by *kayak* and is a member of a class of genes known as Immediate Early Genes (IEGs). IEGs, including Fos, are rapidly induced following activity, stress, or other extracellular stimuli and act to induce transcription of target genes in the nucleus (Riesgo-Escovar and Hafen, 1997; Zeitlinger et al., 1997).

The role that MAPK and Fos signaling play in either neuroprotection or neurodegeneration is controversial. Previous studies have provided evidence to support both a neuroprotective and neurodegenerative role for Fos. It is clear that Fos expression is upregulated *in vivo* in response to acute brain injury (e.g. ischemia or seizure induction) (Cho et al., 2001; Dragunow et al., 1994; Walton et al., 1999a; Walton et al., 1998). However, it is unclear whether Fos is mediating the resulting neuronal apoptosis or simply attempting to protect against it. A few studies have sought to determine a

causal relationship between *c-fos* and neurodegeneration. Administration of *c-fos* antisense oligonucleotides has been shown to protect neurons from glutamate- or NMDA-induced apoptosis *in vitro* or *in vivo*, respectively (Fernandez et al., 2005; Lu et al., 1997). Additionally, genetic elimination of *c-fos* in mice prevents apoptosis of photoreceptors after light exposure (Hafezi et al., 1997). However, there remains a great deal of controversy regarding the neuroprotective or neurodegenerative role of Fos in response to different stimuli. Additionally, a role for Fos in neuronal stability under normal, non-apoptotic conditions has not been resolved.

In the last ten years, a large body of work has emerged which provides indirect evidence for a neuroprotective function of Fos in the nervous system (Lonze et al., 2002; Mabuchi et al., 2001; Mantamadiotis et al., 2002; Palop et al., 2003; Saura et al., 2004; Walton et al., 1999b). In addition to being activated by stimulation of MAPK signaling, *fos* is also a target of cAMP Response Element (CRE)-mediated transcription in neurons, and is upregulated in response to phosphorylation of CRE-binding protein (CREB) (Sheng et al., 1990). Many recent studies have shown a consistent neuroprotective effect of CREB activation (Lonze et al., 2002; Mabuchi et al., 2001; Mantamadiotis et al., 2002; Palop et al., 2003; Saura et al., 2004; Walton et al., 1999b). Although *c-fos* is just one of many CREB target genes, it is tempting to speculate that the robust *c-fos* induction seen after acute brain injury represents an attempt at neuroprotection rather than the execution of a degenerative signaling cascade. It has indeed been reported that *c-fos* induction after ischemia is strongest in cells of the dentate gyrus that are relatively resistant to the ensuing apoptosis (Morgan et al., 1987). Furthermore, studies have investigated the levels

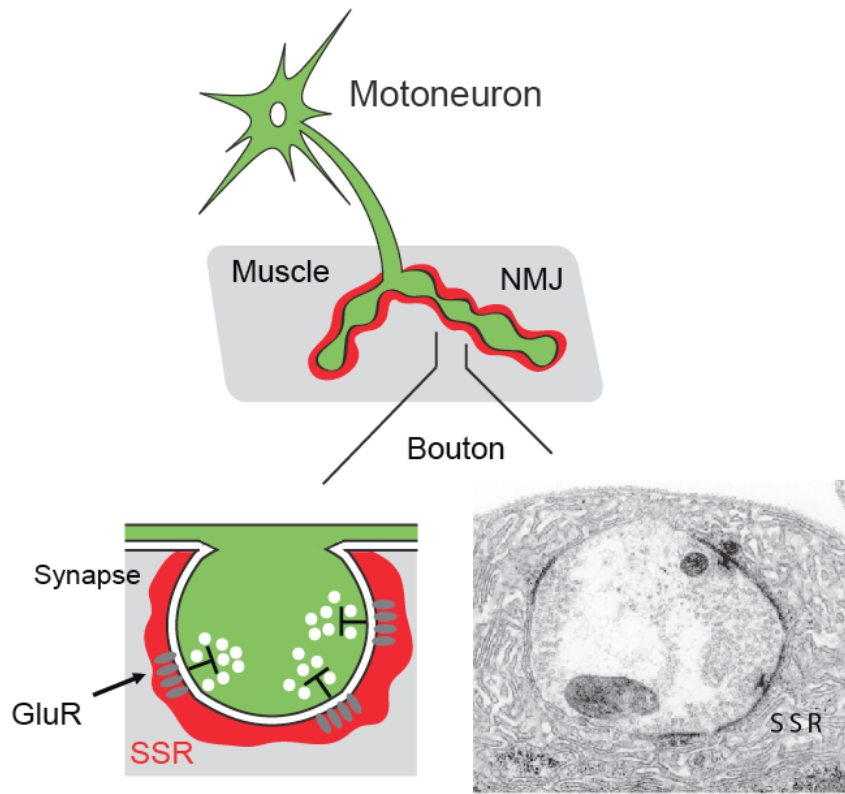
of Fos and CRE-mediated transcription in animal models of neurodegenerative disease. In two animal models of Alzheimer's disease, Fos protein levels are greatly decreased, and this decrease is accompanied by synaptic dysfunction and progressive neurodegeneration (Palop et al., 2003; Saura et al., 2004). As studies have indicated that synapse dysfunction and degeneration may be early pathological events in Alzheimer's disease (Scheff et al., 2006; Selkoe, 2002; Tanzi, 2005), this raises the possibility that Fos may be playing a protective role at the synapse.

My thesis work has attempted to directly investigate a role for MAPK and Fos signaling in maintaining synapse stability and overall motoneuron health. The following chapters will show a clear neuroprotective role for Fos and MAPK activation at the *Drosophila* NMJ, and present evidence that MAPK and Fos participate in an endogenous stress response which provides transient stabilizing activity to the NMJ in the face of cytoskeletal disruption. Additionally, my data suggest that Fos is required for maintaining baseline NMJ stability, and that Fos activity may have broader effects on motoneuron health, beyond simply stabilizing synaptic connections.

### **Figure 1-1. NMJ morphology and stability analysis**

(A) Schematic of the *Drosophila* neuromuscular junction morphology. An identified motoneuron in the CNS projects to an identified muscle cell and forms a multi-bouton synapse. A cross-section of an individual bouton shows that the presynaptic terminal is surrounded by the muscle subsynaptic reticulum, seen in the electron micrograph on the right as multiple microns of complex muscle membrane folds. The schematic cross-section also denotes active zones, where presynaptic release machinery and vesicles are apposed to postsynaptic glutamate receptors (GluR). Active zones can be seen on the electron micrograph as regions of electron dense material. (B) Schematic diagram of the presynaptic motoneuron retraction process that results in a postsynaptic footprint.

A



B



# Chapter 2:

Neuroprotective Fos signaling Enhances Synapse  
Stability Despite Persistent Disruption of the  
Spectrin/Ankyrin/Microtubule Cytoskeleton

## INTRODUCTION

We have previously screened for mutations in genes that are critical for synaptic stability at the *Drosophila* NMJ (Eaton and Davis, 2005; Eaton et al., 2002; Pielage et al., 2008; Pielage et al., 2005). When mutated, these genes cause the presynaptic motoneuron terminal to retract from the muscle fiber in a distal to proximal manner, leaving behind an unopposed postsynaptic apparatus that no longer receives motoneuron input (Eaton and Davis, 2005; Eaton et al., 2002; Koch et al., 2008; Pielage et al., 2008; Pielage et al., 2005). These genes include  $\alpha$ - and  $\beta$ -spectrin (Pielage et al., 2005), *ankyrin2* (Koch et al., 2008; Pielage et al., 2008), as well as genes coding for components of the Dynein/Dynactin complex (Eaton et al., 2002). It is currently unknown whether these mutations represent a cellular stress that triggers an active process of synapse disassembly and retraction at the NMJ, or whether these mutations disrupt cellular mechanisms that directly stabilize the NMJ and therefore cause a passive structural collapse of the presynaptic terminal. Spectrin and Ankyrin2 are prominent cellular components that establish and maintain cell shape (Bennett and Davis, 1983; Bennett and Gilligan, 1993; Bennett and Lambert, 1991). If it is possible to suppress synapse retraction in these mutant animals, then one might be able to distinguish between the mechanisms responsible for structural integrity of the NMJ, and the mechanisms involved in the retraction or elimination of the NMJ.

Here, we demonstrate that synapse retraction following loss of  $\alpha$ -Spectrin can be significantly delayed by over-expression of the *Wallerian degeneration slow* (*Wld<sup>S</sup>*) transgene, as well as by enhanced BMP trophic signaling. In *Drosophila*, recent work

indicates that the NMNAT gene, that is part of the Wld<sup>S</sup> fusion protein, acts as a chaperone to protect against neurodegeneration as has been observed in mouse models of neurodegeneration (Avery et al., 2009; Conforti et al., 2009; Zhai et al., 2008). Thus our new data demonstrate that the disassembly of the *Drosophila* NMJ can be suppressed following a severe cytoskeletal perturbation, and that this process may have mechanistic similarities with Wallerian-type degeneration.

We then use this system to define a novel stabilizing pathway at the *Drosophila* NMJ. The focus of this signaling system is the immediate early gene (IEG) *fos*. Here, we demonstrate that over-expression of Fos effectively reverses many of the hallmark phenotypes of synapse disassembly that are observed in animals lacking presynaptic  $\alpha$ -Spectrin. However, our data suggest that the stabilizing activity provided by endogenous Fos is only transient. Increased Fos protein induces the activity of a negative feedback signaling system that may, ultimately, allow synapse retraction and elimination to proceed in the presence of a persistent cellular stress.

## RESULTS

### **Fos overexpression suppresses presynaptic retraction following depletion of presynaptic $\alpha$ -Spectrin.**

The NMJ in a wildtype animal rarely shows evidence of synapse retraction and when retractions are observed they almost never encompass more than two boutons (Figure 2-1A). By contrast, neuronal expression of UAS- *$\alpha$ -spectrin* RNAi results in frequent and severe synapse retractions. In some cases these retractions can completely eliminate the



presynaptic nerve terminal both anatomically and electrophysiologically (Figure 2-1; see also Pielage et al., 2005). Here we demonstrate that animals co-expressing UAS- $\alpha$ -*spectrin* RNAi and UAS-*fos* have significantly fewer and less severe NMJ retractions compared to animals expressing UAS- $\alpha$ -*spectrin* RNAi alone (Figure 2-1C,F,G). This result suggests that increased Fos signaling can suppress synapse destabilization caused by loss of presynaptic  $\alpha$ -Spectrin. To further investigate this possibility, several controls were performed. First, we controlled for the possibility that co-expression of UAS-*fos* diluted the amount of available GAL4, thereby decreasing the efficiency of UAS- $\alpha$ -*spectrin* RNAi. We controlled for this possibility by co-expressing an inert transgene, UAS-*mRFP(myr)*, along with UAS- $\alpha$ -*spectrin* RNAi. In these animals we see no suppression of synapse retraction frequency or severity (retraction frequency compared to UAS- $\alpha$ -*spectrin* RNAi alone,  $p=0.2$ ,  $n=79$ ; retraction severity compared to UAS- $\alpha$ -*spectrin* RNAi alone,  $p = 0.25$ ,  $n=79$ ). Thus, dilution of GAL4 cannot account for the UAS-*fos*-dependent suppression of synapse retraction. As an additional control, we directly assayed presynaptic  $\alpha$ -Spectrin protein levels. Because muscle expression of  $\alpha$ -Spectrin masks our ability to observe presynaptic  $\alpha$ -Spectrin within the NMJ, we first assayed  $\alpha$ -Spectrin protein levels in the presynaptic axon just prior to innervation of the muscle. We find that  $\alpha$ -Spectrin protein is still absent from the presynaptic axon when UAS-*fos* is co-expressed with UAS- $\alpha$ -*spectrin* RNAi (Supplemental Figure 2-1). Identical results were obtained analyzing the axons of second instar animals demonstrating that  $\alpha$ -Spectrin knockdown occurs early in larval development despite co-expression of UAS-*fos* with UAS- $\alpha$ -*spectrin* RNAi (data not shown). In addition, we

show that simultaneous pre- and postsynaptic expression of UAS- $\alpha$ -spectrin RNAi severely depletes  $\alpha$ -spectrin from the NMJ and co-expression of UAS-*fos* is without effect (Figure 2-1D, E). Thus, the efficiency and extent of  $\alpha$ -Spectrin knockdown by RNAi is not altered by the expression of UAS-*fos*. Finally, examination of synapse morphology in animals over-expressing UAS-*fos* in a wildtype background confirms previous observations that UAS-*fos* expression alone is not sufficient to drive synaptic growth or otherwise alter synapse morphology (data not shown and (Sanyal et al., 2002)). Thus, improved synapse integrity is not a secondary consequence of accelerated synaptic growth. Together, these data suggest that expression of UAS-*fos* enhances synapse stability in the absence of presynaptic  $\alpha$ -Spectrin.

We next confirmed that presynaptic expression of UAS- $\alpha$ -spectrin RNAi causes a significant electrophysiological deficit at the NMJ (Figure 2-2). In these experiments UAS- $\alpha$ -spectrin RNAi is co-expressed with UAS-*mRFP(myr)* as a control (see Figure 2-2 legend). Then we asked whether co-expression of UAS-*fos* with UAS- $\alpha$ -spectrin RNAi would improve synaptic transmission as well as synapse stability. We find that UAS-*fos* co-expression significantly improves every measure of synaptic function when compared to animals that express UAS- $\alpha$ -spectrin RNAi alone. In animals co-expressing UAS-*fos* and UAS- $\alpha$ -spectrin RNAi presynaptically, the average EPSP amplitude is significantly rescued toward wildtype values (Figure 2-2A) and the average quantal content and mini frequency are not statistically different from wildtype (Figure 2-2C,D). This demonstrates that UAS-*fos* co-expression improves synaptic function to near wildtype levels despite the severe depletion of presynaptic  $\alpha$ -Spectrin protein. Taken together,

these data suggest that synapse retraction following depletion of the Spectrin skeleton is not simply due to collapse of neuronal architecture, but reflects a process of synapse destabilization that can be significantly suppressed by overexpression of Fos.

Finally, as a control, we asked whether UAS-*fos* expression could suppress synapse retraction in the *ank2-L* mutant background (Pielage et al., 2008). NMJ retraction in *ank2-L* mutants is significantly more severe than that observed following RNAi-dependent depletion of presynaptic spectrin (Supplemental Figure 2-2F). Although the number of NMJ that show evidence of retraction is unchanged in *ank2-L* animals that also overexpress presynaptic Fos, the severity of NMJ retraction is significantly decreased (Supplemental Figure 2-2D). In addition, we find a significant reduction in the number of NMJ that are completely eliminated when UAS-*fos* is expressed presynaptically in the *ank2-L* mutant (Supplemental Figure 2-2E). Finally, NMJ morphology more closely resembles wildtype when UAS-*fos* is expressed in the *ank2-L* mutant (Supplemental Figure 2-2A,B,C). In conclusion, ectopic expression of Fos confers synapse stabilizing activity that slows the process of NMJ retraction despite the presence of a persistent cellular stress in *ank2-L* mutants.

### **Increased Fos expression improves adult motor behavior following $\alpha$ -Spectrin knockdown**

Although the larval NMJ is ideal for studying NMJ morphology and function, the relatively short developmental period and limited behavior of the larva precludes an analysis of progressive motor deficits that might correlate with impaired NMJ health and

stability. Therefore, we moved to analysis of adult motor behavior in animals with altered Fos activity. To assay motor coordination we used a modified negative geotaxis assay in which we quantified the time necessary for adult flies to transition from the bottom of a vial to the wall of a vial. The advantage of this measure is that all flies attempt to leave the bottom of the vial, but only flies with sufficient motor ability are able to make this transition. This is a robust assay and wild type animals take an average of less than 3 seconds to make this transition (Figure 2-3).

Next we analyzed this behavior in adult animals that express UAS-*α-spectrin* RNAi neuronally throughout development. These animals hatch at a significantly lower frequency than wild type and are analyzed within the first four days of adult eclosion. We were concerned that animals expressing UAS-*α-spectrin* RNAi might have severe developmental abnormalities that would prevent them from ever achieving this behavioral task. Therefore, we excluded those animals with the most severe developmental defects by selecting only animals that were able to transition to the wall of a vial on the first day of adult life. On average the UAS-*α-spectrin* RNAi animals were significantly slower than wild type in transitioning to the wall of a vial, taking an average of greater than 25 seconds (Figure 2-3). These data demonstrate that the neuronal circuitry underlying this behavior is not functioning properly. This could be a consequence of impaired neural development or altered synapse stability. Finally, to determine whether co-expression of UAS-*fos* could improve this behavioral deficit, we analyzed animals co-expressing UAS-*α-spectrin* RNAi and UAS-*fos*. These animals were subjected to the same selection criteria. Remarkably, these animals showed a

significant improvement in this behavioral task (Figure 2-3). While it is unclear how UAS-*fos* might act to achieve this effect, these data demonstrate that expression of UAS-*fos* can have a behaviorally relevant, protective effect on the function of complex neural circuitry.

**Fos overexpression suppresses NMJ retraction despite a persistent disruption of the presynaptic MT cytoskeleton.**

Disruption of the presynaptic microtubule (MT) cytoskeleton is a common feature observed during synapse retraction at the *Drosophila* NMJ (Eaton and Davis, 2005; Pielage et al., 2005) and in many other forms of neuronal retraction and degeneration (Hoopfer et al., 2006; Luo and O'Leary, 2005; Zhai et al., 2003). Indeed, it has been proposed that disruption of neuronal MTs could be causative for Wallerian-type neuronal degeneration (Zhai et al., 2003). It has been shown previously that presynaptic knockdown of  $\alpha$ -Spectrin causes a severe disruption of the Futsch-stabilized MT cytoskeleton at the *Drosophila* NMJ (Pielage et al., 2005). This result is repeated here (Figure 2-4A,B). In wildtype animals, the Futsch-positive MTs extend as a narrow filament throughout the NMJ (Figure 2-4A). Following presynaptic  $\alpha$ -Spectrin knockdown, the Futsch staining becomes disorganized and accumulates in large presynaptic swellings (Figure 2-4B).

One possible mechanism by which UAS-*fos* expression could stabilize the NMJ is through the production of molecules that re-stabilize the MT cytoskeleton at the NMJ.

However, we find that the Futsch-positive MTs remain disorganized when UAS-*fos* is expressed in animals lacking presynaptic  $\alpha$ -Spectrin (Figure 2-4C). Importantly, this MT phenotype is unaltered even though the frequency and severity of NMJ retraction is significantly decreased. These observations indicate that Fos does not achieve synapse stability by restoring the integrity or organization of the presynaptic MT cytoskeleton. Ultimately, we cannot rule out a partial, qualitative improvement in MT organization caused by UAS-*fos* overexpression. However, since UAS-*fos* expression does not restore  $\alpha$ -Spectrin protein to the NMJ and since  $\alpha$ -Spectrin is linked to MT organization via Ank2-L (Pielage et al., 2008), we consider this unlikely.

Previously, loss of presynaptic Spectrin and Ankyrin2-L has been correlated with altered organization of the synaptic cell adhesion molecules Fasciclin II (FasII) and Neuroglian (Nrg, the L1 homologue in *Drosophila*) (Pielage et al., 2008; Pielage et al., 2005). FasII is a homophilic cell adhesion molecule necessary for synapse stability at this NMJ (Schuster et al., 1996). Therefore, we asked whether UAS-*fos* dependent suppression of synaptic retraction might be mediated through upregulation of one or both of these cell adhesion molecules. However, we find no evidence for a Fos-dependent increase in either FasII or Nrg protein at the NMJ (Supplemental Figure 2-3) that could explain enhanced NMJ stability.

### **Overexpression of Wld<sup>S</sup> delays synapse retraction.**

It remains unclear whether the retraction of the presynaptic nerve terminal at the *Drosophila* NMJ is molecularly related to a developmental pruning process, akin to

synapse elimination at the developing vertebrate NMJ, or whether it is related to neurodegeneration. Several lines of evidence have been used to argue that retraction of the motoneuron terminal at the *Drosophila* NMJ is a degenerative event. First, elimination of previously functional NMJ is not a spontaneous event that occurs during normal development (Keshishian et al., 1996; Pielage et al., 2008; Pielage et al., 2005). Second, mutations in genes that cause NMJ retraction in *Drosophila* have similarly been shown to play a role in neural degeneration in vertebrate model systems and humans (Bennett and Healy, 2008; Hafezparast et al., 2003; Ikeda et al., 2006; LaMonte et al., 2002; Levy et al., 2006; Ligon et al., 2005; Parkinson et al., 2001; Puls et al., 2003). Finally, the retraction of the motoneuron terminal is not preceded by motoneuron cell death (Eaton et al., 2002), and we have again confirmed this finding using a tunnel assay, examining wildtype and mutant CNS (data not shown).

Recently, a molecular distinction has been made between the mechanisms responsible for developmental pruning of neuronal arbors and neurodegeneration. *Wld<sup>S</sup>* is a spontaneously occurring dominant genetic aberration that fuses the 5' end of *ube4b* and the *nmnat* gene (Lyon et al., 1993; Mack et al., 2001; Martin-Blanco et al., 1998; Ring and Martinez Arias, 1993). In vertebrates, the *Wld<sup>S</sup>* mutation has been shown to slow Wallerian degeneration as well as other forms of neural degeneration (Ferri et al., 2003; Fischer et al., 2005; Hoopfer et al., 2006; Luo and O'Leary, 2005; Perry et al., 1991; Perry et al., 1990; Sajadi et al., 2004; Wang et al., 2001; Wang et al., 2002). In *Drosophila*, neuronal expression of a *Wld<sup>S</sup>* transgene is sufficient to suppress neurodegeneration caused by axon transection (Hoopfer et al., 2006). However, in both

Drosophila and vertebrate systems, *Wld<sup>S</sup>* does not alter the process of developmental pruning of neuronal arborizations (Hoopfer et al., 2006; Parson et al., 1997). Therefore, we asked whether expression of the *Wld<sup>S</sup>* transgene could suppress or slow the process of presynaptic retraction at the Drosophila NMJ.

Here we demonstrate that animals neuronally co-expressing UAS-*α-spectrin* RNAi and UAS-*Wld<sup>S</sup>* have significantly fewer and less severe synapse retractions compared to animals expressing UAS-*α-spectrin* RNAi alone (Figure 2-5B,C,D,E). Expression of UAS-*Wld<sup>S</sup>* in a wildtype background has no effect on synaptic stability (data not shown). These data are consistent with the conclusion that loss of *α-Spectrin* induces a degenerative retraction of the presynaptic nerve terminal.

In vertebrate systems, the withdrawal of trophic factors from cultured motoneurons also induces a neurodegenerative response and elevated expression of trophic signaling molecules can suppress neuromuscular degeneration in mouse models of amyotrophic lateral sclerosis (ALS) (Pun et al., 2006). At the Drosophila NMJ, bone morphogenetic protein (BMP) signaling functions as a trophic signaling system that supports NMJ growth (Aberle et al., 2002), and it has been shown that impaired BMP signaling causes synapse retraction at the NMJ (Eaton et al., 2002). Therefore, we asked whether neuronal expression of the BMP ligand *glass bottom boat* (*gbb*) could suppress synapse retraction following depletion of *α-Spectrin*. Here we show that neuronal co-expression of UAS-*gbb* with UAS-*α-spectrin* RNAi significantly suppresses the frequency and severity of NMJ retractions compared to expression of UAS-*α-spectrin* RNAi alone (Figure 2-5F,G; see also materials and methods section for supplemental discussion relevant to this



figure). Taken together, these data support the conclusion that retraction of the presynaptic motoneuron terminal at the *Drosophila* NMJ following loss of  $\alpha$ -Spectrin may be related to neurodegenerative processes in vertebrate systems.

**Evidence for the induction of Fos-MAP Kinase signaling following cytoskeletal disruption.**

Since the over-expression of UAS-*fos* is sufficient to suppress neuromuscular retraction, we sought to determine whether Fos protein levels are altered following expression of UAS- *$\alpha$ -spectrin* RNAi. Available Fos antibodies do not work well *in situ*, but can reliably report a 50% decrease in Fos protein in heterozygous *fos/+* null mutant animals on western blots (Figure 2-6B top row) (the *fos* gene is also called *kayak* (*kay*) in *Drosophila* and the terms are used interchangeably). When we assayed Fos protein levels from the CNS of third instar larvae that express UAS- *$\alpha$ -spectrin* RNAi throughout development and have significant NMJ retraction, we find no change in total Fos protein compared to controls (Figure 2-6B bottom row). Thus, neuromuscular retraction is not correlated with a persistent change in Fos protein relative to controls.

Since Fos is an immediate early gene, we next considered the possibility that Fos protein levels transiently increase at some time during larval development following the loss of  $\alpha$ -Spectrin and the ensuing cytoskeletal disruption. To test this hypothesis, we acutely disrupted the neuronal cytoskeleton, *in vivo*, and assayed Fos protein levels. Pharmacological reagents to disrupt Spectrin are not available. However, loss of  $\alpha$ -Spectrin results in a severe disruption of the underlying microtubule cytoskeleton (Figure

2-4; (Pielage et al., 2005)). We reasoned that pharmacological perturbation of MTs might represent a similar, generalized, cytoskeletal stress, though clearly not identical to that caused by the developmental loss of  $\alpha$ -Spectrin. Several prior studies support such a conclusion (Hoopfer et al., 2006; Luo and O'Leary, 2005; Zhai et al., 2003). Therefore, we assayed Fos protein levels after disruption of the neuronal MTs through application of 50-100 $\mu$ M nocodazole (Noc) to larval neuromuscular preparations. This concentration of Noc efficiently disrupts the dynamic population of microtubules in *Drosophila* motoneuron axons and at the *Drosophila* NMJ without an immediate effect on Futsch-stabilized microtubule organization (GWD and Catherine Pawson, unpublished data). We assayed Fos protein in animals incubated in Noc for either 30 minutes or 2 hours (Fig 2-6E,F). At the 30 min time point, we observe a highly significant, greater than two-fold, increase in Fos protein levels compared to controls. At the 2 hour time point, Fos levels have returned to baseline. These data are consistent with a rapid induction and decay of Fos protein following perturbation of the neuronal microtubule cytoskeleton. Since Fos overexpression is sufficient to suppress neuromuscular degeneration, we suggest that the increase in endogenous Fos protein may provide a transient stabilizing effect following cytoskeletal disruption.

Fos is embedded within a negative feedback signaling system that includes the dual specificity, VH1 family phosphatase *puckered* (*puc*) (Figure 6A). Increased Fos activity leads to elevation of *puckered* transcription, decreased JNK activity and, ultimately, decreased Fos phosphorylation (Figure 2-6A) (Agnes et al., 1999; Dobens et al., 2001; Martin-Blanco et al., 1998; Ring and Martinez Arias, 1993). We asked whether this

negative feedback system might be induced following cytoskeletal disruption. To do so we monitored the activity of a previously published *puckered* reporter (Dobens et al., 2001; Martin-Blanco et al., 1998). First, we validated the use of this reporter by showing that there is a statistically significant ~50% reduction in reporter activity in the heterozygous null *fos*/+ mutant background that parallels the observed 50% reduction in Fos protein (Figure 2-6C). We then find that there is a highly significant (> two-fold) induction of *puckered* reporter expression in the *α-spectrin* RNAi animals (Figure 6C). A similar induction of the *puckered* reporter can also be observed in central neurons, confirming the neuronal expression of this signaling pathway as well as a neuronal induction of this pathway in response to loss of  $\alpha$ -Spectrin (Figure 2-6D). One interpretation is that an initial elevation of Fos protein induced a persistent elevation in *puckered* transcription. Persistent activity of this negative feedback would constitutively inhibit Fos activity and prevent re-activation of elevated Fos protein during a persistent cytoskeletal perturbation. If the induction of Puckered-dependent negative feedback signaling favors NMJ retraction in the presence of a cytoskeletal perturbation, then loss-of-function mutations in the *puckered* gene might function similar to UAS-*fos* overexpression and suppress NMJ disassembly in animals lacking  $\alpha$ -Spectrin. Therefore, we went on to test this hypothesis genetically.

**Mutations in the JNK phosphatase *puckered* suppress synapse retraction following loss of presynaptic  $\alpha$ -Spectrin**

Homozygous *puckered* mutations are embryonic lethal. Therefore, we asked whether a hypomorphic loss-of-function *puckered* allelic combination could suppress synapse retraction in the background of animals expressing UAS- $\alpha$ -spectrin RNAi in neurons. First, we find that the *puckered* hypomorphic mutation alone did not show any significant defects in synapse stability compared to wildtype (Figure 2-7A,B,E,F). We then assayed synapse stability in the *elav-GAL4; UAS- $\alpha$ -spectrin RNAi/+; puc<sup>1</sup>/puc<sup>A251</sup>* double mutant animals. We find that the presence of the *puckered* mutation significantly improves synapse stability as shown by a statistically significant decrease in both retraction frequency and severity (Figure 2-7C,D,E,F). Note that it was necessary, due to genetic considerations, to initiate synapse retractions by expressing a single copy of the UAS- $\alpha$ -spectrin RNAi transgene. A single copy of the RNAi transgene results in a less severe (though still highly significant) synapse retraction phenotype (see materials and methods for supplemental discussion). These data support a model in which transient Fos activity is initially stabilizing, but is then attenuated by the induction of negative feedback via *puckered*. To further test this model, we examined mutations in a second gene, *highwire*, which has been previously shown to negatively regulate MAPK protein levels and Fos (Collins et al., 2006).

### **Mutations in *highwire* suppress synapse retraction following loss of presynaptic $\alpha$ -Spectrin**

The *highwire* gene encodes a large protein with putative E3 ubiquitin ligase activity (Aberle et al., 2002; Wan et al., 2000; Wu et al., 2005). In both *Drosophila* and *C.*

*elegans*, the *highwire* (or *RPM-1*) mutation leads to increased levels of the MAP3K protein encoded by *wallenda* (*Drosophila*) or *dlk* (*C. elegans*) (Collins et al., 2006; Nakata et al., 2005). In *Drosophila*, the *highwire* mutation leads to increased synaptic growth that is dependent upon *wallenda*, *JNK* and *fos* (Collins et al., 2006). Therefore, we tested whether *highwire*-dependent activation of Fos could suppress synapse retraction following loss of presynaptic  $\alpha$ -Spectrin. In these experiments, two copies of the UAS- *$\alpha$ -spectrin* RNAi transgene were used (as shown in Figure 2-1).

First, we find that the presence of a heterozygous *highwire*/+ mutation in the background of animals that express UAS- *$\alpha$ -spectrin* RNAi neuronally causes a slight but statistically significant suppression of synapse retraction severity (Figure 2-8F). There is also a trend toward a lower frequency of synapse retractions, though this is not statistically significant (Figure 2-8E). Importantly, in these animals, the NMJ is not overgrown, demonstrating that improved synapse stability can occur without a change in bouton number. Next we analyzed synapse stability in animals harboring a hemizygous *highwire* mutation (*highwire*/Y) that also neuronally express UAS- *$\alpha$ -spectrin* RNAi. A hemizygous *highwire* mutation does not have any effect on stability in a wildtype background (Figure 2-8C,E,F). However, we observe that a hemizygous *highwire* mutation results in a strong, statistically significant, suppression of both synapse retraction frequency and severity in animals lacking presynaptic  $\alpha$ -Spectrin (Figure 2-8D,E,F). It is possible that NMJ overgrowth contributes to the suppression of synapse retraction in this experiment. However, since *highwire*/+ can partially suppress synapse retractions without causing NMJ overgrowth, we speculate that NMJ overgrowth is not

required to achieve increased synapse stability following loss of presynaptic  $\alpha$ -Spectrin. This is further supported by the demonstration that Fos over-expression suppresses synapse retraction without inducing NMJ overgrowth. Together these data support our model in which induction of negative feedback signaling via *puckered* attenuates the stabilizing activity of Fos, leading to more rapid NMJ disassembly. It should also be noted that the stabilizing activity of the *hiw* mutation could be due to elevated BMP signaling in this background (McCabe et al., 2004), which we have shown to be sufficient to suppress NMJ retraction (Figure 2-5).

## **DISCUSSION**

Here we define genetic and transgenic conditions capable of conferring enhanced NMJ stability following the loss of presynaptic  $\alpha$ -Spectrin, a molecule that is necessary for normal microtubule organization and which has been termed a master organizer of the cell membrane (Lacas-Gervais et al., 2004). Enhanced NMJ stability in the absence of Spectrin suggests that NMJ destabilization and degeneration are not simply a catastrophic collapse of the NMJ, but might be mediated through additional signaling processes. Consistent with this hypothesis we show a molecular link to Wallerian-type degeneration. These advances could provide insight into the molecular processes underlying neural degeneration caused by spectrin mutations in vertebrate model systems and humans (Bennett and Healy, 2008; Hafezparast et al., 2003; Ikeda et al., 2006; LaMonte et al., 2002; Levy et al., 2006; Ligon et al., 2005; Parkinson et al., 2001; Puls et al., 2003).

We then go on to define a molecular pathway that appears to be centrally involved in the degenerative process at this synapse. We have documented a sequence of events that occur following a persistent cytoskeletal disruption. We demonstrate that an acute cytoskeletal perturbation causes a transient induction of the immediate early gene *fos*. Since transgenic expression of Fos is sufficient to suppress synapse retraction in this system, we suggest that the transient elevation of Fos represents an initial stabilizing response. We then provide evidence that elevated Fos activates a negative feedback loop by increasing transcription of the dual specificity phosphatase *puckered*. The induction of Puckered-dependent negative feedback is delayed relative to the stabilizing increase in Fos and is observed to persist throughout the life of the larvae. Thus, our data suggest that during a prolonged cytoskeletal perturbation, transient stabilizing Fos activity is replaced by a strong induction of *puckered*. The induction of *puckered* has been shown to suppress baseline JNK/Fos activity and should, therefore, prevent re-activation of stabilizing Fos signaling during a persistent cellular stress. The delayed activation of Puckered-dependent negative feedback in the presence of a persistent cytoskeletal stress could represent an endogenous mechanism to ensure that Fos activity is inhibited in the presence of ongoing stress and switch the motoneuron into a state that favors rapid NMJ retraction. Such a system would favor synapse stability when it is possible to repair cellular damage, but favor the elimination of a neuron when damage persists.

This model predicts that prolonging Fos expression or inhibiting Puckered transcription should prolong synapse stability despite the presence of a persistent cytoskeletal disruption (Figure 2-9). This is precisely what we observe. In addition, loss

of function mutation in the E3 ubiquitin ligase *highwire*, which is believed to potentiate baseline Fos signaling (Collins et al., 2006), also significantly suppresses NMJ retraction (Figure 2-9).

The model for a temporal switch from stabilization to disassembly shares similarity to a model for stress induced cell death that involves the induction of the unfolded protein response (UPR) (Lin et al., 2007). The UPR can elicit both a protective response by re-establishing appropriate levels of unfolded protein as well as pro-apoptotic signaling. A recent study has provided evidence that the switch from protective to pro-apoptotic signaling correlates with the duration of activation for different signaling systems downstream of UPR induction. All downstream signaling systems are initially induced, but the switch to pro-apoptotic signaling is correlated with the decay of IRE1 signaling and the prolonged activation of PERK signaling (Lin et al., 2007). Again, the switch from protective to cell-destructive signaling is achieved by temporal changes in the balance of signaling systems that reside downstream of a persistent cellular stress.

### **Sustaining motoneuron integrity despite loss of presynaptic $\alpha$ -Spectrin.**

We previously demonstrated that loss of presynaptic  $\alpha$ -Spectrin causes profound synaptic loss at the NMJ (Pielage et al., 2005). Impaired NMJ stability was correlated with the loss of synaptic cell adhesion, a severely disorganized microtubule cytoskeleton, and the appearance of large protein aggregations in motor axons (Pielage et al., 2005). It is remarkable, therefore, that increased expression of *Wld<sup>S</sup>*, *Gbb* or *Fos* can significantly preserve synapse stability in animals that lack presynaptic  $\alpha$ -Spectrin.



Several studies have documented a neuroprotective effect of synaptic growth. Increased expression of CNTF is neuroprotective in a mouse model of amyotrophic lateral sclerosis (ALS) (Pun et al., 2006). It was also shown that NMJs with an increased endogenous capacity for synaptic growth and remodeling are more resistant to degeneration in a mouse model of ALS (Frey et al., 2000; Pun et al., 2006). Consistent with the importance of growth factor signaling, we show that Gbb overexpression is able to rescue synapse stability. However, overexpression of Wld<sup>S</sup> or UAS-*fos* has no effect on synaptic growth ((Sanyal et al., 2002); data not shown). In addition, a heterozygous *highwire* mutation is sufficient to rescue some aspects of synapse stability in animals that lack presynaptic  $\alpha$ -Spectrin without stimulating significant NMJ growth (Fig 2-8). Therefore, while the stabilizing function of Wld<sup>S</sup> or Fos may be related to the mechanisms that are required for synaptic growth (Collins et al., 2006), enhanced NMJ growth is not necessary for the stabilizing actions of Fos.

We considered the possibility that loss of Spectrin causes motor axons to break, followed by a neurodegenerative response. The basis for this consideration is the recent demonstration that loss of Spectrin in *C. elegans* causes motor axons to break during animal motility (Hammarlund et al., 2007; Hammarlund et al., 2009). In *Drosophila*, it does not appear that motor axons break following loss of neuronal Spectrin. It was previously shown that the severity of NMJ degeneration precisely correlates with the disruption of synaptic transmission at the NMJ (Pielage et al., 2005). Specifically, a small degenerative event that encompasses ~25% of the NMJ was not associated with any defect in synaptic transmission, whereas a degenerative event encompassing >60% of

the NMJ was associated with a significant decrease in synaptic transmission. However, in both cases, the presynaptic action potentials clearly invade the presynaptic nerve terminal and reliably evoke neurotransmitter release. This would not be the case if there were axonal breaks. It is interesting; however, that MAPK signaling is emerging as an important pathway involved in axon regeneration (Ayaz et al., 2008; Hammarlund et al., 2009) and, as shown here, the transition from stabilization to disassembly at the NMJ.

Finally, a recently published study provides evidence that Wallenda and JNK function specifically in distal neuronal processes, severed from the neuronal soma, to promote Wallerian-type degeneration (Miller et al., 2009). These recent data are in apparent contrast with the neuronal growth promoting function of Wallenda/JNK/Fos during neural development (Collins et al., 2006; DiAntonio et al., 2001; Sanyal et al., 2002; Wan et al., 2000) and axon regeneration (Hammarlund et al., 2009). Furthermore, previous studies have shown that both Wallenda and JNK normally promote axonal transport, which is required for ongoing neuronal health (Byrd et al., 2001; Horiuchi et al., 2007). One possible way to reconcile these recent data from Miller and colleagues with our current model is to consider the cellular compartment in which the signaling pathways have been examined. In an intact cell, MAPK/JNK/Fos signaling appears to generally promote synapse stability, axonal transport, cell growth and neuroprotection. By contrast, within an axonal process that has been severed from the cell body and is destined to degenerate, Wallenda and JNK may function to facilitate the induction of the degenerative process. Thus, there may be context-dependent and compartment-specific functions of this important, stress response pathway.

## FIGURES

### Figure 2-1. Overexpression of Fos, but not Jun, suppresses synaptic instability at the NMJ

(A-C) Representative images of muscle 6/7 NMJs stained for the presynaptic active zone protein Brp (green) and postsynaptic Dlg (red). (A) A wildtype NMJ shows Brp in apposition to Dlg throughout the NMJ. (B) An NMJ lacking presynaptic  $\alpha$ -Spectrin shows a large retraction (arrowheads), encompassing over 50% of the NMJ. (C) A similar loss of presynaptic innervation is not seen when Fos is expressed presynaptically, even in the absence of presynaptic  $\alpha$ -Spectrin. (D) Image of a wildtype animal (top) with  $\alpha$ -Spectrin expression (green) visible both in the muscle and innervating axon (as visualized by HRP). Expression of UAS- $\alpha$ -spectrin-dsRNA both neuronally and in the muscle eliminates  $\alpha$ -Spectrin staining throughout the NMJ (middle). Elimination of  $\alpha$ -Spectrin is not altered by concomitant expression of UAS-*fos* (bottom). (E)  $\alpha$ -Spectrin immunoreactivity is quantified at 12 NMJs per genotype. (F,G) Quantification of retraction frequency (F) is measured as the average % of NMJs with >1 or >7 boutons retracted. Retraction severity (G) is measured as the number of boutons per NMJ that are retracted and the data are plotted as a cumulative frequency histogram for each genotype. WT =  $w^{1118}$  (n = 128 NMJs/30 animals).  $\alpha$ -spec RNAi = *elav<sup>C155</sup>-GAL4/+; 2x UAS- $\alpha$ -spectrin dsRNA* (n = 177 NMJs/18 animals).  $\alpha$ -spec RNAi; UAS-*fos* = *elav<sup>C155</sup>-GAL4/+; 2x UAS- $\alpha$ -spectrin-dsRNA; UAS-*fos** (n= 137 NMJs/14 animals).  $\alpha$ -spec RNAi; UAS-*jun* = *elav<sup>C155</sup>-GAL4/+; 2x UAS- $\alpha$ -spectrin-dsRNA; UAS-*jun** (n = 90 NMJs/9 animals). Error bars represent SEM; P-values for retraction frequency were

determined using one-way ANOVA with post-hoc Tukey-Kramer; P-values for retraction severity were determined using a Kruskal-Wallis test with a post-hoc Dunn's test for multiple comparisons: \* $p < 0.05$ , \*\* $p < 0.01$ , \*\*\* $p < 0.001$ . Statistical differences remain when comparisons are made using Student's t-test. Scale bar = 10 $\mu$ m.

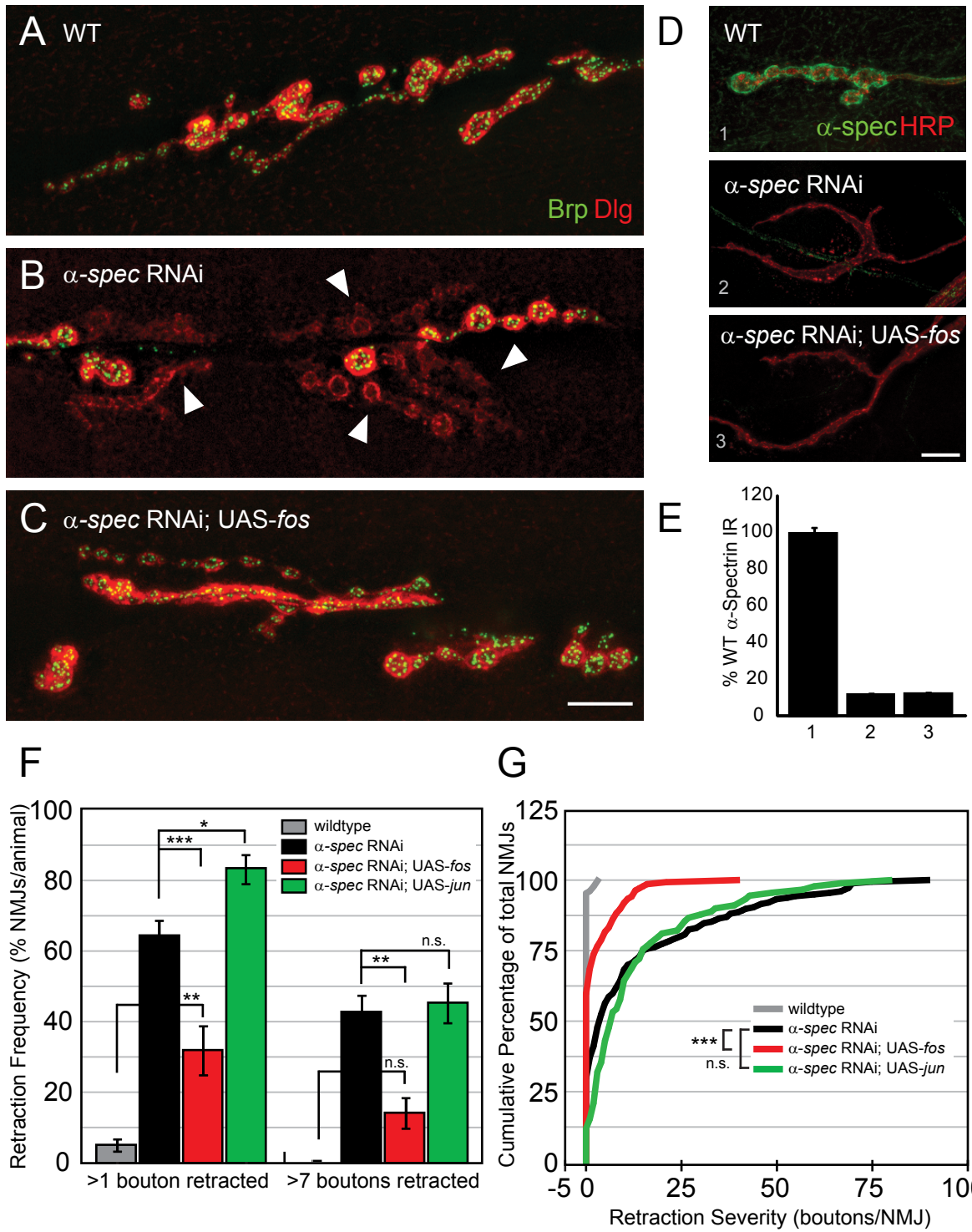


**Figure 2-2. Overexpression of Fos rescues synaptic function following loss of presynaptic  $\alpha$ -Spectrin**

(A-D) Average EPSP amplitude (A), mEPSP amplitude (B), quantal content (C) and mEPSP frequency (D) are plotted for three genotypes. Averages are shown in bar graph format. Superimposed on each bar are the individual averages for each parameter recorded from single NMJ. There is a significant decrease in EPSP amplitude ( $p < 0.001$ ) and quantal content ( $p < 0.001$ ) in  $\alpha$ -spec RNAi animals compared to wild type. There is a significant increase in average EPSP amplitude and quantal content toward wildtype levels by co-expression of UAS-*fos* (EPSP amplitude comparing  $\alpha$ -spec RNAi to  $\alpha$ -spec RNAi; UAS-*fos*:  $p < 0.01$ ) (quantal content comparing  $\alpha$ -spec RNAi to  $\alpha$ -spec RNAi; UAS-*fos*,  $p < 0.001$ ). WT =  $w^{1118}$  (n = 13 NMJs).  $\alpha$ -spec RNAi =  $elav^{C155}$ -GAL4/+; 2x UAS- $\alpha$ -spectrin-dsRNA; UAS-*mRFP*(myr) (n = 21 NMJs).  $\alpha$ -spec RNAi; UAS-*fos* =  $elav^{C155}$ -GAL4/+; 2x UAS- $\alpha$ -spectrin-dsRNA; UAS-*fos* (n = 12). P-values were determined using one-way ANOVA with post-hoc Tukey-Kramer. Statistical differences remain when comparisons are made using Student's t-test.

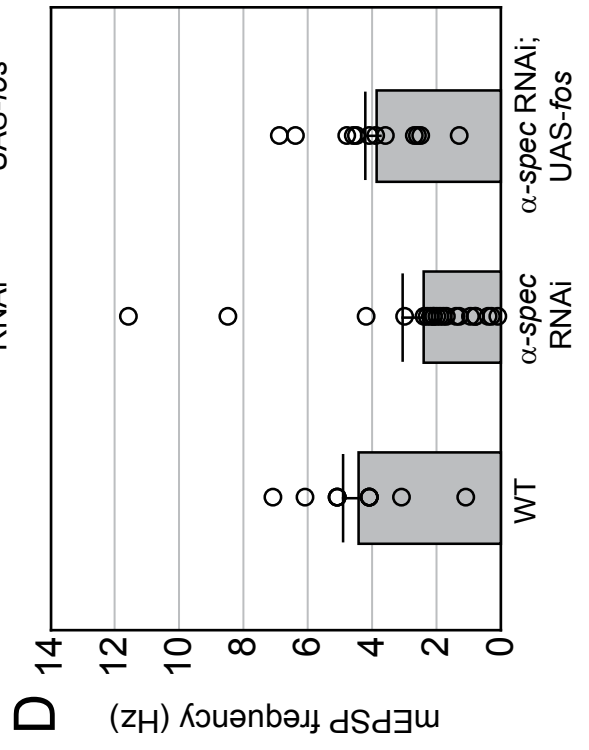
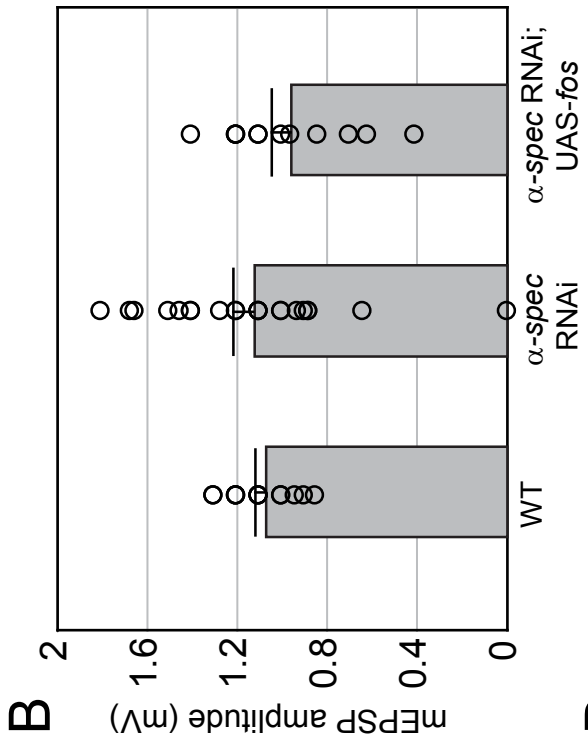
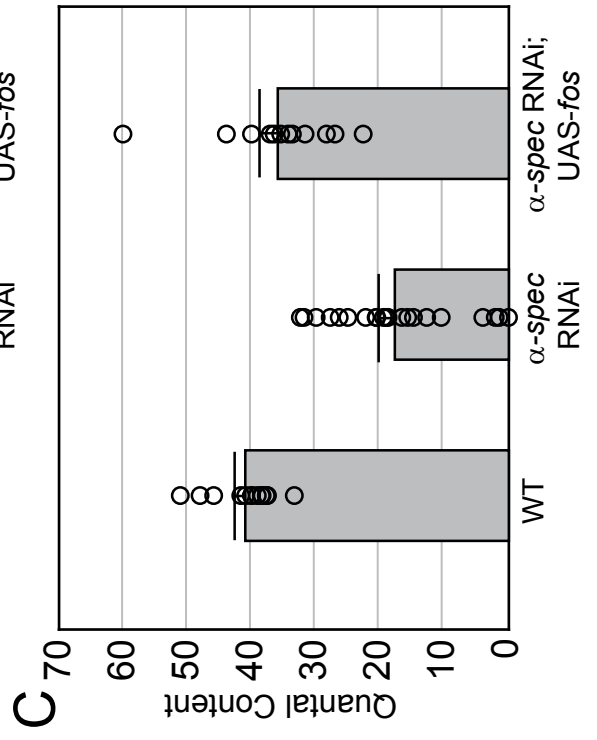
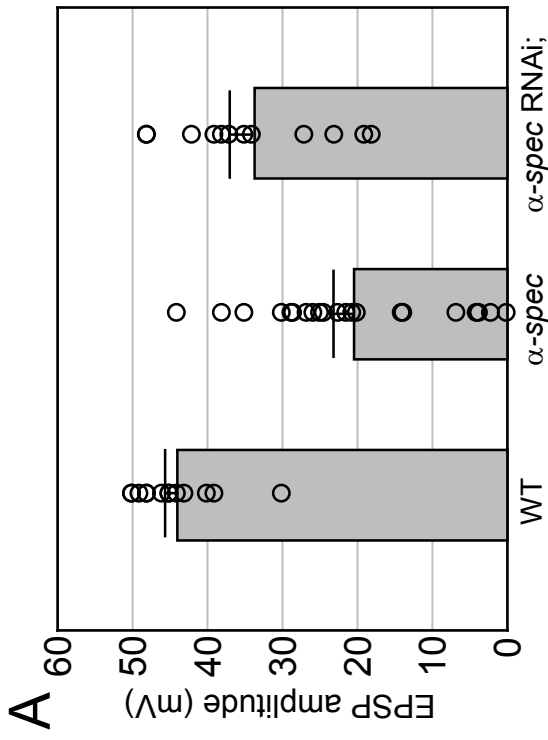


**Figure 2-3. Increased Fos expression improves adult motor behavior following  $\alpha$ -Spectrin knockdown**

Overexpression of Fos improves motor function in flies that lack presynaptic  $\alpha$ -Spectrin. Data was collected for 4 days after eclosure, and motor ability was scored as the time required to transition from the bottom of a vial to the wall of a vial after being knocked down. Female flies were tested individually and three trials were conducted for each fly on a given day. WT = w<sup>1118</sup> (n = 21 animals).  $\alpha$ -spec RNAi = *elav*<sup>C155</sup>-GAL4/+; 2x UAS- *$\alpha$ -spectrin*-dsRNA (n = 11 animals).  $\alpha$ -spec RNAi; UAS-*fos* = *elav*<sup>C155</sup>-GAL4/+; 2x UAS- *$\alpha$ -spectrin*-dsRNA; UAS-*fos* (n = 25 animals). Error bars represent SEM; P-values were determined using a t-test: \*p<0.05, \*\*p<0.01, \*\*\*p<0.001.



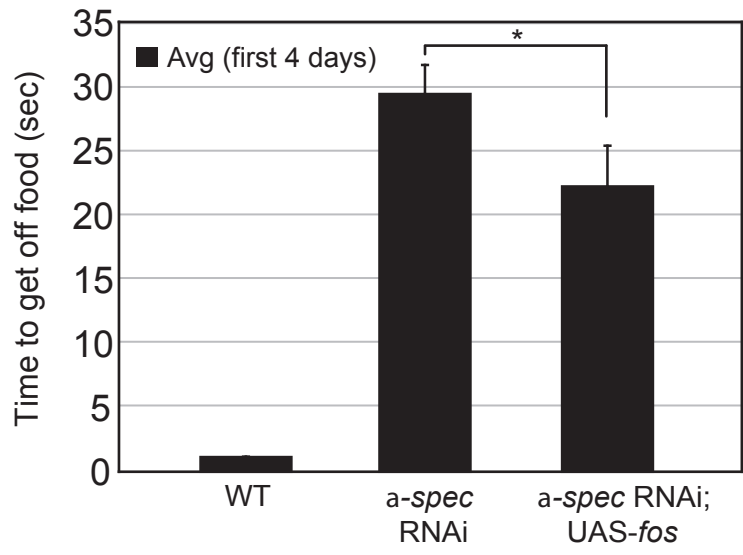


**Figure 2-4. Overexpression of Fos suppresses instability despite persistent microtubule disruption**

(A-C) Representative images of muscle 6/7 NMJs stained for the microtubule associated protein Futsch (green; second row), the presynaptic membrane marker HRP (red; third row), and the presynaptic protein Dap160 (blue; bottom row). (A) A wildtype NMJ. (B) An NMJ lacking presynaptic  $\alpha$ -Spectrin shows disorganized Futsch staining.

Accumulation of Futsch within boutons (arrowheads) and a lack of Futsch staining in distal boutons (arrows) can be observed. (C) Neuronal over-expression of Fos does not restore microtubule integrity. Distal boutons lacking Futsch staining (arrows), as well as large accumulations of Futsch (arrowheads) are still observed. WT =  $w^{1118}$ .  $\alpha$ -spec RNAi =  $elav^{C155}$ -GAL4/+; 2x UAS- $\alpha$ -spectrin-dsRNA.  $\alpha$ -spec RNAi; UAS- $fos$  =  $elav^{C155}$ -GAL4/+; 2x UAS- $\alpha$ -spectrin-dsRNA; UAS- $fos$ . Scale bar = 10 $\mu$ m.

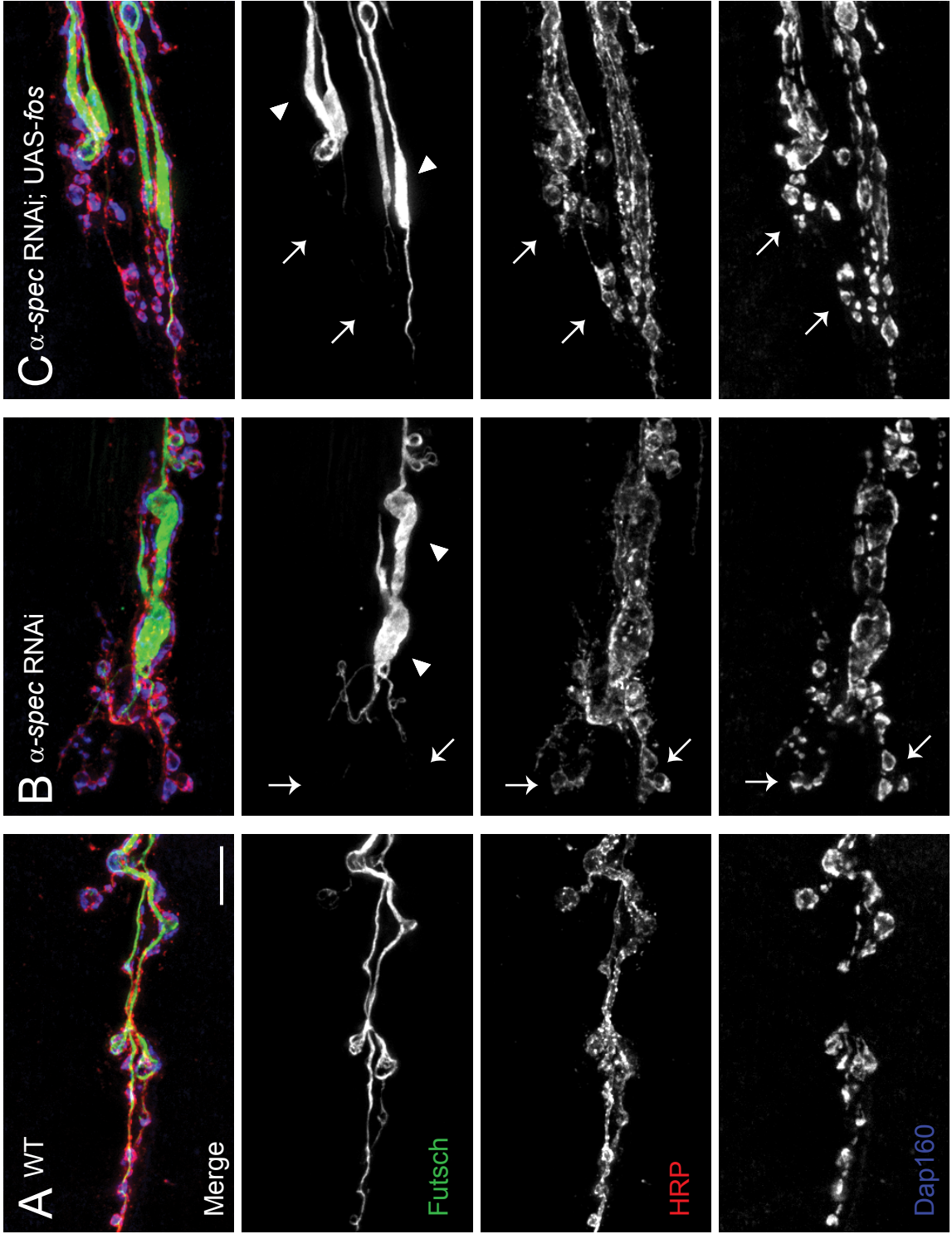


**Figure 2-5. Wld<sup>S</sup> expression and potentiation of trophic signaling suppress instability at the NMJ in animals lacking presynaptic  $\alpha$ -Spectrin**

(A-C) Representative images of muscle 6/7 NMJs stained for the presynaptic active zone protein Brp (green) and postsynaptic Dlg (red). (A) A wildtype NMJ. (B) An NMJ lacking presynaptic  $\alpha$ -Spectrin shows a large retraction (arrowheads), encompassing a majority of the NMJ. (C) Neuronal expression of UAS-Wld<sup>S</sup> slows the synaptic retraction process. (D,E) Wld<sup>S</sup> decreases the severity of synaptic instability as well as the frequency of larger retraction events. Retraction frequency (D) is measured as the average % of NMJs with >1 or >7 boutons retracted. Retraction severity (E) is measured as the number of boutons per NMJ that are retracted and the data are plotted as a cumulative frequency histogram for each genotype. WT = *w<sup>1118</sup>* (n = 137 NMJs/14 animals).  $\alpha$ -*spec* RNAi = *elav<sup>C155</sup>-GAL4/+; 2x UAS- $\alpha$ -spectrin-dsRNA* (n = 134 NMJs/14 animals).  $\alpha$ -*spec* RNAi; UAS-Wld<sup>S</sup> = *elav<sup>C155</sup>-GAL4/+; 2x UAS- $\alpha$ -spectrin-dsRNA; UAS-Wld<sup>S</sup>* (n = 127 NMJs/13 animals). (F,G) Neuronal expression of UAS-*gbb* decreases the severity (F) and frequency (G) of synaptic retractions. WT = *w<sup>1118</sup>* (n = 119 NMJs/12 animals).  $\alpha$ -*spec* RNAi = *elav<sup>C155</sup>-GAL4/+; UAS- $\alpha$ -spectrin-dsRNA* (n = 100 NMJs/10 animals).  $\alpha$ -*spec* RNAi; UAS-*gbb* = *elav<sup>C155</sup>-GAL4/+; UAS- $\alpha$ -spectrin-dsRNA; UAS-*gbb** (n = 67 NMJs/7 animals). Error bars represent SEM; P-values for retraction frequency were determined using one-way ANOVA with post-hoc Tukey-Kramer; P-values for retraction severity were determined using a Kruskal-Wallis test with a post-hoc Dunn's test for multiple comparisons: \*p<0.05, \*\*p<0.01, \*\*\*p<0.001. Statistical differences remain when comparisons are made using Student's t-test. Scale bar = 10 $\mu$ m.

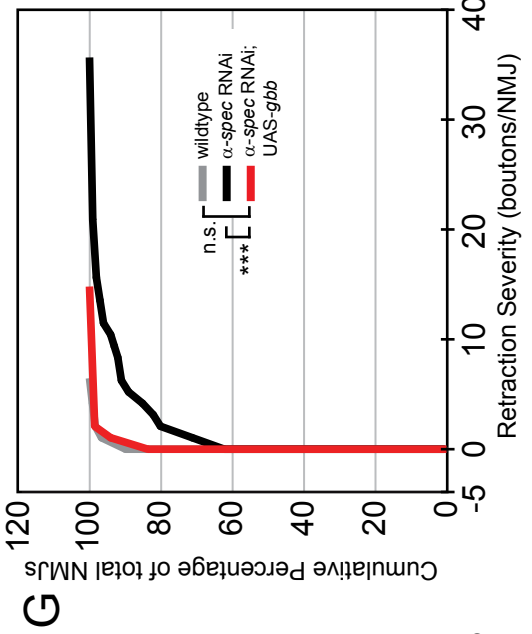
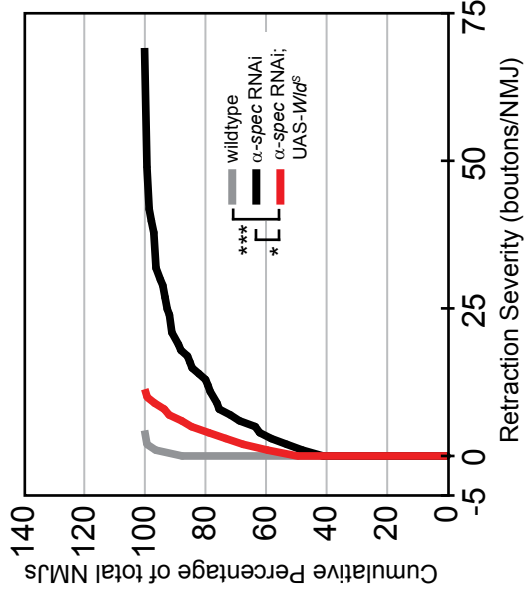
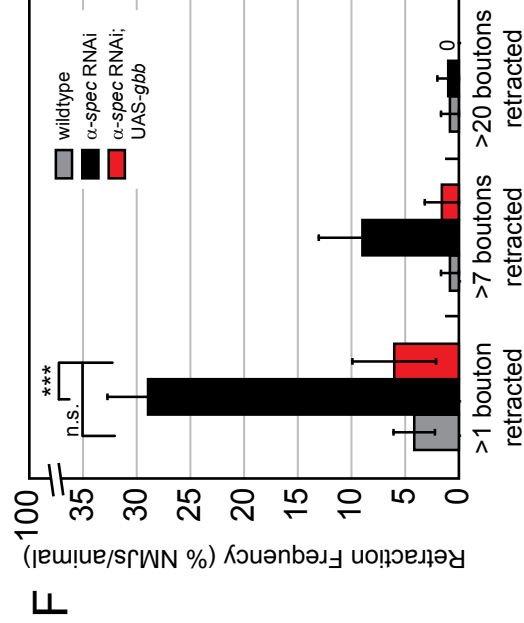
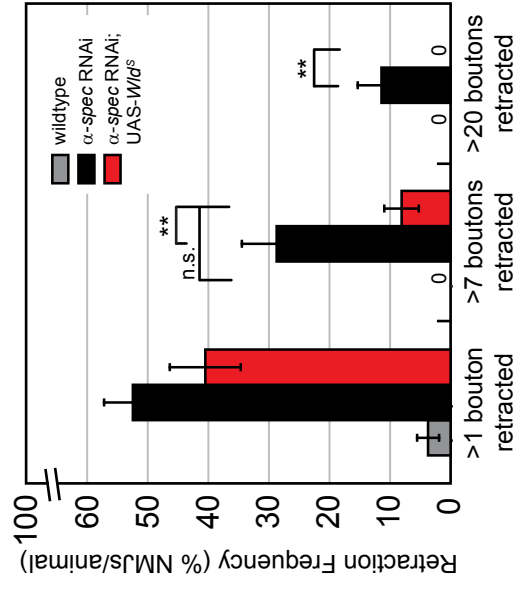
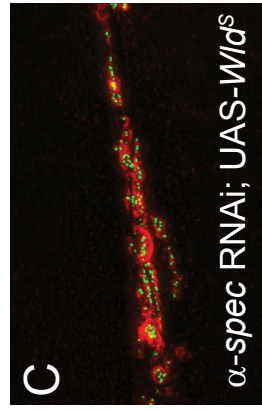
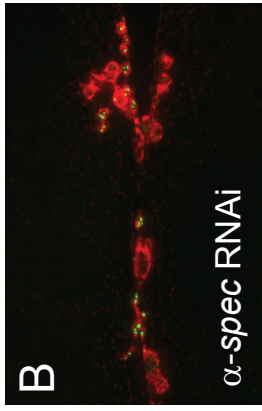
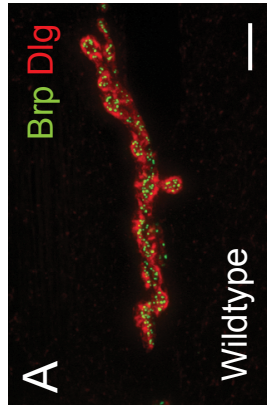


**Figure 2-6. Fos-MAPK signaling is induced following cytoskeletal disruption**

(A) Schematic diagram representing MAPK signaling that converges on Fos. Puckered (Puc) is shown as both a downstream target of Fos and Jun, as well as an upstream regulator of Fos and Jun activity through negative regulation of the upstream MAPK, Jun-Kinase (JNK). (B) Representative Western Blot lanes and corresponding quantification for different genotypes. Images show bands for Dfos and the corresponding loading control for those lanes (tubulin or actin). Quantification shows average Fos protein levels normalized to loading control levels. Fos band intensity for each lane was normalized to the loading control band intensity for the same lane. Fos protein is decreased by 50% in *kay*<sup>1/+</sup> animals, confirming the specificity of the antibodies (data is aggregated from two different experiments with different anti-Fos antibodies). Wt (top) = *w*<sup>1118</sup> (6 CNS total). *kay*<sup>1/+</sup> (6 CNS total). Wt (bottom) = *w*<sup>1118</sup> (12 CNS total). *α-spec* RNAi = *elav*<sup>C155</sup>-GAL4/+; 2x UAS-*α-spectrin*-dsRNA (12 CNS total). (C,D) puckered reporter is induced in the CNS in animals lacking presynaptic *α*-Spectrin. (C) Beta-gal levels are quantified in wildtype animals, *kay*<sup>1/+</sup> animals, and animals lacking presynaptic *α*-Spectrin. WT = *puc*<sup>A251.1F3/+</sup> (6 animals). *kay*<sup>1/+</sup> = *kay*<sup>1/puc</sup><sup>A251.1F3</sup> (3 animals). *α-spec* RNAi = *elav*<sup>C155</sup>-GAL4/+; *puc*<sup>A251.1F3/+</sup>; 2x UAS-*α-spectrin*-dsRNA (6 animals). (D) Representative images of ventral nerve cords stained with an antibody against Beta-gal to visualize expression of the puckered reporter in the CNS of a wildtype animal and an animal lacking pre-synaptic *α*-Spectrin. (E,F) Representative Western Blot lanes (E) and corresponding quantification (F) for control and nocodazole-treated animals. Images show bands for Dfos and the corresponding loading control for those

lanes (tubulin). Quantification shows average Fos protein levels normalized to loading control levels. Fos band intensity for each lane was normalized to the loading control band intensity for the same lane. Quantification shows a greater than 2-fold increase in Fos protein after 30min nocodazole incubation. All animals = *w<sup>1118</sup>* (30min: control n = 3 trials/15 CNS total, nocodazole n = 3 trials/15 CNS total; 2hr control n = 4 trials/20 CNS total, nocodazole n = 5 trials/25 CNS total). Error bars represent SEM; P-values were determined using Student's t-test: \* $p < 0.05$ , \*\* $p < 0.01$ , \*\*\* $p < 0.001$ . Scale bar = 20 $\mu$ m.

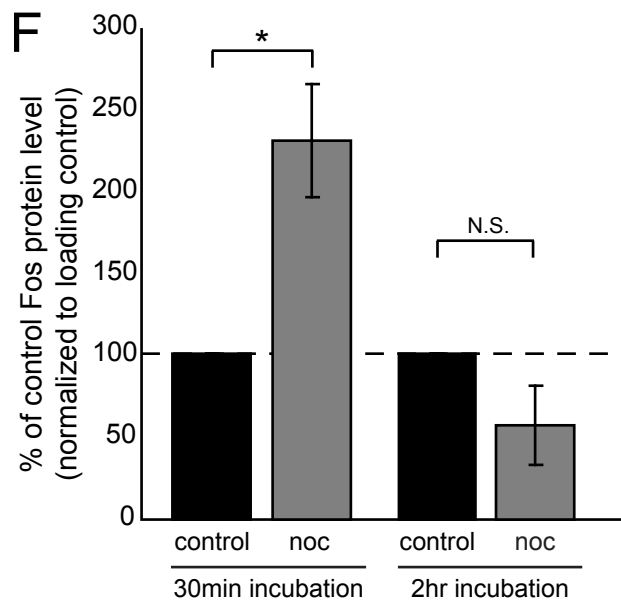
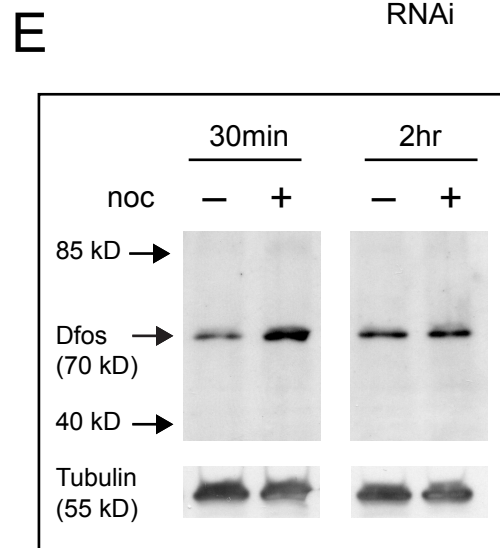
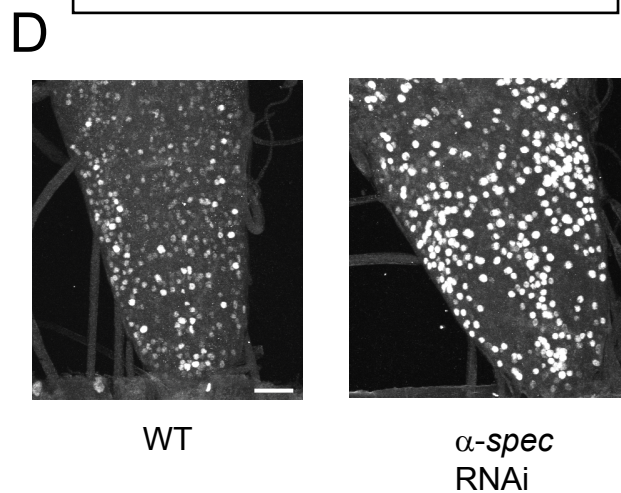
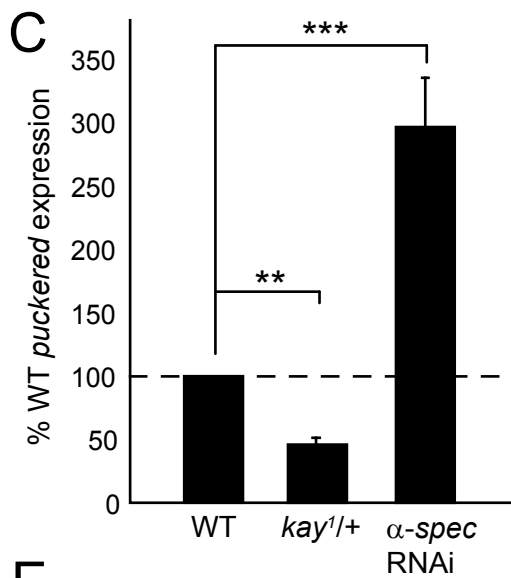
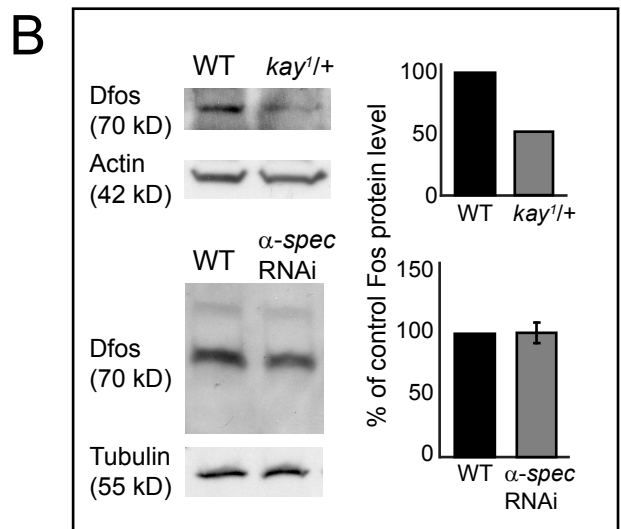
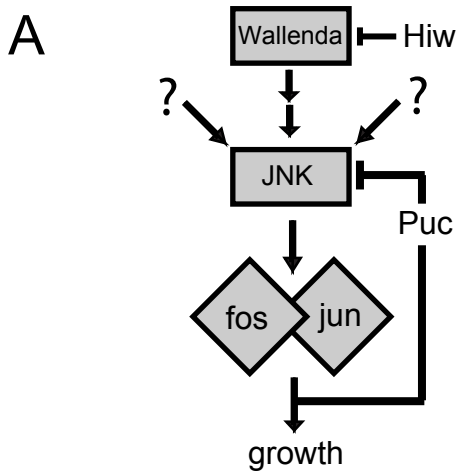




### Figure 2-7. Loss of Puckered suppresses synaptic instability at the NMJ

(A-D) Representative images of muscle 6/7 NMJs stained for the presynaptic active zone protein Brp (green) and postsynaptic Dlg (red). (A) A control NMJ. (B) An NMJ from a larva with mutations in puckered ( $puc^1/puc^{A251.1F3}$ ) shows maintenance of this apposition of pre- and postsynaptic markers. (C) An NMJ lacking presynaptic  $\alpha$ -Spectrin shows a severe retraction (arrowheads). (D) This phenotype is suppressed in puckered mutants. (E,F) Quantification of retraction frequency (E) is measured as the average % of NMJs with  $>1$  or  $>7$  boutons retracted. Retraction severity (F) is measured as the number of boutons retracted per NMJ and the data are plotted as a cumulative frequency histogram for each genotype. control = 1x UAS- $\alpha$ -spectrin-dsRNA (no GAL4) (n = 39 NMJs/4 animals).  $puc^1/puc^{A251}$  control = 1x UAS- $\alpha$ -spectrin-dsRNA;  $puc^1/puc^{A251.1F3}$  (no GAL4) (n = 97 NMJs/10 animals).  $\alpha$ -spec RNAi =  $elav^{C155}$ -GAL4/+ or  $elav^{C155}$ -GAL4/Y; 1x UAS- $\alpha$ -spectrin-dsRNA (n = 96 NMJs/10 animals).  $\alpha$ -spec RNAi;  $puc^1/puc^{A251}$  =  $elav^{C155}$ -GAL4/+; 1x UAS  $\alpha$ -spectrin-dsRNA;  $puc^1/puc^{A251.1F3}$  (n = 136 NMJs/14 animals). Error bars represent SEM; P-values for retraction frequency were determined using one-way ANOVA with post-hoc Tukey-Kramer; P-values for retraction severity were determined using a Kruskal-Wallis test with a post-hoc Dunn's test for multiple comparisons: \*p<0.05, \*\*p<0.01, \*\*\*p<0.001. Statistical differences remain when comparisons are made using Student's t-test. Scale bar = 10 $\mu$ m.

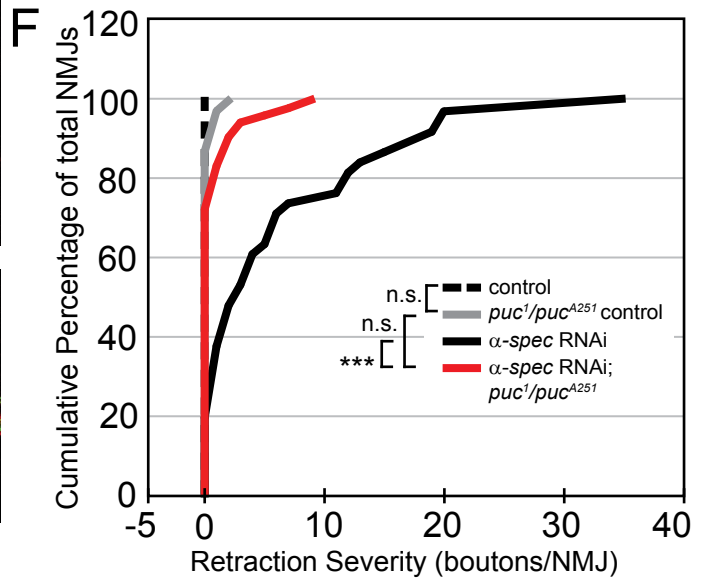
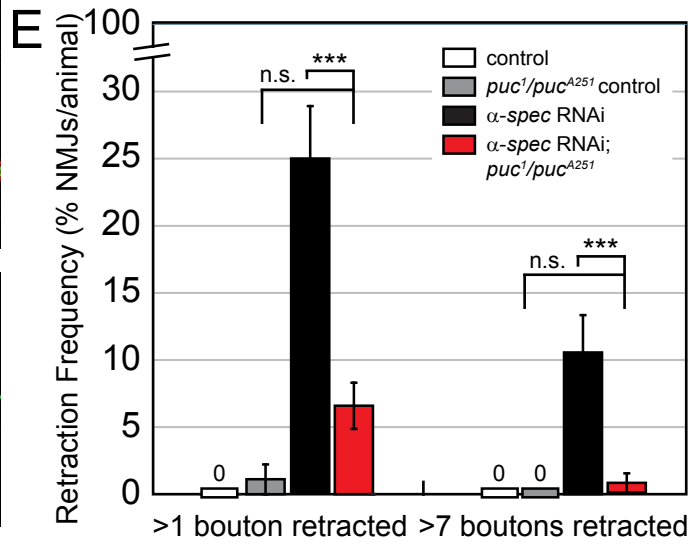
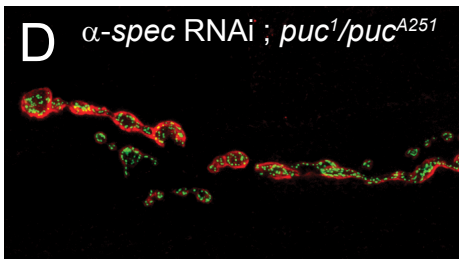
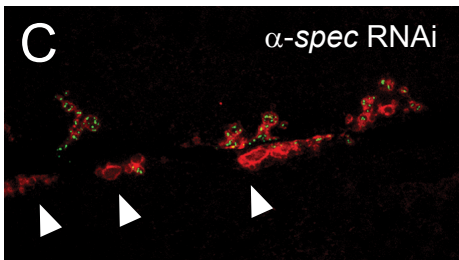
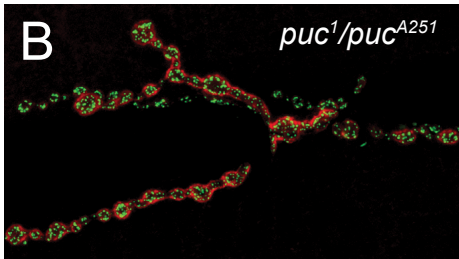
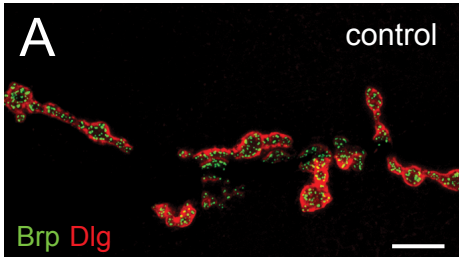


## Figure 2-8. Highwire mutation suppress synaptic instability at the NMJ

(A-D) Representative images of muscle 6/7 NMJs stained for the presynaptic active zone protein Brp (green) and postsynaptic Dlg (red). (A) A wildtype NMJ. (B) An NMJ lacking presynaptic  $\alpha$ -Spectrin shows a large retraction, encompassing an entire branch (arrowhead). (C)  $hiw^{ND9}$  NMJs show altered morphology and overgrowth, but they maintain apposition of pre- and postsynaptic markers and do not show a substantial amount of retractions (2x magnification of boxed region is shown below). (D) Presynaptic expression of UAS- $\alpha$ -spec-dsRNA in homozygous  $hiw^{ND9}$  mutants results in a much abrogated frequency and severity of synaptic retractions as compared to expression in a wildtype background.  $hiw^{ND9}$  NMJs that lack presynaptic  $\alpha$ -Spectrin show a characteristic  $hiw^{ND9}$  morphology and maintain good apposition of pre- and postsynaptic markers (2x magnification of boxed region is shown below). (E,F) Quantification of retraction frequency (E) is plotted as the average % of NMJs with >1 or >7 boutons retracted. Retraction severity (F) is measured as the number of boutons per NMJ that are retracted and the data are plotted as a cumulative frequency histogram for each genotype. WT =  $w^{1118}$  (n = 70 NMJs/7 animals).  $hiw^{ND9}$  =  $hiw^{ND9}/hiw^{ND9}$  or  $hiw^{ND9}/Y$  (n = 65 NMJs/7 animals).  $\alpha$ -spec RNAi =  $elav^{C155}$ -GAL4/+ or  $elav^{C155}$ -GAL4/Y; 2x UAS- $\alpha$ -spectrin-dsRNA (n = 182 NMJs/19 animals).  $hiw^{ND9}/+$ ;  $\alpha$ -spec RNAi; =  $elav^{C155}$ -GAL4,  $hiw^{ND9}/+$ ; 2x UAS- $\alpha$ -spectrin-dsRNA (n = 106 NMJs/11 animals).  $hiw^{ND9}$ ;  $\alpha$ -spec RNAi; =  $elav^{C155}$ -GAL4,  $hiw^{ND9}/Y$ ; 2x UAS- $\alpha$ -spectrin-dsRNA (n = 149 NMJs/15 animals). Error bars represent SEM; P-values for retraction frequency were determined using one-way ANOVA with post-hoc Tukey-Kramer; P-values for

retraction severity were determined using a Kruskal-Wallis test with a post-hoc Dunn's test for multiple comparisons: \* $p < 0.05$ , \*\* $p < 0.01$ , \*\*\* $p < 0.001$ . Statistical differences remain when comparisons are made with Student's t-test. Scale bar = 10 $\mu$ m.

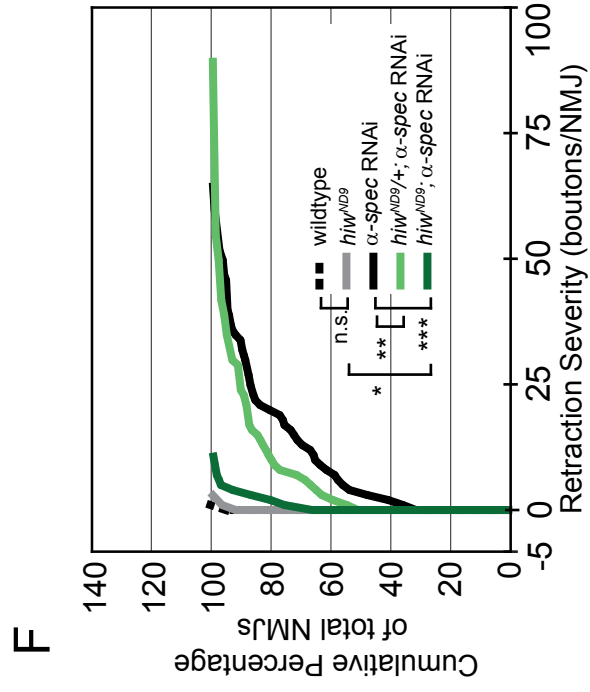
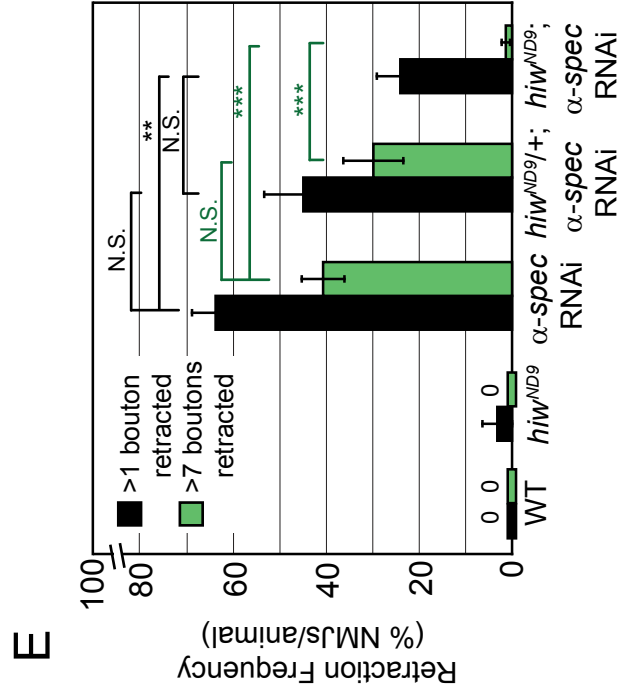
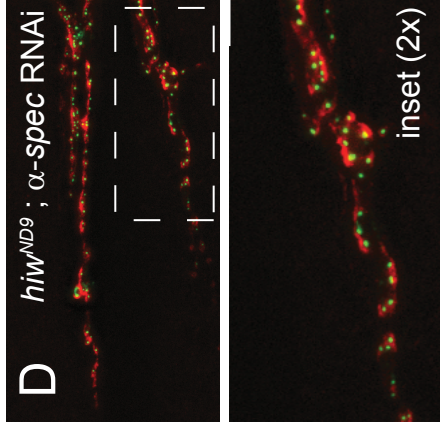
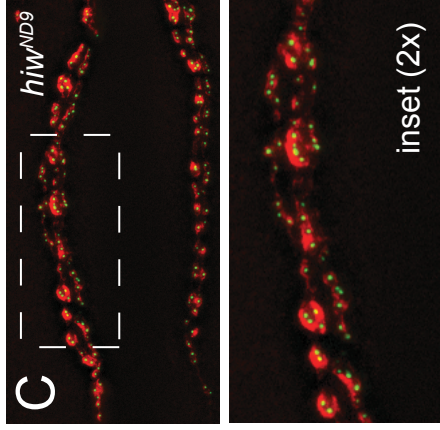
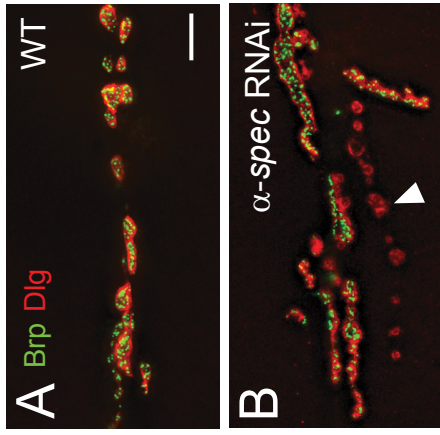
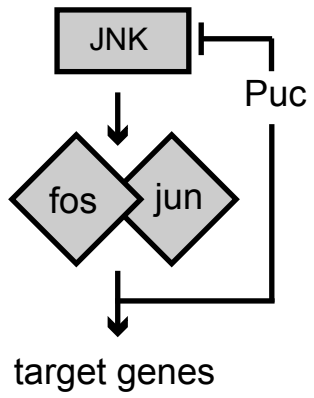


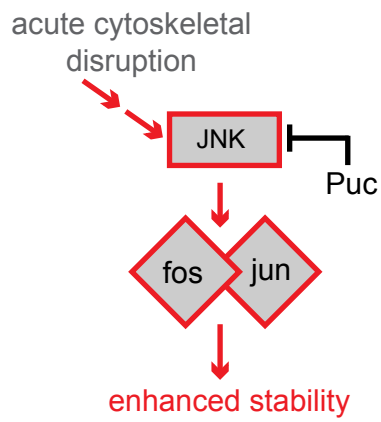
**Figure 2-9. Model for synapse stabilizing effects of MAPK signaling**

(A-C) Effects of stress on MAPK signaling. (A) In the absence of cellular stress this JNK-Fos pathway is at steady state (shown in black) and is not necessary for endogenous synapse stability. (B) Acute cellular stress (e.g. cytoskeletal disruption) induces activation (shown in red) of JNK and Fos which enhances synapse stabilization. The elevation of Fos is transient. (C) In the presence of a persistent cellular stress, negative feedback via the phosphatase Puckered prevents re-activation of Fos and the neuron switches toward a state that favors disassembly or instability. (D-F) Experimental manipulations (shown in blue) that result in enhanced synapse stability in the presence of a persistent cellular stress. (D) Fos over-expression results in enhanced stability. (E) Loss of Puckered-dependent feedback inhibition promotes synapse stability, likely through enhanced Fos activity. (F) Loss of Highwire potentiates upstream MAPK signaling, acting through Fos to promote synapse stability.

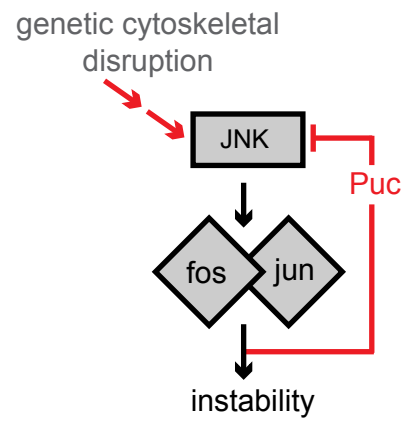
**A** NO STRESS



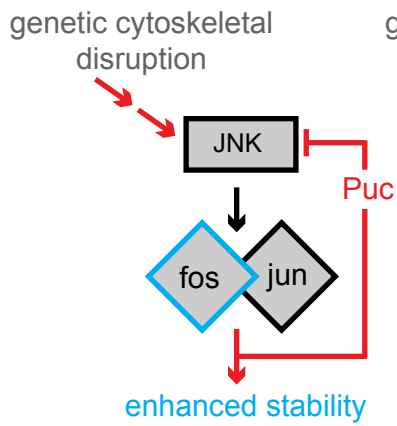
**B** ACUTE STRESS



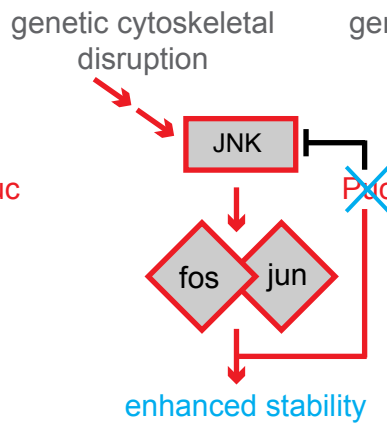
**C** PERSISTENT STRESS



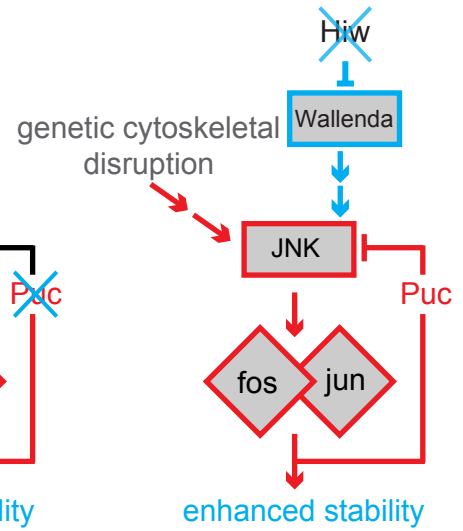
**D** PERSISTENT STRESS SUPPRESSION 1



**E** PERSISTENT STRESS SUPPRESSION 2



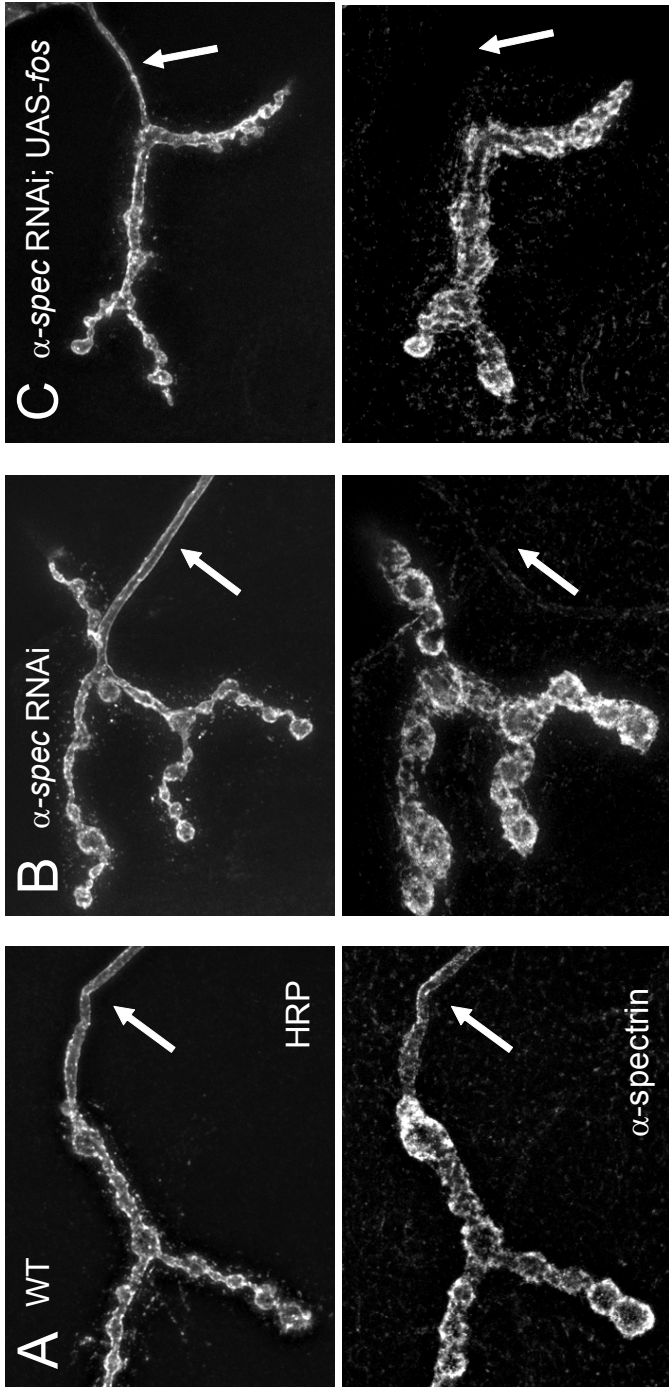
**F** PERSISTENT STRESS SUPPRESSION 3



**Supplemental Figure 2-1. Overexpression of Fos does not increase presynaptic  $\alpha$ -Spectrin levels**

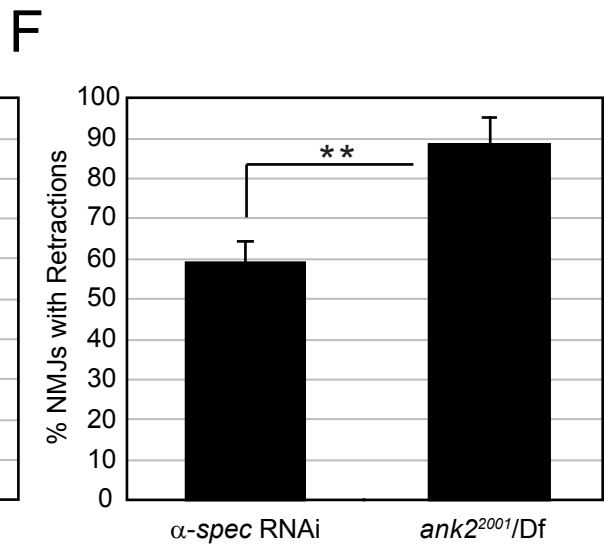
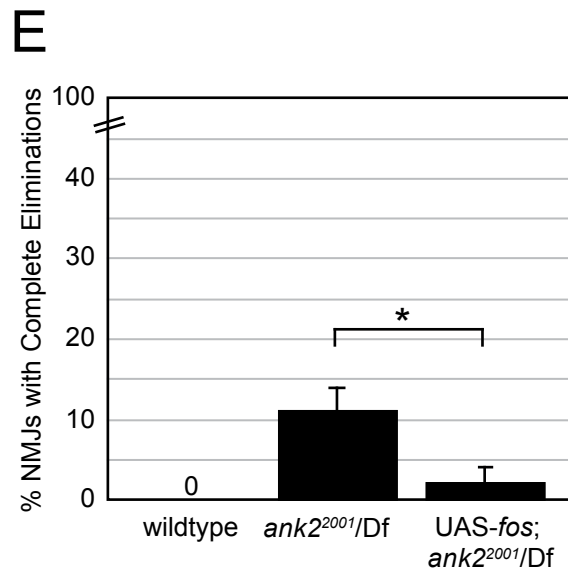
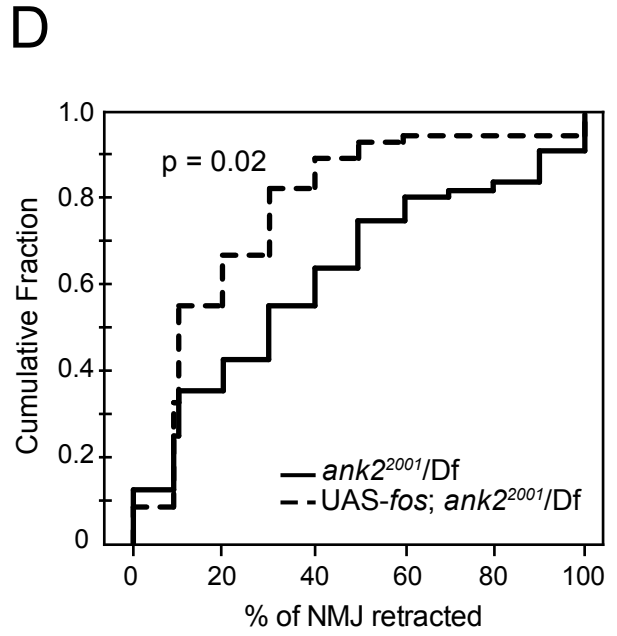
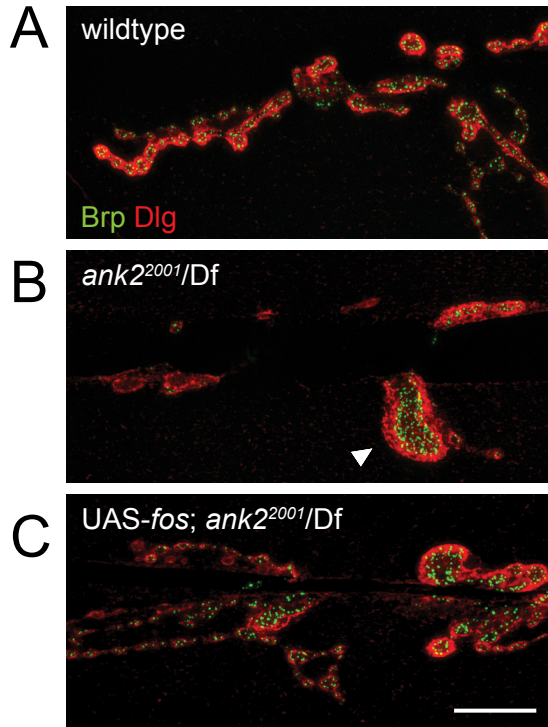
(A-C) Representative images of muscle 4 stained for the presynaptic membrane marker HRP (top panel) and  $\alpha$ -Spectrin protein (bottom panel). Efficiency of the  *$\alpha$ -spectrin*-dsRNA can be seen by the loss of  $\alpha$ -Spectrin immunoreactivity presynaptically in the nerve (arrow). (A) Image of a wildtype animal with  $\alpha$ -Spectrin expression visible both in the muscle and innervating axon (as visualized by HRP; arrow). (B) Expression of UAS- *$\alpha$ -spectrin*-dsRNA eliminates  $\alpha$ -Spectrin staining in the motoneuron axon (arrow). (C) Presynaptic elimination of  $\alpha$ -Spectrin is not altered by concomitant presynaptic expression of UAS-*fos* (arrow). WT = *w<sup>1118</sup>*.  *$\alpha$ -spec* RNAi = *elav<sup>C155</sup>-GAL4/+; 2x UAS- $\alpha$ -spectrin*-dsRNA.  *$\alpha$ -spec* RNAi; UAS-*fos* = *elav<sup>C155</sup>-GAL4/+; 2x UAS- $\alpha$ -spectrin*-dsRNA; UAS-*fos*. Scale bar = 10 $\mu$ m.





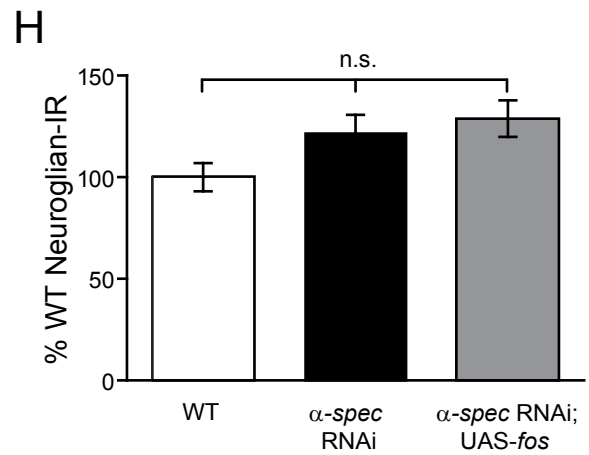
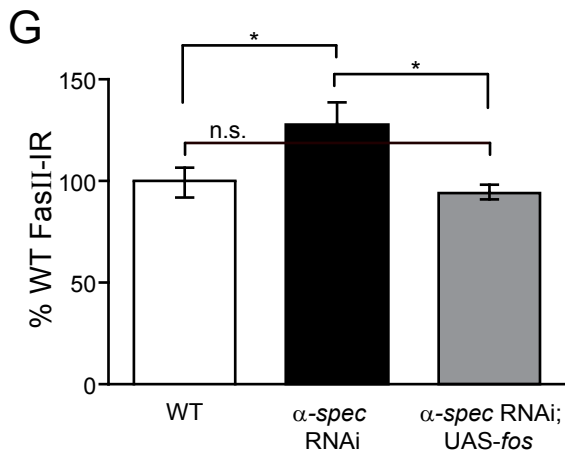
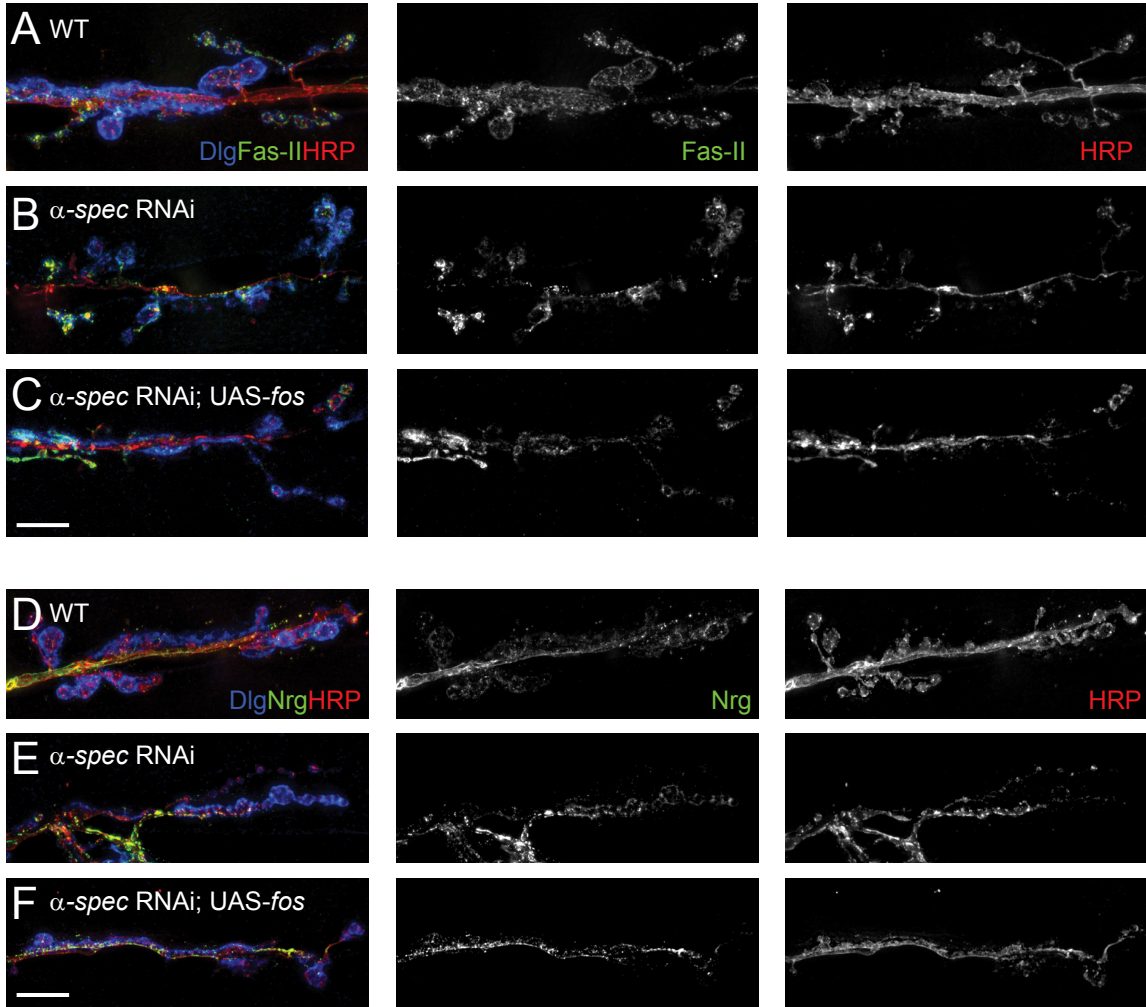
**Supplemental Figure 2-2. Overexpression of Fos suppresses synaptic instability due to *ank2* mutation**

(A-C) Representative images of muscle 6/7 NMJs stained for the presynaptic active zone protein Brp (green) and postsynaptic Dlg (red). (A) A wildtype NMJ shows Brp in apposition to Dlg throughout the NMJ. (B) An NMJ from an *ank2* mutant animal shows a large retraction and a clearly disrupted synapse morphology (arrowhead indicates an abnormally large bouton compartment), while less severe NMJ retraction and improved synapse morphology are seen when Fos is expressed presynaptically (C). A retraction is defined as an area of the NMJ where clearly defined postsynaptic Dlg staining is not apposed by presynaptic Brp staining. (D) Quantification of retraction phenotype is shown as a cumulative fraction histogram of the percentage of an NMJ that has undergone retraction. (E) The average number of complete eliminations (defined as an NMJ which lacks all presynaptic antigen, while maintaining a clear postsynaptic density) in *ank2* mutants is also significantly reduced by neuronal expression of Fos protein. (F) Retractions occur at a higher frequency in *ank2* mutant animals than in animals expressing presynaptic  *$\alpha$ -spec* RNAi. Wildtype =  $w^{1118}$ . *ank2<sup>2001</sup>/Df = ank2<sup>2001</sup>/Df(3L)RM5-2* (n = 56 NMJs/6 animals). UAS-*fos*; *ank2<sup>2001</sup>/Df = elav<sup>C155</sup>-GAL4/y*; UAS-*fos*; *ank2<sup>2001</sup>/Df(3L)RM5-2* (n = 58 NMJs/6 animals).  *$\alpha$ -spec* RNAi; UAS-*fos = elav<sup>C155</sup>-GAL4/+*; 2x UAS- *$\alpha$ -spectrin*-dsRNA (n = 135NMJs/14 animals). P-value for (D) was determined using a Kolmogorov-Smirnov Test. P-values for (E,F) were determined using a t-test: \*p<0.05, \*\*p<0.01, \*\*\*p<0.001; Error bars represent SEM. Scale bar = 10 $\mu$ m.



**Supplemental Figure 2-3. Over-expression of Fos does not upregulate cell adhesion proteins at the NMJ**

(A-C) Neuronal Fos expression does not upregulate levels of Fasciclin-II (Fas-II) at the NMJ. Representative images of muscle 6/7 NMJs stained for the presynaptic cell adhesion protein Fas-II (green), the presynaptic membrane marker HRP (red), and the postsynaptic scaffold protein Dlg (blue). Single channel images are shown for Fas-II (middle column) and HRP (right column). (A) A wildtype NMJ shows normal presynaptic Fas-II staining. (B,C) In animals lacking presynaptic  $\alpha$ -Spectrin, co-expression of UAS-*fos* does not result in increased Fas-II staining at the NMJ. (D-F) Representative images of muscle 6/7 NMJs stained for Nrg (green), the presynaptic membrane marker HRP (red), and the postsynaptic scaffold protein Dlg (blue). Single channel images are shown for Nrg (middle column) and HRP (right column). (F) A wildtype NMJ shows normal presynaptic Nrg staining. (D,E) In animals lacking presynaptic  $\alpha$ -Spectrin, co-expression of UAS-*fos* does not result in increased Nrg staining at the NMJ. (G,H) Fas-II and Nrg staining is quantified. WT =  $w^{1118}$  (n = 5 NMJs/3 animals).  $\alpha$ -*spec* RNAi = *elav<sup>C155</sup>-GAL4/+; 2x UAS- $\alpha$ -spectrin-dsRNA* (n = 5 NMJs/3 animals).  $\alpha$ -*spec* RNAi; UAS-*fos* = *elav<sup>C155</sup>-GAL4/+; 2x UAS- $\alpha$ -spectrin-dsRNA; UAS-*fos** (n = 5 NMJs/3 animals). Error bars represent SEM; P-values were determined using one-way ANOVA with post-hoc Tukey Kramer: \*p<0.05, \*\*p<0.01, \*\*\*p<0.001. Scale bar = 10 $\mu$ m.



# Chapter 3:

Fos is Required to Maintain Synaptic Stability at the  
Drosophila Neuromuscular Junction

## INTRODUCTION

We have shown that synapse degeneration following loss of presynaptic  $\alpha$ -Spectrin can be slowed or suppressed via multiple genetic manipulations that increase Fos protein or potentiate upstream MAPK signaling. Additionally, our data show that MAPK-Fos signaling is activated endogenously in response to microtubule disruption and/or neuronal injury. These data are consistent with Fos activity playing a role in maintaining normal NMJ stability during development. However, we sought to show this more directly by impairing Fos function presynaptically and then assaying NMJ stability.

Null mutations in *fos* are embryonic lethal (Riesgo-Escovar and Hafen, 1997; Zeitlinger et al., 1997). Therefore, we disrupted neuronal Fos signaling by expressing a previously published dominant negative Fos transgene (UAS-*fos*<sup>DN</sup>) (Ciapponi et al., 2001; Collins et al., 2006; Eresh et al., 1997; Riese et al., 1997; Sanyal et al., 2002; Szuts and Bienz, 2000). This transgene expresses only the DNA binding and dimerization domains of Fos and has been shown to cause defects in diverse developmental contexts that phenocopy the *fos* mutations (Ciapponi et al., 2001; Szuts and Bienz, 2000; Zeitlinger et al., 1997). At the NMJ UAS-*fos*<sup>DN</sup> expression has been shown to disrupt both NMJ growth and function, demonstrating that this transgene can have effects at the NMJ (Sanyal et al., 2002). We find that neuronal expression of UAS-*fos*<sup>DN</sup> drastically impairs synapse stability at the *Drosophila* NMJ. We also asked whether Fos functions in concert with Jun in the AP1 complex to control synapse stability. To do so we over-expressed a similar dominant negative Jun transgene (UAS-*jun*<sup>DN</sup>). Neuronal expression of this transgene has been previously shown to disrupt both NMJ growth and function

with similar efficiency to that observed when UAS-*fos*<sup>DN</sup> is expressed neuronally (Sanyal et al., 2002). However, we do not see a similar impairment of NMJ stability when UAS-*jun*<sup>DN</sup> is expressed presynaptically.

Lastly, we sought to determine whether the role Fos plays in regulating NMJ stability extends to a more general role in regulating overall motoneuron health. We assayed two measures of motor function as well as viability in adult animals expressing UAS-*fos*<sup>DN</sup> neuronally. We find that motor function and overall organismal health, as measure by viability, are both significantly impaired when Fos function is disrupted. These data suggest that Fos plays a broad role in promoting motoneuron health, both during NMJ development and in the adult animal.

## **RESULTS**

### **Fos activity is necessary for synapse stability**

Expression of UAS-*fos*<sup>DN</sup> in neurons results in a dramatic increase in synapse retraction frequency and severity (Figure 3-1A, B, C, E). These data demonstrate that Fos activity is necessary for synapse stability at the *Drosophila* NMJ. Expression of UAS-*jun*<sup>DN</sup> in neurons results in only a slight, but statistically significant, increase in synapse retraction frequency compared to wild type (Figure 3-1C,E). However, retraction severity is not significantly different from wild type. Furthermore, the phenotype of synapse retraction is far less severe than that observed following UAS-*fos*<sup>DN</sup> expression (Figure 3-1E). It is possible that differences in the levels of expression of these transgenic proteins contribute to the observed difference in synapse stability. However, these transgenes have been



shown to function comparably in other contexts (Sanyal et al., 2002; Zeitlinger et al., 1997), and the effect of these constructs on synaptic growth is repeated here (Supplemental Figure 3-1). Therefore, an alternate possibility is that Fos has a Jun-independent function during synapse stability. Fos is transcriptionally active in the absence of Jun (Perkins et al., 1990) and a Jun-independent function for Fos during *highwire*-dependent NMJ overgrowth has been suggested (Collins et al., 2006; Perkins et al., 1990). Interestingly, expression of UAS-*fos*<sup>DN</sup> does not cause an obvious disorganization of synaptic MTs or an accumulation of Futsch staining in presynaptic swellings, as is seen in *α-spectrin* RNAi animals (Figure 3-1D), suggesting that Fos does not promote synapse stability by influencing the integrity or organization of the presynaptic MT cytoskeleton.

In an effort to further analyze the role of Fos in NMJ stability during normal development, we also analyzed a heterozygous *fos* null mutant (*kayak*<sup>1/+</sup>) and a hypomorphic *fos* mutant (*kayak*<sup>2</sup>). The heterozygous null mutants survive to be normally sized third instar larvae and we find no change in synapse stability compared to wildtype (Figure 3-1E). The hypomorphic *fos* mutants survive until mid-larval stages, so we assayed NMJ stability at the second instar stage and found no evidence of NMJ degeneration (Figure 3-1E). However, we have previously shown that NMJ degeneration following loss of *ankyrin2-L* is a progressive process such that second instar animals show relatively few retractions and retraction frequency increases significantly over the ensuing two days of larval development (Pielage et al., 2008). Therefore, we aged second instar *fos* hypomorphic mutants for an additional three days before assaying the

NMJ for degeneration. The *fos* hypomorphic mutants survive for at least three days as growth arrested second instar larvae. Again, we found no evidence of NMJ degeneration in aged second instar *fos* mutant larvae (data not shown). These data seem to contradict the Fos<sup>DN</sup> data, which indicates a critical role for Fos in maintaining baseline NMJ stability. However, it remains possible that low levels of Fos activity are sufficient for synapse stability or that NMJ disassembly occurs only during the late stages of larval neuromuscular growth and development.

### **Impaired Fos activity causes a progressive motor deficit and decreased viability**

The demonstration that expression of UAS-*fos*<sup>DN</sup> causes NMJ degeneration suggests that expression of this transgene could cause behavioral deficits and decreased viability in the adult system. To our surprise, we find that adults expressing UAS-*fos*<sup>DN</sup> in the nervous system throughout development hatch as normally behaving adults that are capable of flight. However, there is an obvious and progressive decay in the motor behavior of these animals. Initially, animals that neuronally express UAS-*fos*<sup>DN</sup> (GAL4; UAS-*fos*<sup>DN</sup>) are able to transition to the wall of a vial with a latency comparable to that observed in wild type (Figure 3-2A). However, this behavior significantly deteriorates compared to wild type over a one-week period (Figure 3-2A). We do not see a similar deterioration of motor behavior in animals that neuronally express UAS-*jun*<sup>DN</sup>, a genetic condition that does not result in synapse retraction (Figure 3-2A). In the same experiment, we also scored motor behavior in control flies harboring either a neuronal GAL4 or UAS-*fos*<sup>DN</sup> transgene, but not both. Neither of these genotypes showed any behavioral impairments

when compared to WT (Figure 3-2A). Animals neuronally expressing UAS-*fos*<sup>DN</sup> were significantly different (by Mann-Whitney test) than all other populations tested (  $p < 0.01$  compared to GAL4 control;  $p < 0.001$  compared to WT, UAS-*fos*<sup>DN</sup> control, and neuronal UAS-*jun*<sup>DN</sup>). This progressive motor impairment in animals neuronally expressing *fos*<sup>DN</sup> is also evident when examining wing posture. Animals with neuronal expression of the UAS-*fos*<sup>DN</sup> transgene initially hold their wings in a posture which is only slightly impaired when compared to wild type (Figure 3-2B). However, after 7-14 days, the majority of these animals have severely perturbed wing posture consistent with impaired motor function (Figure 3-2B). Together, these data demonstrate that expression of UAS-*fos*<sup>DN</sup> causes progressive motor impairment in adults.

Finally, we assessed the viability of animals that neuronally express the UAS-*fos*<sup>DN</sup> transgene. These animals hatch at an equivalent frequency to wild type when raised at room temperature. However, after one week ~40% of animals expressing UAS-*fos*<sup>DN</sup> have died, while 100% of wild type animals remain alive (Figure 3-2C). This difference becomes even greater by two weeks of age with greater than 60% of the UAS-*fos*<sup>DN</sup> animals having died, compared to 100% viability in the wild type population (Figure 3-2C). Thus, neuronal expression of UAS-*fos*<sup>DN</sup> not only causes cellular phenotypes that are consistent with models of motoneuron degenerative disease and progressive motor deficits, but also significantly decreases lifespan.

**Evidence that upstream Map Kinase signaling is not required for NMJ stability.**

Finally, we asked whether the MAPK-JNK signaling upstream of Fos is required to prevent synapse retraction at the NMJ during normal development. First, we over-expressed the phosphatase *puckered*, which has been shown to inhibit JNK activity in *Drosophila* (Dobens et al., 2001; Martin-Blanco et al., 1998; Ring and Martinez Arias, 1993). Overexpression of UAS-*puckered* has no effect on synapse stability (Figure 3-3). We also find no change in synapse stability in the *wallenda* (MAPKKK) mutant background or when a dominant negative JNK transgene is neuronally expressed (Figure 3-3). From these data we conclude that inhibition of this MAPK signaling pathway does not trigger an underlying neurodegenerative response. This is consistent with the observation that Wallenda protein levels are normally maintained at low steady state levels in *Drosophila* neurons through the activity of the ubiquitin proteasome system (Collins et al., 2006). This is also consistent with recent work in *C. elegans* where it has been shown that disruption of the homologous MAPK signaling system does not alter synapse stability (Hammarlund et al., 2009). Finally, we assayed Wnd protein levels, comparing wildtype and  $\alpha$ -Spectrin depleted-animals, examining both the ventral nerve cord and the NMJ. Wnd protein levels are kept low through the activity of the ubiquitin proteasome system and, therefore, increased Wnd function would be expected to correlate with increased Wnd protein (Collins et al., 2006). However, we did not find an induction of Wnd protein (data not shown). This suggests that cytoskeletal disruption induces a neuronal stress response that is independent or downstream of Wnd.

Thus, while activation of MAP Kinase signaling appears sufficient to activate Fos and suppress synapse retraction in animals that lack presynaptic  $\alpha$ -Spectrin, the

Wallenda-JNK signaling pathway is not necessary for synapse stability in a wild type animal. Based on these data we speculate that the Fos activity necessary for synapse stability in wild type animals does not depend on Wallenda-JNK signaling. However, hyper-activation of this signaling system is sufficient to stimulate Fos and suppress synapse retraction in a degenerative background.

## **DISCUSSION**

We have shown a critical role for Fos activity in maintaining NMJ stability during larval development. While the embryonic lethality resulting from null *fos* mutations precludes a perfect analysis of NMJ stability in the absence of Fos activity, we disrupted Fos function post-embryonically by expressing a dominant-negative *fos* transgene presynaptically. Neuronal expression of this transgene results in a very severe synapse retraction phenotype. The frequency and severity of NMJ retraction in animals expressing UAS-*fos*<sup>DN</sup> is surpassed only by the retraction phenotype seen in *spectrin* or *ankyrin* mutants. It is impressive that impairing the function of a transcription factor in the nucleus can have a destructive effect on the NMJ which rivals that seen when a key structural component of the presynaptic terminal is removed.

As is observed when Fos is overexpressed to suppress NMJ retractions, Fos's role in maintaining baseline NMJ stability appears to be downstream of the synaptic microtubule cytoskeleton. We cannot rule out the possibility that Fos is communicating with the cytoskeleton to monitor its integrity, but our data suggest that neuroprotective

signaling downstream of Fos is executed independently of signaling that would repair the synaptic microtubule cytoskeleton.

In addition to playing a role in maintaining normal NMJ stability, our data also show a role for Fos in maintaining adult motor function and organismal health. While we cannot directly link motor function in adults to NMJ stability in larvae, we can say that Fos has broad, behaviorally relevant effects on motoneuron and organismal health both during development and in adults.

## FIGURES

### Figure 3-1. Fos is critical for synaptic stability downstream of the NMJ cytoskeleton

(A-D) Representative images of muscle 6/7 NMJs stained for the presynaptic active zone marker nc82 (green) and postsynaptic Dlg (red). Presynaptic expression of UAS-*fos*<sup>DN</sup> results in severe retractions at the NMJ (C, D). (B) A single-channel image of nc82 immunoreactivity (same NMJ as (A)) reveals a complete absence of this presynaptic marker throughout most of the NMJ. (D) Presynaptic expression of UAS-*jun*<sup>DN</sup> results in a low frequency of mild retractions. (E) Representative images of muscle 6/7 NMJs stained for the microtubule associated protein Futsch (green; middle row) and the presynaptic protein Dap160 (red; bottom row). A wildtype NMJ (left column) shows characteristic Futsch staining in the presynaptic nerve. Presynaptic expression of UAS-*fos*<sup>DN</sup> (right column) does not appear to disrupt normal Futsch staining, consistent with the persistence of a stable microtubule population, even in the presence of severe NMJ instability. (F) Retraction frequency is quantified for multiple genetic manipulations of MAPK signaling. Quantification of retraction frequency (F) is measured as the average % of NMJs with >1 bouton retracted. Jun<sup>DN</sup> = *elav*<sup>C155</sup>-GAL4/+; UAS-*jun*<sup>DN</sup> (n = 95 NMJs/10 animals). Fos<sup>DN</sup> = *elav*<sup>C155</sup>-GAL4/+; UAS-*fos*<sup>DN</sup> (n = 119 NMJs/12 animals). *kay*<sup>1/+</sup> (n = 118 NMJs/12 animals). *kay*<sup>2</sup>(L2) (n = 72 NMJs/8 animals). Error bars represent SEM; P-values were determined using a t-test: \*p<0.05, \*\*p<0.01, \*\*\*p<0.001. Scale bar = 10µm.

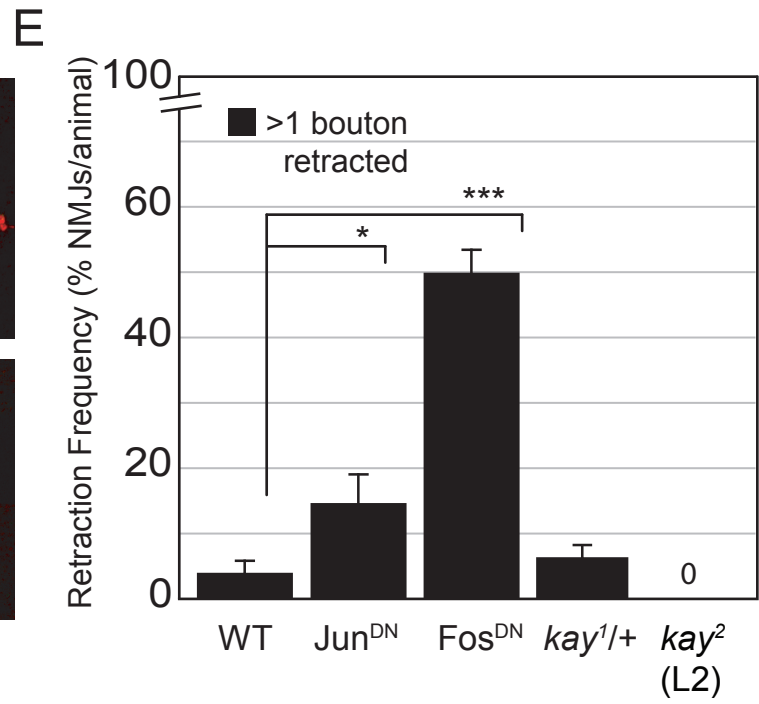
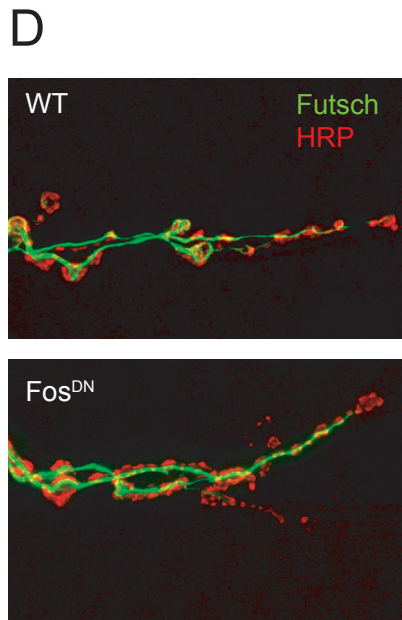
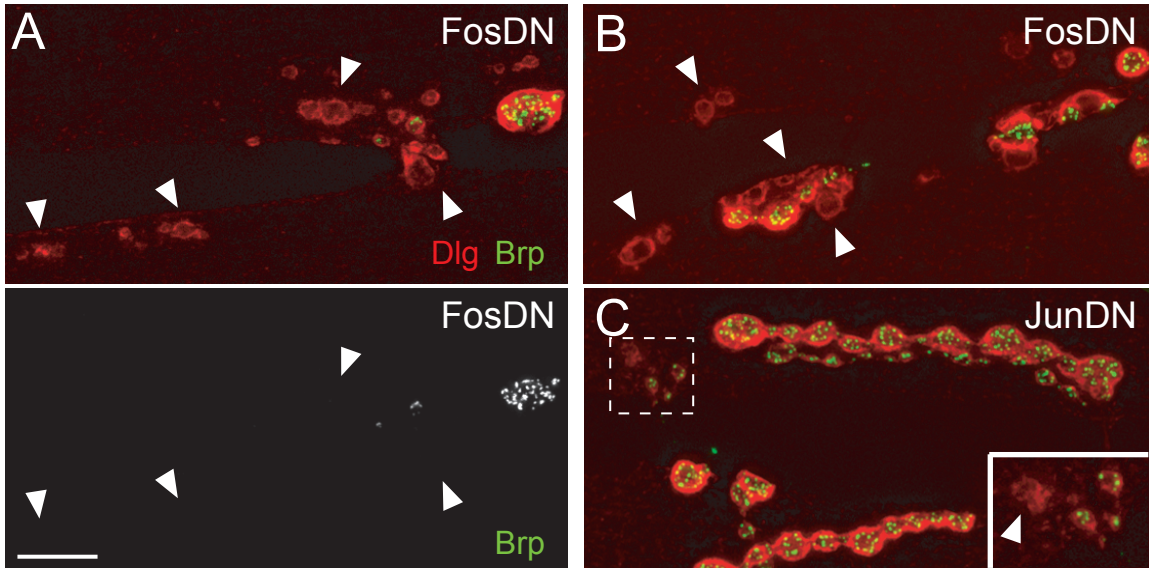
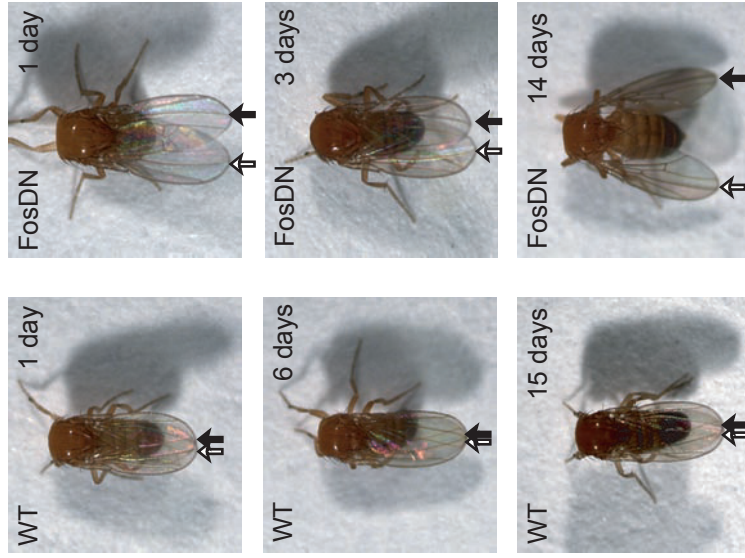


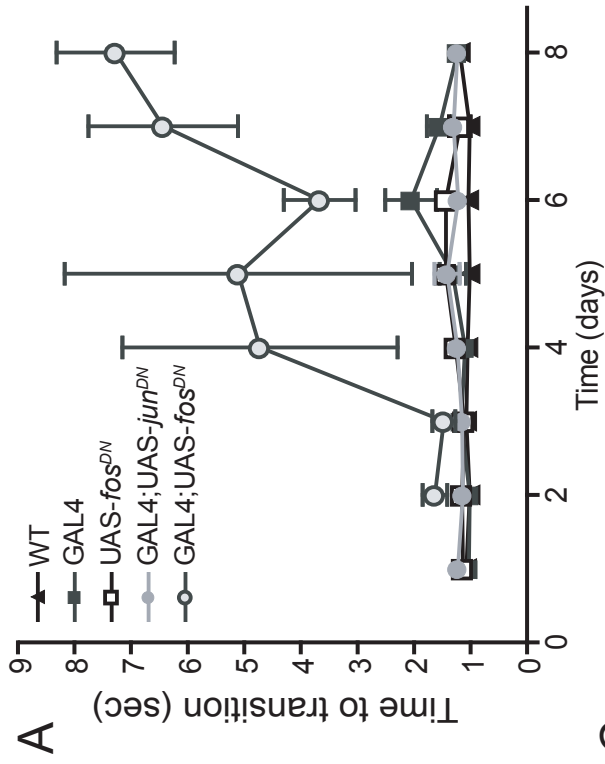


### Figure 3-2. Fos signaling regulates motor function and viability in adult flies

(A) Neuronal expression of a dominant negative *fos* transgene results in a progressive deterioration in motor function in adult flies. Data was collected for 7 days after eclosure, and motor ability was scored as the time required to transition from the bottom of a vial to the wall of a vial after being knocked down. Female flies were tested individually and three trials were conducted for each group on a given day. WT = w<sup>1118</sup> (n = 18 animals). GAL4 = *elav*<sup>C155</sup>-GAL4/+ (n = 20 animals). UAS-*fos*<sup>DN</sup> = UAS-*fos*<sup>DN</sup> (no GAL4; n = 20 animals). GAL4;UAS-*jun*<sup>DN</sup> = *elav*<sup>C155</sup>-GAL4/+; UAS-*jun*<sup>DN</sup> (n = 20 animals). GAL4;UAS-*fos*<sup>DN</sup> = *elav*<sup>C155</sup>-GAL4/+; UAS-*fos*<sup>DN</sup> (n = 19 animals). Error bars represent SEM. (B) Disruption of Fos signaling results in an inability to maintain wing posture. Wildtype flies (left column) show a characteristic wing posture which is maintained beyond the two week observation period (arrows point to the apexes of each wing). This posture is characterized by overlapping wings that are held parallel to the body axis. In contrast, *fos*<sup>DN</sup> flies (right column) are unable to maintain a similar wing posture during the two week period. After two weeks, the wings no longer overlap and they drop to either side of the animal, suggesting a loss of motor function required to maintain a rigid wing posture. WT = w<sup>1118</sup>. FosDN = *elav*<sup>C155</sup>-GAL4/Y; UAS-*fos*<sup>DN</sup>. (C) Neuronal expression of a dominant negative Fos transgene shortens lifespan. Lifespan was measured as the % of each population that was still alive at a given time point. The averages for 1 week and 2 weeks are shown. WT = w<sup>1118</sup> (n = 3 groups). Fos<sup>DN</sup> = *elav*<sup>C155</sup>-GAL4/Y; UAS-*fos*<sup>DN</sup> (n = 4 groups). Error bars represent SEM; P-values were determined using a t-test: \*p<0.05, \*\*p<0.01, \*\*\*p<0.001.



B



C

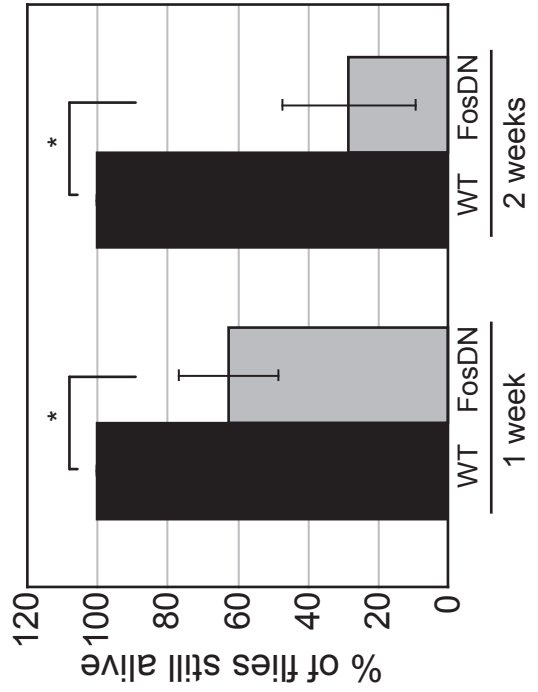
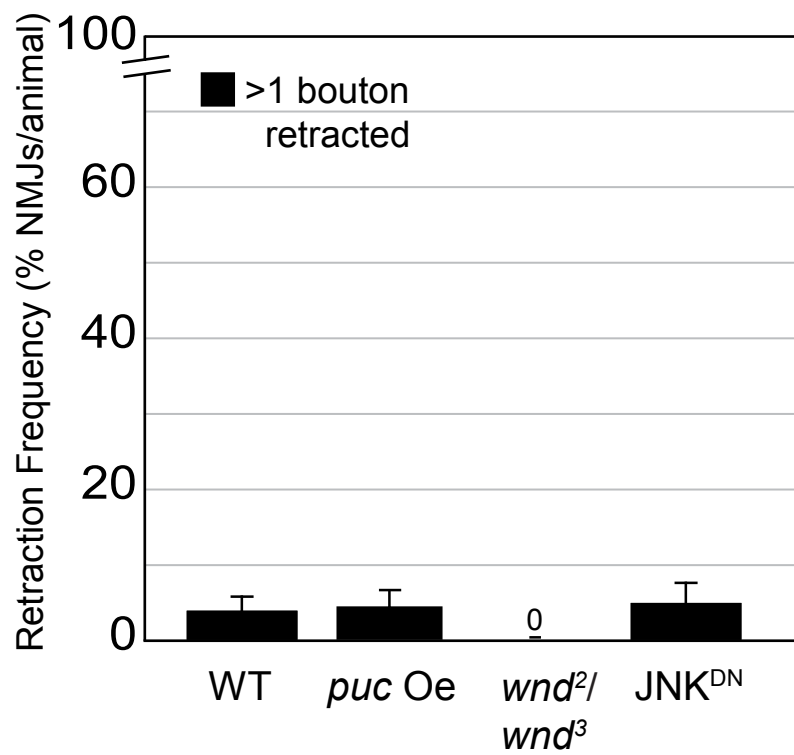


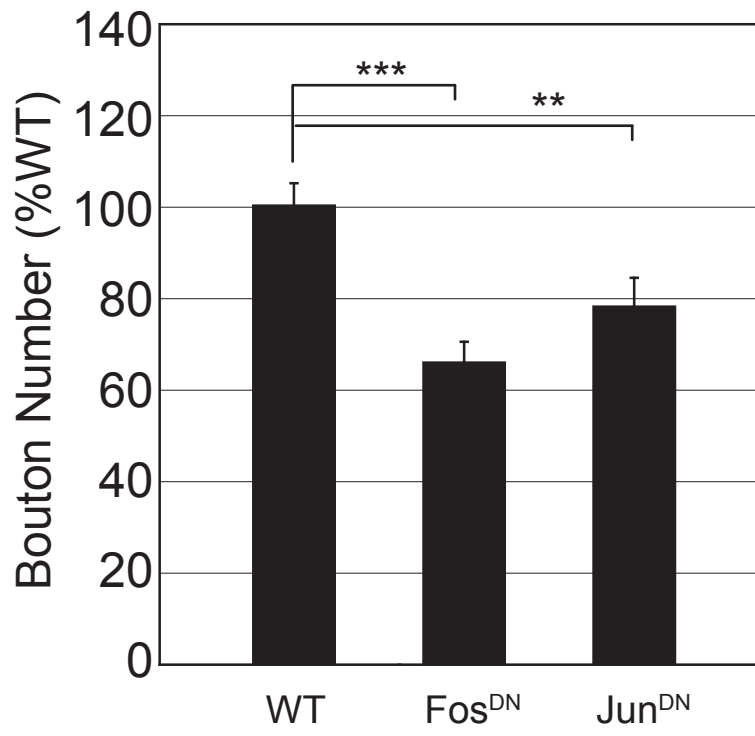
### **Figure 3-3. Upstream Wnd/JNK signaling is not required for stability**

Retraction frequency is quantified for multiple genetic manipulations of MAPK signaling. Quantification of retraction frequency is measured as the average % of NMJs with >1 bouton retracted. *puc* Oe = *elav*<sup>C155</sup>-GAL4/+; UAS-*puc* (n = 97 NMJs/10 animals). *wnd*<sup>2</sup>/*wnd*<sup>3</sup> (n = 105 NMJs/11 animals). *JNK*<sup>DN</sup> = *elav*<sup>C155</sup>-GAL4/+; UAS-*JNK*<sup>DN</sup> (n = 108 NMJs/11 animals). Error bars represent SEM. Neither one-way ANOVA nor Student's t-test determined any significant differences in mean retraction frequency between genotypes.



**Supplemental Figure 3-1. Dominant-negative Fos and Jun constructs both impair synaptic growth at the NMJ**

Bouton number is quantified for animals expressing dominant-negative constructs presynaptically. Quantification of retraction frequency is measured as the average number of type Ib boutons on segment A2, muscle 4. WT =  $w^{1118}$  (n = 16NMJs/8 animals). Jun<sup>DN</sup> = *elav<sup>C155</sup>-GAL4/+; UAS-jun<sup>DN</sup>* (n = 10 NMJs/5 animals). Fos<sup>DN</sup> = *elav<sup>C155</sup>-GAL4/+; UAS-fos<sup>DN</sup>* (n = 10 NMJs/5 animals). Error bars represent SEM; P-values were determined using a t-test: \*p<0.05, \*\*p<0.01, \*\*\*p<0.001..



# Chapter 4:

## MAPK-Fos Signaling and Axonal Transport

## INTRODUCTION

In *Drosophila*, disruption of axonal transport results in aberrant accumulation of synaptic proteins in the motor axons, which have been referred to as axonal blockages (Bowman et al., 2000; Horiuchi et al., 2007; Martin et al., 1999). These axonal protein accumulations result from mutations in both retrograde and anterograde motor proteins (Martin et al., 1999). The presence of axonal protein aggregates has been correlated with NMJ retraction in animals with impaired Dynein/Dynactin function and in animals with presynaptic expression of  *$\alpha$ -spectrin* RNAi (Eaton et al., 2002; Pielage et al., 2005).

Recent work has implicated MAPK signaling in axonal transport, suggesting that JNK-interacting proteins (JIPs) play a role in scaffolding MAPK signaling molecules to the axonal transport machinery, where they regulate attachment of vesicles to the motor protein (Bowman et al., 2000; Byrd et al., 2001; Horiuchi et al., 2005; Horiuchi et al., 2007). Both the MAPKKK, Wallenda, and the MAPKK, JNK, have been shown to be critical for preventing the formation of axonal blockages. Dominant-negative constructs for these proteins cause significant accumulation of synaptic proteins within axons. Therefore, we tested whether downstream Fos and Jun signaling also influence the presence of axonal protein aggregates. We find that overexpression of Fos protein or increased Fos activity is sufficient to clear axonal blockages in animals that lack presynaptic  *$\alpha$ -Spectrin*. We also find that impairment of Fos, but not Jun, signaling results in accumulation of synaptic proteins within axons, consistent with a role for Fos signaling in regulating axonal transport and/or signaling within the axonal compartment.



## RESULTS

### Fos activity prevents aberrant axonal protein aggregation

First, we confirmed that neuronal expression of  $\alpha$ -spectrin RNAi causes a dramatic increase in the accumulation of the active zone marker, Bruchpilot (Brp), within axons (Figure 4-1A). Next we show that expression of UAS-*fos* alone has no effect on axonal Brp aggregation (Figure 4-1A). Finally, we demonstrate that co-expression of UAS-*fos* with UAS- $\alpha$ -spectrin RNAi appears to diminish the appearance of accumulated Brp within the axon (Figure 4-1A). Similarly, mutation of the E3 Ubiquitin ligase Highwire, whose effects at the NMJ are mediated through Fos activity (Collins et al., 2006), also significantly decreases the number of axonal Brp aggregates (Figure 4-1B,C). Lastly, we find that neuronal expression of UAS-*fos*<sup>DN</sup> causes a striking increase in axonal accumulation of Brp (Figure 4-1D, top row), synaptotagmin (Figure 4-1D, bottom row), and cysteine string protein (not shown). As with the control of synapse stability, this effect appears specific to UAS-*fos*<sup>DN</sup> expression since expression of UAS-*jun*<sup>DN</sup> does not cause axonal protein aggregates. Thus, Fos activity is sufficient to suppress axonal protein aggregation following  $\alpha$ -Spectrin knockdown and, when inhibited, causes axonal protein aggregates in an otherwise wild type background.

## DISCUSSION

It is remarkable that UAS-*fos*<sup>DN</sup> expression causes axonal protein aggregates since this phenotype is generally associated with mutations in the axonal transport machinery (Eaton et al., 2002; Horiuchi et al., 2007; Martin et al., 1999). However, data presented

here dissociates, for the first time, the presence of axonal protein aggregates and synapse retraction at the NMJ. The expression of UAS-*JNK<sup>DN</sup>* has been shown to cause axonal protein aggregates in *Drosophila* (Horiuchi et al., 2007) consistent with a role for JNK interacting proteins in axonal transport in both worms and flies (Bowman et al., 2000; Byrd et al., 2001; Horiuchi et al., 2005; Horiuchi et al., 2007). However, UAS-*JNK<sup>DN</sup>* does not cause synapse retraction. Furthermore, *wallenda* mutations cause axonal protein aggregates (Horiuchi et al., 2007) but this same mutation does not cause synapse retraction.

Thus, axonal protein aggregation, or impaired axonal transport, is often associated with synapse retraction, but it does not appear to be sufficient to induce and execute disassembly of the presynaptic terminal. One possibility is that MAPK signaling upstream of Fos plays a dual role both as a regulator of axonal transport and as a key component of the signal that translates a neuronal insult into a degenerative program. In other words, JNK and Wallenda help to ensure that axonal transport runs smoothly, and in case things break down, they also signal back to the cell body to initiate a repair and/or disassembly program. If this model is correct, one would not predict axonal blockages in *wallenda* or *bsk* (JNK) mutants to translate into NMJ retractions, as the signaling between those processes has been disabled. This model also helps to explain a recent study from Aaron DiAntonio's group, in which they suggest that MAPK-JNK signaling is pro-degenerative (Miller et al., 2009). In this study, they show that mutation of *wnd* and/or pharmacological inhibition of JNK slows Wallerian degeneration resulting from axon transection or microtubule depolymerizing drugs. This result seems to be in conflict with

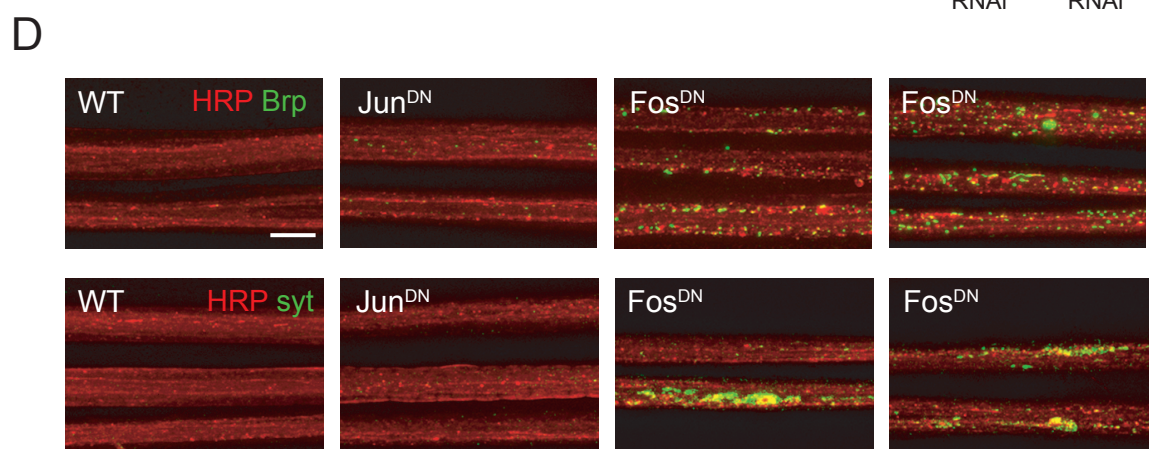
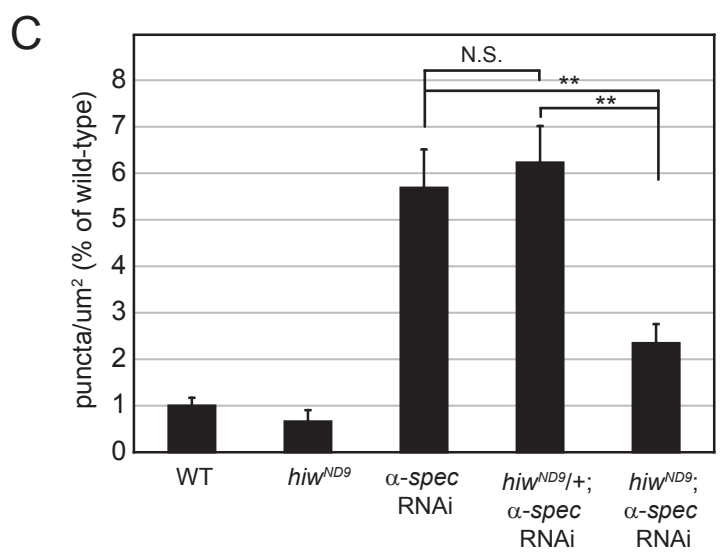
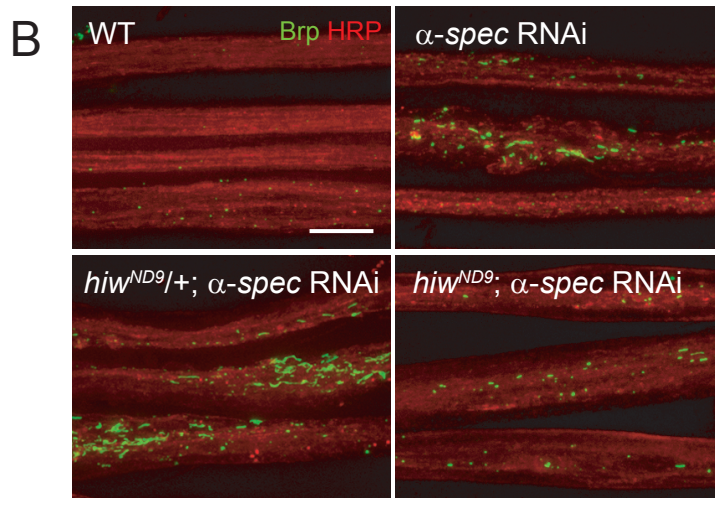
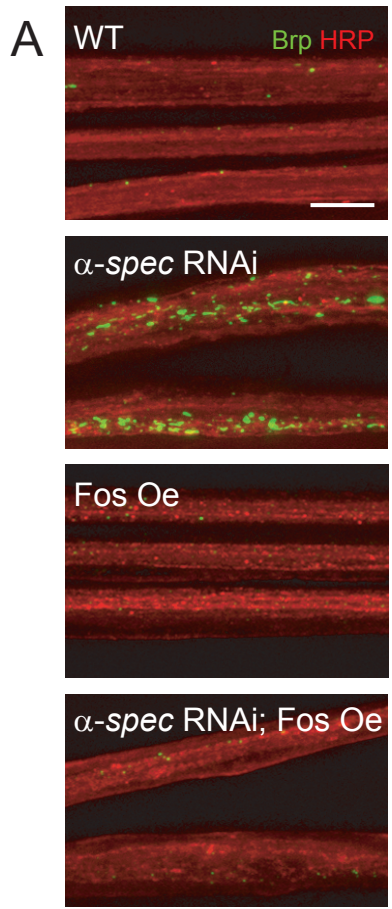
our data, which shows that MAPK-JNK signaling is neuroprotective. However, if this signaling pathway is indeed protective, but also plays a role in signaling the presence of a neuronal stress, removing key MAPK signaling molecules would prevent a neuronal insult from being translated into a active degenerative program. Understanding the exact nature of this signaling cascade and identifying key executors of the degenerative program at the presynaptic terminal are critical to parsing out the specifics of a link between axonal transport and NMJ stability.

## FIGURES

### Figure 4-1. MAPK-Fos signaling regulates accumulation of protein within axons

(A) Representative images of peripheral nerves from third instar larvae stained for the neuronal membrane marker HRP (red) and the presynaptic active zone marker Brp (green). While Brp immunoreactivity is low in wildtype animals and animals over-expressing presynaptic Fos (top two rows), animals lacking presynaptic  $\alpha$ -Spectrin (middle) show large aberrant accumulations of Brp staining within peripheral nerves. Concurrent presynaptic over-expression of Fos (bottom) eliminates accumulation of nc82 staining. (B) Representative images of peripheral nerves from third instar larvae stained for the neuronal membrane marker HRP (red) and the presynaptic active zone marker Brp (green). While Brp immunoreactivity is low in the axons of wildtype animals and *Hiw*<sup>ND9</sup> animals, animals lacking presynaptic  $\alpha$ -Spectrin show large aberrant accumulations of Brp staining within peripheral nerves. Removal of *Hiw* drastically decreases the accumulation of Brp staining within axons. (C) Brp puncta density is measured as the number of puncta per micron<sup>2</sup>. (D) Representative images of peripheral nerves from third instar larvae stained for the neuronal membrane marker HRP (red) and either the presynaptic active zone marker Brp (left column; green), or the presynaptic protein Synaptotagmin (right column; green). Only presynaptic expression of UAS-*fos*<sup>DN</sup> (bottom two rows) resulted in accumulation of synaptic proteins within peripheral nerves. This is consistent with a critical role for Fos in preventing aberrant accumulation of protein in the axons. wildtype = w<sup>1118</sup>.  $\alpha$ -*spec* RNAi = *elav*<sup>C155</sup>-GAL4/+; 2x UAS- $\alpha$ -*spectrin*-dsRNA.  $\alpha$ -*spec* RNAi; Fos Oe = *elav*<sup>C155</sup>-GAL4/+; 2x UAS- $\alpha$ -*spectrin*-dsRNA; UAS-

*fos*. Fos Oe = *elav*<sup>C155</sup>-GAL4/+; UAS-*fos*. Jun<sup>DN</sup> = *elav*<sup>C155</sup>-GAL4/+; UAS-*jun*<sup>DN</sup>. Fos<sup>DN</sup>  
= *elav*<sup>C155</sup>-GAL4/+; UAS-*fos*<sup>DN</sup>. Scale bar = 10μm.



# Conclusions

Our understanding of neurodegenerative disease has been significantly advanced by the identification of causal genetic mutations. However, for many neurodegenerative diseases such as amyotrophic lateral sclerosis (ALS), the majority of the disease is sporadic and of unknown cause. Furthermore, knowing the causal molecular perturbation does not necessarily suggest a pathway toward effective disease intervention. Recently, an alternate strategy has emerged. There is increasing evidence that the mechanisms of neurodegeneration include the activation of auto-destructive signaling systems. For example, the ubiquitin proteasome system (UPS) participates in the mechanisms of both developmental and insult-induced degeneration. Strikingly, inhibition of the UPS has been shown to slow both developmental axonal pruning and Wallerian type degeneration (DiAntonio et al., 2001; Hoopfer et al., 2006; Watts et al., 2003; Zhai et al., 2003). These data not only identify a fundamental process that appears to execute the elimination of neuronal structure, but highlights the potential power of interfering with auto-destructive signaling systems to slow the mechanisms of nervous system degeneration. This possibility is further supported by the identification and characterization of the *Wallerian degeneration slow* ( $Wld^S$ ) mutation in mice. In heterozygous  $Wld^S$  mice, transected or injured axons survive for 1-2 weeks, while similarly treated axons survive only a few days in wildtype mice (Parson et al., 1997). How  $Wld^S$  functions to slow degeneration is not clear. Indeed, the  $Wld^S$  mutation is effective in slowing Wallerian and other forms of insult-induced degeneration (Bommel et al., 2002; Ferri et al., 2003; Martin et al., 2002; Sajadi et al., 2004; Wang et al., 2001; Wang et al., 2002; Zhai et al., 2003; Zhai et al.,



2008), but it does not interfere with the mechanisms of developmental neuronal remodeling (Hoopfer et al., 2006). If neurodegenerative signaling systems include mechanisms of auto-destructive signaling, it may be possible to define the nature of these signaling systems using forward genetic approaches in *Drosophila*. This has been the goal of my dissertation. The ultimate goal will be to not only define the molecular players, but define how these signaling systems are controlled in order to uncover possible avenues for therapeutic intervention.

### **A model for the neuroprotective actions of Fos**

Taken together, our data argue that loss of presynaptic  $\alpha$ -Spectrin does not cause a simple structural collapse of the NMJ. Instead, we propose that the loss of presynaptic  $\alpha$ -Spectrin triggers a cellular response that may include the inhibition of a constitutively active, Fos signaling system. The inhibition of Fos signaling could then mediate a neurodegenerative response in two ways. One possibility is that loss of Fos activity de-represses an auto-destructive signaling pathway. In this scenario, UAS-*fos* over-expression would continue to repress this auto-destructive pathway despite the loss of presynaptic  $\alpha$ -Spectrin. This is based on current models of Wallerian-type degeneration where a rapid degeneration of distal neural processes is observed following nerve injury or transection. The demonstration that the rate of Wallerian degeneration can be substantially slowed in the *Wld<sup>S</sup>* mutant mouse is also consistent with the ability to repress an active process of neural degeneration (reviewed in (Luo and O'Leary, 2005)). It has been proposed that disruption of the axonal microtubule cytoskeleton may be the

perturbation that initiates Wallerian degeneration (Zhai et al., 2003). In this context, it is interesting that Fos rescues synapse stability and neuronal health but does not restore microtubule organization suggesting that Fos could act downstream of a signaling system triggered by microtubule disruption.

Another possibility is that inhibition of Fos signaling deprives the cell of a constitutive neuroprotective signaling pathway such as that found downstream of neurotrophic signaling. Indeed, Fos has been shown to be a target of TGF-beta signaling during *Drosophila* development (Riese et al., 1997; Riesgo-Escovar and Hafen, 1997; Zeitlinger et al., 1997). In this scenario, loss of  $\alpha$ -Spectrin would not only perturb the cell but also repress a protective neurotrophic response, resulting in degeneration. Among the constitutive neuroprotective functions of Fos would be the production of factors that actively prevent the accumulation of protein aggregates in axons since expression of UAS-*fos*<sup>DN</sup> causes axonal protein aggregation and overexpression of Fos protein protects against it.

Ultimately, we favor the hypothesis that Fos constitutively represses an active auto-destructive mechanism in the neuron. We find that UAS-*fos* expression rescues synapse stability, axonal protein aggregation and synaptic function to nearly wild type levels without causing overgrowth or any other evidence of a compensatory growth response. It seems unlikely that activation of a neurotrophic response mediated by Fos could achieve such precise preservation of neural function in the absence of presynaptic  $\alpha$ -Spectrin. Additionally, it will likely be simpler to block an auto-destructive program

than to titrate a neurotrophic protective signal, providing us with more promising therapeutic avenues.

# Experimental Procedures

## Fly Stocks

Flies were maintained at 25° on normal food, unless otherwise noted. The following strains were used in the study: *w*<sup>1118</sup> (wildtype), *elav*<sup>C155</sup>-GAL4 (neuron-specific; (Lin and Goodman, 1994)), *BG57*-GAL4 (muscle specific; (Budnik et al., 1996)), *hiw*<sup>ND9</sup> (Wan et al., 2000), *puc*<sup>1</sup> and *puc*<sup>A251.1F3</sup> (Martin-Blanco et al., 1998), *wnd*<sup>2</sup> and *wnd*<sup>3</sup> (Collins et al., 2006), *kay*<sup>1</sup> (Riesgo-Escovar and Hafen, 1997), *kay*<sup>2</sup> (courtesy of D. Bohmann), GAL4-responsive UAS-*Wld*<sup>8</sup> (Hoopfer et al., 2006), UAS-*gbb* (Stephan Thor; (Wharton et al., 1999)), UAS-*puc* (Martin-Blanco et al., 1998), UAS-*jun*, UAS-*fos*, UAS-*jbz* (DN-*jun*), and UAS-*fbz* (DN-*fos*) (Eresh et al., 1997), UAS-*bsk*<sup>DN</sup> (Weber et al., 2000), UAS-*α-spectrin*-dsRNA (Pielage et al., 2005), *Pbac(WH)CG32373*<sup>02001</sup> [*P(CG32373*<sup>2001</sup>) or *ank2*<sup>2001</sup>] (identified in the BDGP/Exelixis gene disruption project), and Df(3L)RM5-2 (from the Bloomington stock center, Indiana). All UAS-constructs were driven presynaptically with *elav*<sup>C155</sup>-GAL4, except for Figure 2-1D,E where UAS-constructs were simultaneously driven both presynaptically with *elav*<sup>C155</sup>-GAL4 and postsynaptically with *BG57*-GAL4.

Throughout this paper we make use of multiple genomic insertions of the UAS-*α-spectrin* RNAi transgene. To allow for construction of double mutants in different experiments, either one or two copies of the RNAi transgene were used. This results in different baseline retraction phenotypes in different experiments, with a single copy of the RNAi transgene causing a lower frequency and severity of retractions than the two copies. The milder phenotype seen with a single copy of UAS-*α-spectrin* RNAi is significantly different from wild type and is qualitatively identical to the more severe

phenotype seen with two copies of UAS-*α-spectrin* RNAi. One copy of UAS-*α-spectrin* RNAi was used in the following: Figure 2-5F, G and Figure 2-7. Two copies of UAS-*α-spectrin* RNAi were used in the following figures: Figures 2-1, 2-2, 2-3, 2-4, 2-5A,B,C,D,E, 2-8, 4-1 and Supplemental Figures 2-1, 2-2, 2-3.

### **Immunocytochemistry and imaging**

Wandering third instar larvae were dissected in HL3 saline (Stewart et al., 1994) and fixed in Bouin's fixative (Sigma) except for stainings for CSP and Synaptotagmin where larvae were fixed with 4% paraformaldehyde in PBS. Primary antibodies were applied at 4°C overnight. Primary antibodies were used at the following dilutions: anti-bruchpilot (nc82), 1:50; anti-Futsch (22C10), 1:20; anti-*α*-Spectrin (3A9), 1:20; anti-Fasciclin II, 1:10; anti-Neuroglian, 1:10; anti-Synaptotagmin, 1:25; anti-CSP, 1:25 (all provided by the Developmental Studies Hybridoma Bank, Iowa); rabbit-anti-Wallenda, 1:100 (courtesy of A. DiAntonio); anti-*β*-Galactosidase (14B7), 1:50 (Cell Signaling Technology); and rabbit polyclonal anti-Dlg, 1:10,000 (Budnik et al., 1996). Secondary Alexa Fluor antibodies (goat-anti-mouse-488, goat-anti-rabbit-555, and goat-anti-rabbit-647) were obtained from Molecular Probes and used at a 1:600 dilution. All other secondary antibodies and Cy3-conjugated HRP were obtained from Jackson Immunoresearch Laboratories or Molecular Probes and used at a 1:200 dilution. All secondary antibodies were applied for 1-2 hours at room temperature. All NMJ and axon image stacks were captured using an Axiovert 200 (Zeiss) inverted microscope with a Zeiss Plan-APOCHROMAT 100x oil-immersion lens (numerical aperture = 1.40), a

cooled CCD camera (Photometrics CoolSnapHQ) and piezo controlled z-axis positioning. All images were taken at room temperature, using Zeiss Immersol imaging oil. Hardware and software analysis was driven by Intelligent Imaging Innovations (3I) software, specifically the Slidebook imaging program. Using the Slidebook software, images were deconvolved with the nearest neighbor algorithm, and z-stacks were combined into a single projection image. Further processing of images, specifically cropping and adjustment of levels was done in Adobe Photoshop. No thresholding was incorporated into the images shown. Ventral Nerve Cord image stacks (Fig 5D) were captured using a Zeiss Axioskop 2 inverted microscope and the Zeiss LSM 510 Meta Laser Scanning System. Images were acquired with a Zeiss Plan-APOCHROMAT 40x oil-immersion lens (numerical aperture = 1.3), a CCD camera (QImaging Rolera-XR Mono Fast 1394) and piezo controlled z-axis positioning. All images were taken at room temperature, using Zeiss Immersol imaging oil. Hardware and software analysis was driven by Zeiss LSM 510 software. Using the Zeiss LSM 510 software, z-stacks were combined into a single projection image, and further processing of images, specifically cropping and adjustment of levels was done in Adobe Photoshop.

### **Image Quantification**

All retractions and bouton numbers were counted at 40x magnification, and the observer was blind to genotype. Retractions were counted on m67 of segments A2 through A6, and a retraction was defined as an area of the NMJ where clearly defined postsynaptic Dlg staining is not apposed by presynaptic nc82 staining. Bouton numbers were counted

on m4 of segment A2, using postsynaptic Dlg staining to label bouton profiles. Levels of immunoreactivity and Brp puncta density were quantified (Figures 2-1, 2-S3, and 4-1) using the masking function in Slidebook. Image stacks were taken at the same exposure from animals that were dissected and stained together. Images were deconvolved and projected into a single 3D stack before masking. No alterations were made to the images before quantification.

### **Electrophysiology**

Recordings were performed as described previously (Albin and Davis, 2004). Wandering third-instar larvae were selected after leaving the food. Larvae were recorded in HL3 saline with 0.3 mM  $\text{Ca}^{2+}$ , 10mM  $\text{Mg}^{2+}$ . Muscle recordings were achieved using sharp electrodes (12-18M $\Omega$ ) filled with 3M potassium chloride. Recordings were performed using an Axoclamp2B amplifier (Axon Instruments), Master-8 stimulator (AMPI) and digitized using Axon Instruments hardware and P-Clamp software (Axon Instruments). Electrodes were positioned using Sutter Instruments MP285 micromanipulators. The preparation was visualized using a compound, fixed stage microscope (Olympus BX50WI ) and 40x water immersion lens (0.8NA). Quantal content was calculated by dividing the average maximal EPSP amplitude by the average amplitude of the spontaneous miniature release events (mEPSP) for each recording. Multiple recordings were averaged per genotype. Measurements of maximal EPSP and input resistance were done by hand using the cursor option in Clampfit (Molecular Devices). Measurements of spontaneous miniature release events were semi-automated using MiniAnalysis software



(Synaptosoft, Decatur, GA). For each recording, 100-300 mEPSP events were averaged to determine the average mEPSP amplitude.

### **$\beta$ -Gal Activity Assay**

$\beta$ -galactosidase activity was measured using the Galacto-Light Plus System (Applied Biosystems, Foster City, CA). Samples consisted of at least three animals for each condition, and all assays were conducted in duplicate. For genetics experiments (i.e. comparisons between animals of different genotype), animals were dissected in HL3 saline with 0mM  $\text{Ca}^{2+}$ , 20mM  $\text{Mg}^{2+}$ , and then transferred to lysis buffer for homogenization immediately following dissection. For nocodazole experiments, animals were dissected in HL3 saline with 0.5mM  $\text{Ca}^{2+}$ , 10mM  $\text{Mg}^{2+}$  and then incubated for 30min, 1hr, 2 hrs, or 4hrs in identical HL3 solution with nocodazole in DMSO or DMSO only (control condition). After incubation, animals were transferred to lysis buffer for homogenization. A standard Bradford assay for protein concentration was performed on each sample, and  $\beta$ -galactosidase activity was normalized to within-sample protein concentration for each condition.

### **Western Blotting**

For genetics experiments (i.e. comparisons between animals of different genotype), animals were dissected in HL3 saline with 0mM  $\text{Ca}^{2+}$ , 20mM  $\text{Mg}^{2+}$ . The CNS was removed from each animal and homogenized in sample buffer (95% 2x Laemmli Sample Buffer with 5% 2-Mercaptoethanol). For nocodazole experiments, animals were

dissected in HL3 saline with 0.5mM Ca<sup>2+</sup>, 10mM Mg<sup>2+</sup> and then incubated for 30min or 2hrs in identical HL3 solution with nocodazole in DMSO or DMSO only (control condition). After incubation, the CNS was removed from each animal and homogenized in sample buffer. Samples consisted of at least five CNS for each condition. Samples were boiled for 15min and then run on 7.5% tris-HCl gels at 35mA. Gels were transferred to PVDF membrane for one hour at 100V, and then membranes were probed with one of two rabbit-anti-Fos antibodies (101AP from Fabgennix, Inc. or courtesy of D. Bohmann) at 1:1000. Secondary antibody (goat-anti-rabbit-HRP) was obtained from Jackson Immunoresearch and used at 1:5,000. To control for protein loading, membranes were stripped with Restore<sup>TM</sup> Western Blot Stripping Buffer (Thermo Scientific) and re-probed with mouse-anti- $\beta$ -tubulin (courtesy of U. Heberlein) at 1:1,000 or mouse-anti-actin (Sigma) at 1:10,000. Secondary antibody (goat-anti-mouse-HRP) was obtained from Jackson Immunoresearch and used at 1:10,000. All antibody incubations were done at room temperature for 1 hr in 2% milk in TBS with 0.1% Tween-20. All membranes were developed with ECL substrate (Amersham) and exposed to film. Films were quantified with ImageJ (NIH) gel analysis tool.

## **Behavior**

### *Fos suppression of motor impairment in animals lacking $\alpha$ -Spectrin*

Animals were raised as larvae at 25° and transferred to room temperature during pupation. Pupae were carefully removed from vials and transferred to empty vials containing a moist Kim Wipe. On the day of eclosure, each female adult was transferred

to new vial with food (no yeast). Flies were maintained in individual vials for the duration of behavioral testing. Testing began on the day after eclosure. Each day, flies were tested in a simplified negative geotaxis assay. Each fly was knocked to the bottom of the vial (onto the food) and the time taken to transition from the food to the wall of the vial was recorded. Any fly taking more than 60 seconds to transition from the food was given a score of 60 seconds and the trial was ended. Each fly was given three sequential trials on the given test day. Any flies that were unable to complete the task (i.e. took more than 60 seconds) on the first day of testing, were excluded from further testing.

*Expression of Fos<sup>DN</sup> induces a progressive motor impairment*

Animals were maintained at 25°C throughout larval and adult stages. On the day of eclosure, each female adult was transferred to new vial with food (no yeast). Flies were maintained in individual vials for the duration of behavioral testing. Testing began on the day after eclosure. Each day, flies were tested in a simplified negative geotaxis assay. Each fly was knocked to the bottom of the vial (onto the food) and the time taken to transition from the food to the wall of the vial was recorded. Any fly taking more than 60 seconds to transition from the food was given a score of 60 seconds and the trial was ended. Each fly was given three sequential trials on the given test day.

*Expression of Fos<sup>DN</sup> impairs adult wing posture*

Animals were maintained at 25°C throughout larval and adult stages. On the day of eclosure, individual females were transferred to a new vial with food. Animals were

imaged on a dissecting microscope at 1, 3, 6, 14, or 15 days after eclosure. In order to prevent animals from escaping, the head was chopped off immediately prior to imaging. Each animal was only imaged at one time point.

*Expression of Fos<sup>DN</sup> decreases lifespan*

Animals were maintained at room temperature throughout larval and adult stages. On the day of eclosure, male adults were separated into groups of 4-5 flies and transferred to new vial with food (no yeast). The percentage of flies alive in each group was scored each day for two weeks.

## REFERENCES

- Aberle, H., A.P. Haghghi, R.D. Fetter, B.D. McCabe, T.R. Magalhaes, and C.S. Goodman. 2002. wishful thinking encodes a BMP type II receptor that regulates synaptic growth in *Drosophila*. *Neuron*. 33:545-58.
- Agnes, F., M. Suzanne, and S. Noselli. 1999. The *Drosophila* JNK pathway controls the morphogenesis of imaginal discs during metamorphosis. *Development*. 126:5453-62.
- Albin, S.D., and G.W. Davis. 2004. Coordinating structural and functional synapse development: postsynaptic p21-activated kinase independently specifies glutamate receptor abundance and postsynaptic morphology. *J Neurosci*. 24:6871-9.
- Avery, M.A., A.E. Sheehan, K.S. Kerr, J. Wang, and M.R. Freeman. 2009. Wld S requires Nmnat1 enzymatic activity and N16-VCP interactions to suppress Wallerian degeneration. *J Cell Biol*. 184:501-13.
- Ayaz, D., M. Leyssen, M. Koch, J. Yan, M. Srahna, V. Sheeba, K.J. Fogle, T.C. Holmes, and B.A. Hassan. 2008. Axonal injury and regeneration in the adult brain of *Drosophila*. *J Neurosci*. 28:6010-21.
- Bennett, V., and J. Davis. 1983. Spectrin and ankyrin in brain. *Cell Motil*. 3:623-33.
- Bennett, V., and D.M. Gilligan. 1993. The spectrin-based membrane skeleton and micron-scale organization of the plasma membrane. *Annu Rev Cell Biol*. 9:27-66.
- Bennett, V., and J. Healy. 2008. Organizing the fluid membrane bilayer: diseases linked to spectrin and ankyrin. *Trends Mol Med*. 14:28-36.
- Bennett, V., and S. Lambert. 1991. The spectrin skeleton: from red cells to brain. *J Clin Invest*. 87:1483-9.
- Bommel, H., G. Xie, W. Rossoll, S. Wiese, S. Jablonka, T. Boehm, and M. Sendtner. 2002. Missense mutation in the tubulin-specific chaperone E (Tbce) gene in the mouse mutant progressive motor neuronopathy, a model of human motoneuron disease. *J Cell Biol*. 159:563-9.
- Bowman, A.B., A. Kamal, B.W. Ritchings, A.V. Philp, M. McGrail, J.G. Gindhart, and L.S. Goldstein. 2000. Kinesin-dependent axonal transport is mediated by the sunday driver (SYD) protein. *Cell*. 103:583-94.
- Budnik, V., Y.H. Koh, B. Guan, B. Hartmann, C. Hough, D. Woods, and M. Gorczyca. 1996. Regulation of synapse structure and function by the *Drosophila* tumor suppressor gene *dlg*. *Neuron*. 17:627-40.
- Byrd, D.T., M. Kawasaki, M. Walcoff, N. Hisamoto, K. Matsumoto, and Y. Jin. 2001. UNC-16, a JNK-signaling scaffold protein, regulates vesicle transport in *C. elegans*. *Neuron*. 32:787-800.
- Cho, S., E.M. Park, Y. Kim, N. Liu, J. Gal, B.T. Volpe, and T.H. Joh. 2001. Early c-Fos induction after cerebral ischemia: a possible neuroprotective role. *J Cereb Blood Flow Metab*. 21:550-6.

- Ciapponi, L., D.B. Jackson, M. Mlodzik, and D. Bohmann. 2001. Drosophila Fos mediates ERK and JNK signals via distinct phosphorylation sites. *Genes Dev.* 15:1540-53.
- Collins, C.A., Y.P. Wairkar, S.L. Johnson, and A. DiAntonio. 2006. Highwire restrains synaptic growth by attenuating a MAP kinase signal. *Neuron.* 51:57-69.
- Conforti, L., A. Wilbrey, G. Morreale, L. Janeckova, B. Beirowski, R. Adalbert, F. Mazzola, M. Di Stefano, R. Hartley, E. Babetto, T. Smith, J. Gilley, R.A. Billington, A.A. Genazzani, R.R. Ribchester, G. Magni, and M. Coleman. 2009. Wld S protein requires Nmnat activity and a short N-terminal sequence to protect axons in mice. *J Cell Biol.* 184:491-500.
- DiAntonio, A., A.P. Haghghi, S.L. Portman, J.D. Lee, A.M. Amaranto, and C.S. Goodman. 2001. Ubiquitination-dependent mechanisms regulate synaptic growth and function. *Nature.* 412:449-52.
- Dobens, L.L., E. Martin-Blanco, A. Martinez-Arias, F.C. Kafatos, and L.A. Raftery. 2001. Drosophila puckered regulates Fos/Jun levels during follicle cell morphogenesis. *Development.* 128:1845-56.
- Dragunow, M., E. Beilharz, E. Sirimanne, P. Lawlor, C. Williams, R. Bravo, and P. Gluckman. 1994. Immediate-early gene protein expression in neurons undergoing delayed death, but not necrosis, following hypoxic-ischaemic injury to the young rat brain. *Brain Res Mol Brain Res.* 25:19-33.
- Eaton, B.A., and G.W. Davis. 2005. LIM Kinase1 controls synaptic stability downstream of the type II BMP receptor. *Neuron.* 47:695-708.
- Eaton, B.A., R.D. Fetter, and G.W. Davis. 2002. Dynactin is necessary for synapse stabilization. *Neuron.* 34:729-41.
- Eresh, S., J. Riese, D.B. Jackson, D. Bohmann, and M. Bienz. 1997. A CREB-binding site as a target for decapentaplegic signalling during Drosophila endoderm induction. *Embo J.* 16:2014-22.
- Fernandez, M., S. Pirondi, T. Antonelli, L. Ferraro, L. Giardino, and L. Calza. 2005. Role of c-Fos protein on glutamate toxicity in primary neural hippocampal cells. *J Neurosci Res.* 82:115-25.
- Ferri, A., J.R. Sanes, M.P. Coleman, J.M. Cunningham, and A.C. Kato. 2003. Inhibiting axon degeneration and synapse loss attenuates apoptosis and disease progression in a mouse model of motoneuron disease. *Curr Biol.* 13:669-73.
- Fischer, L.R., D.G. Culver, A.A. Davis, P. Tennant, M. Wang, M. Coleman, S. Asress, R. Adalbert, G.M. Alexander, and J.D. Glass. 2005. The WldS gene modestly prolongs survival in the SOD1G93A fALS mouse. *Neurobiol Dis.* 19:293-300.
- Frey, D., C. Schneider, L. Xu, J. Borg, W. Spooren, and P. Caroni. 2000. Early and selective loss of neuromuscular synapse subtypes with low sprouting competence in motoneuron diseases. *J Neurosci.* 20:2534-42.
- Guan, B., B. Hartmann, Y.H. Kho, M. Gorczyca, and V. Budnik. 1996. The Drosophila tumor suppressor gene, dlg, is involved in structural plasticity at a glutamatergic synapse. *Curr Biol.* 6:695-706.

- Hafezi, F., J.P. Steinbach, A. Marti, K. Munz, Z.Q. Wang, E.F. Wagner, A. Aguzzi, and C.E. Reme. 1997. The absence of c-fos prevents light-induced apoptotic cell death of photoreceptors in retinal degeneration in vivo. *Nat Med.* 3:346-9.
- Hafezparast, M., R. Klocke, C. Ruhrberg, A. Marquardt, A. Ahmad-Annuar, S. Bowen, G. Lalli, A.S. Witherden, H. Hummerich, S. Nicholson, P.J. Morgan, R. Oozageer, J.V. Priestley, S. Averill, V.R. King, S. Ball, J. Peters, T. Toda, A. Yamamoto, Y. Hiraoka, M. Augustin, D. Korthaus, S. Wattler, P. Wabnitz, C. Dickneite, S. Lampel, F. Boehme, G. Peraus, A. Popp, M. Rudelius, J. Schlegel, H. Fuchs, M. Hrabe de Angelis, G. Schiavo, D.T. Shima, A.P. Russ, G. Stumm, J.E. Martin, and E.M. Fisher. 2003. Mutations in dynein link motor neuron degeneration to defects in retrograde transport. *Science.* 300:808-12.
- Hammarlund, M., E.M. Jorgensen, and M.J. Bastiani. 2007. Axons break in animals lacking beta-spectrin. *J Cell Biol.* 176:269-75.
- Hammarlund, M., P. Nix, L. Hauth, E.M. Jorgensen, and M. Bastiani. 2009. Axon regeneration requires a conserved MAP Kinase pathway. *Science.* 323:802-806.
- Herdegen, T., and V. Waetzig. 2001. AP-1 proteins in the adult brain: facts and fiction about effectors of neuroprotection and neurodegeneration. *Oncogene.* 20:2424-37.
- Hoopfer, E.D., T. McLaughlin, R.J. Watts, O. Schuldiner, D.D. O'Leary, and L. Luo. 2006. Wlds protection distinguishes axon degeneration following injury from naturally occurring developmental pruning. *Neuron.* 50:883-95.
- Horiuchi, D., R.V. Barkus, A.D. Pilling, A. Gassman, and W.M. Saxton. 2005. APLIP1, a kinesin binding JIP-1/JNK scaffold protein, influences the axonal transport of both vesicles and mitochondria in Drosophila. *Curr Biol.* 15:2137-41.
- Horiuchi, D., C.A. Collins, P. Bhat, R.V. Barkus, A. Diantonio, and W.M. Saxton. 2007. Control of a kinesin-cargo linkage mechanism by JNK pathway kinases. *Curr Biol.* 17:1313-7.
- Ikeda, Y., K.A. Dick, M.R. Weatherspoon, D. Gincel, K.R. Armbrust, J.C. Dalton, G. Stevanin, A. Durr, C. Zuhlke, K. Burk, H.B. Clark, A. Brice, J.D. Rothstein, L.J. Schut, J.W. Day, and L.P. Ranum. 2006. Spectrin mutations cause spinocerebellar ataxia type 5. *Nat Genet.* 38:184-90.
- Keshishian, H., K. Broadie, A. Chiba, and M. Bate. 1996. The drosophila neuromuscular junction: a model system for studying synaptic development and function. *Annu Rev Neurosci.* 19:545-75.
- Koch, I., H. Schwarz, D. Beuchle, B. Goellner, M. Langegger, and H. Aberle. 2008. Drosophila ankyrin 2 is required for synaptic stability. *Neuron.* 58:210-22.
- Lacas-Gervais, S., J. Guo, N. Strenzke, E. Scarfone, M. Kolpe, M. Jahkel, P. De Camilli, T. Moser, M.N. Rasband, and M. Solimena. 2004. BetaIVSigma1 spectrin stabilizes the nodes of Ranvier and axon initial segments. *J Cell Biol.* 166:983-90.
- LaMonte, B.H., K.E. Wallace, B.A. Holloway, S.S. Shelly, J. Ascano, M. Tokito, T. Van Winkle, D.S. Howland, and E.L. Holzbaur. 2002. Disruption of dynein/dynactin inhibits axonal transport in motor neurons causing late-onset progressive degeneration. *Neuron.* 34:715-27.

- Lau, L.F., and D. Nathans. 1987. Expression of a set of growth-related immediate early genes in BALB/c 3T3 cells: coordinate regulation with c-fos or c-myc. *Proc Natl Acad Sci U S A.* 84:1182-6.
- Levy, J.R., C.J. Sumner, J.P. Caviston, M.K. Tokito, S. Ranganathan, L.A. Ligon, K.E. Wallace, B.H. LaMonte, G.G. Harmison, I. Puls, K.H. Fischbeck, and E.L. Holzbaur. 2006. A motor neuron disease-associated mutation in p150Glued perturbs dynactin function and induces protein aggregation. *J Cell Biol.* 172:733-45.
- Ligon, L.A., B.H. LaMonte, K.E. Wallace, N. Weber, R.G. Kalb, and E.L. Holzbaur. 2005. Mutant superoxide dismutase disrupts cytoplasmic dynein in motor neurons. *Neuroreport.* 16:533-6.
- Lin, D.M., and C.S. Goodman. 1994. Ectopic and increased expression of Fasciclin II alters motoneuron growth cone guidance. *Neuron.* 13:507-23.
- Lin, J.H., H. Li, D. Yasumura, H.R. Cohen, C. Zhang, B. Panning, K.M. Shokat, M.M. Lavail, and P. Walter. 2007. IRE1 signaling affects cell fate during the unfolded protein response. *Science.* 318:944-9.
- Lonze, B.E., A. Riccio, S. Cohen, and D.D. Ginty. 2002. Apoptosis, axonal growth defects, and degeneration of peripheral neurons in mice lacking CREB. *Neuron.* 34:371-85.
- Lu, X.C., F.C. Tortella, H.S. Ved, G.E. Garcia, and J.R. Dave. 1997. Neuroprotective role of c-fos antisense oligonucleotide: in vitro and in vivo studies. *Neuroreport.* 8:2925-9.
- Ludwin, S.K., and M.A. Bisby. 1992. Delayed wallerian degeneration in the central nervous system of Ola mice: an ultrastructural study. *J Neurol Sci.* 109:140-7.
- Lunn, E.R., V.H. Perry, M.C. Brown, H. Rosen, and S. Gordon. 1989. Absence of Wallerian Degeneration does not Hinder Regeneration in Peripheral Nerve. *Eur J Neurosci.* 1:27-33.
- Luo, L., and D.D. O'Leary. 2005. Axon retraction and degeneration in development and disease. *Annu Rev Neurosci.* 28:127-56.
- Lyon, M.F., B.W. Ogunkolade, M.C. Brown, D.J. Atherton, and V.H. Perry. 1993. A gene affecting Wallerian nerve degeneration maps distally on mouse chromosome 4. *Proc Natl Acad Sci U S A.* 90:9717-20.
- Mabuchi, T., K. Kitagawa, K. Kuwabara, K. Takasawa, T. Ohtsuki, Z. Xia, D. Storm, T. Yanagihara, M. Hori, and M. Matsumoto. 2001. Phosphorylation of cAMP response element-binding protein in hippocampal neurons as a protective response after exposure to glutamate in vitro and ischemia in vivo. *J Neurosci.* 21:9204-13.
- Mack, T.G., M. Reiner, B. Beirowski, W. Mi, M. Emanuelli, D. Wagner, D. Thomson, T. Gillingwater, F. Court, L. Conforti, F.S. Fernando, A. Tarlton, C. Andressen, K. Addicks, G. Magni, R.R. Ribchester, V.H. Perry, and M.P. Coleman. 2001. Wallerian degeneration of injured axons and synapses is delayed by a Ube4b/Nmnat chimeric gene. *Nat Neurosci.* 4:1199-206.
- Mantamadiotis, T., T. Lemberger, S.C. Bleckmann, H. Kern, O. Kretz, A. Martin Villalba, F. Tronche, C. Kellendonk, D. Gau, J. Kapfhammer, C. Otto, W.



- Schmid, and G. Schutz. 2002. Disruption of CREB function in brain leads to neurodegeneration. *Nat Genet.* 31:47-54.
- Martin-Blanco, E., A. Gampel, J. Ring, K. Virdee, N. Kirov, A.M. Tolkovsky, and A. Martinez-Arias. 1998. puckered encodes a phosphatase that mediates a feedback loop regulating JNK activity during dorsal closure in *Drosophila*. *Genes Dev.* 12:557-70.
- Martin, M., S.J. Iyadurai, A. Gassman, J.G. Gindhart, Jr., T.S. Hays, and W.M. Saxton. 1999. Cytoplasmic dynein, the dynactin complex, and kinesin are interdependent and essential for fast axonal transport. *Mol Biol Cell.* 10:3717-28.
- Martin, N., J. Jaubert, P. Gounon, E. Salido, G. Haase, M. Szatanik, and J.L. Guenet. 2002. A missense mutation in *Tbce* causes progressive motor neuronopathy in mice. *Nat Genet.* 32:443-7.
- Massaro, C.M., J. Pielage, and G.W. Davis. 2009. Molecular mechanisms that enhance synapse stability despite persistent disruption of the spectrin/ankyrin/microtubule cytoskeleton. *J Cell Biol.* 187:101-17.
- McCabe, B.D., S. Hom, H. Aberle, R.D. Fetter, G. Marques, T.E. Haerry, H. Wan, M.B. O'Connor, C.S. Goodman, and A.P. Haghghi. 2004. Highwire regulates presynaptic BMP signaling essential for synaptic growth. *Neuron.* 41:891-905.
- Miller, B.R., C. Press, R.W. Daniels, Y. Sasaki, J. Milbrandt, and A. DiAntonio. 2009. A dual leucine kinase-dependent axon self-destruction program promotes Wallerian degeneration. *Nat Neurosci.* 12:387-9.
- Morgan, J.I., D.R. Cohen, J.L. Hempstead, and T. Curran. 1987. Mapping patterns of *c-fos* expression in the central nervous system after seizure. *Science.* 237:192-7.
- Nakata, K., B. Abrams, B. Grill, A. Goncharov, X. Huang, A.D. Chisholm, and Y. Jin. 2005. Regulation of a DLK-1 and p38 MAP kinase pathway by the ubiquitin ligase RPM-1 is required for presynaptic development. *Cell.* 120:407-20.
- Palop, J.J., B. Jones, L. Kekonius, J. Chin, G.Q. Yu, J. Raber, E. Masliah, and L. Mucke. 2003. Neuronal depletion of calcium-dependent proteins in the dentate gyrus is tightly linked to Alzheimer's disease-related cognitive deficits. *Proc Natl Acad Sci U S A.* 100:9572-7.
- Parkinson, N.J., C.L. Olsson, J.L. Hallows, J. McKee-Johnson, B.P. Keogh, K. Noben-Trauth, S.G. Kujawa, and B.L. Tempel. 2001. Mutant beta-spectrin 4 causes auditory and motor neuropathies in quivering mice. *Nat Genet.* 29:61-5.
- Parson, S.H., C.L. Mackintosh, and R.R. Ribchester. 1997. Elimination of motor nerve terminals in neonatal mice expressing a gene for slow wallerian degeneration (C57Bl/Wlds). *Eur J Neurosci.* 9:1586-92.
- Perkins, K.K., A. Admon, N. Patel, and R. Tjian. 1990. The *Drosophila* Fos-related AP-1 protein is a developmentally regulated transcription factor. *Genes Dev.* 4:822-34.
- Perry, V.H., M.C. Brown, and E.R. Lunn. 1991. Very Slow Retrograde and Wallerian Degeneration in the CNS of C57BL/Ola Mice. *Eur J Neurosci.* 3:102-105.
- Perry, V.H., E.R. Lunn, M.C. Brown, S. Cahusac, and S. Gordon. 1990. Evidence that the Rate of Wallerian Degeneration is Controlled by a Single Autosomal Dominant Gene. *Eur J Neurosci.* 2:408-413.

- Pielage, J., L. Cheng, R.D. Fetter, P.M. Carlton, J.W. Sedat, and G.W. Davis. 2008. A presynaptic giant ankyrin stabilizes the NMJ through regulation of presynaptic microtubules and transsynaptic cell adhesion. *Neuron*. 58:195-209.
- Pielage, J., R.D. Fetter, and G.W. Davis. 2005. Presynaptic spectrin is essential for synapse stabilization. *Curr Biol*. 15:918-28.
- Puls, I., C. Jonnakuty, B.H. LaMonte, E.L. Holzbaur, M. Tokito, E. Mann, M.K. Floeter, K. Bidus, D. Drayna, S.J. Oh, R.H. Brown, Jr., C.L. Ludlow, and K.H. Fischbeck. 2003. Mutant dynactin in motor neuron disease. *Nat Genet*. 33:455-6.
- Pun, S., A.F. Santos, S. Saxena, L. Xu, and P. Caroni. 2006. Selective vulnerability and pruning of phasic motoneuron axons in motoneuron disease alleviated by CNTF. *Nat Neurosci*. 9:408-19.
- Riese, J., G. Tremml, and M. Bienz. 1997. D-Fos, a target gene of Decapentaplegic signalling with a critical role during Drosophila endoderm induction. *Development*. 124:3353-61.
- Riesgo-Escovar, J.R., and E. Hafen. 1997. Common and distinct roles of DFos and DJun during Drosophila development. *Science*. 278:669-72.
- Ring, J.M., and A. Martinez Arias. 1993. puckered, a gene involved in position-specific cell differentiation in the dorsal epidermis of the Drosophila larva. *Dev Suppl*:251-9.
- Saitoe, M., T.L. Schwarz, J.A. Umbach, C.B. Gundersen, and Y. Kidokoro. 2001. Absence of junctional glutamate receptor clusters in Drosophila mutants lacking spontaneous transmitter release. *Science*. 293:514-7.
- Sajadi, A., B.L. Schneider, and P. Aebischer. 2004. Wlds-mediated protection of dopaminergic fibers in an animal model of Parkinson disease. *Curr Biol*. 14:326-30.
- Sanyal, S., D.J. Sandstrom, C.A. Hoeffler, and M. Ramaswami. 2002. AP-1 functions upstream of CREB to control synaptic plasticity in Drosophila. *Nature*. 416:870-4.
- Saura, C.A., S.Y. Choi, V. Beglopoulos, S. Malkani, D. Zhang, B.S. Shankaranarayana Rao, S. Chattarji, R.J. Kelleher, 3rd, E.R. Kandel, K. Duff, A. Kirkwood, and J. Shen. 2004. Loss of presenilin function causes impairments of memory and synaptic plasticity followed by age-dependent neurodegeneration. *Neuron*. 42:23-36.
- Scheff, S.W., D.A. Price, F.A. Schmitt, and E.J. Mufson. 2006. Hippocampal synaptic loss in early Alzheimer's disease and mild cognitive impairment. *Neurobiol Aging*. 27:1372-84.
- Schuster, C.M., G.W. Davis, R.D. Fetter, and C.S. Goodman. 1996. Genetic dissection of structural and functional components of synaptic plasticity. II. Fasciclin II controls presynaptic structural plasticity. *Neuron*. 17:655-67.
- Selkoe, D.J. 2002. Alzheimer's disease is a synaptic failure. *Science*. 298:789-91.
- Sheng, M., G. McFadden, and M.E. Greenberg. 1990. Membrane depolarization and calcium induce c-fos transcription via phosphorylation of transcription factor CREB. *Neuron*. 4:571-82.

- Stewart, B.A., H.L. Atwood, J.J. Renger, J. Wang, and C.F. Wu. 1994. Improved stability of *Drosophila* larval neuromuscular preparations in haemolymph-like physiological solutions. *J Comp Physiol [A]*. 175:179-91.
- Szuts, D., and M. Bienz. 2000. An autoregulatory function of Dfos during *Drosophila* endoderm induction. *Mech Dev*. 98:71-6.
- Tanzi, R.E. 2005. The synaptic Abeta hypothesis of Alzheimer disease. *Nat Neurosci*. 8:977-9.
- Thomas, U., S. Ebitsch, M. Gorczyca, Y.H. Koh, C.D. Hough, D. Woods, E.D. Gundelfinger, and V. Budnik. 2000. Synaptic targeting and localization of disc-large is a stepwise process controlled by different domains of the protein. *Curr Biol*. 10:1108-17.
- Walton, M., B. Connor, P. Lawlor, D. Young, E. Sirimanne, P. Gluckman, G. Cole, and M. Dragunow. 1999a. Neuronal death and survival in two models of hypoxic-ischemic brain damage. *Brain Res Brain Res Rev*. 29:137-68.
- Walton, M., G. MacGibbon, D. Young, E. Sirimanne, C. Williams, P. Gluckman, and M. Dragunow. 1998. Do c-Jun, c-Fos, and amyloid precursor protein play a role in neuronal death or survival? *J Neurosci Res*. 53:330-42.
- Walton, M., A.M. Woodgate, A. Muravlev, R. Xu, M.J. During, and M. Dragunow. 1999b. CREB phosphorylation promotes nerve cell survival. *J Neurochem*. 73:1836-42.
- Wan, H.I., A. DiAntonio, R.D. Fetter, K. Bergstrom, R. Strauss, and C.S. Goodman. 2000. Highwire regulates synaptic growth in *Drosophila*. *Neuron*. 26:313-29.
- Wang, M., Y. Wu, D.G. Culver, and J.D. Glass. 2001. The gene for slow Wallerian degeneration (Wld(s)) is also protective against vincristine neuropathy. *Neurobiol Dis*. 8:155-61.
- Wang, M.S., A.A. Davis, D.G. Culver, and J.D. Glass. 2002. WldS mice are resistant to paclitaxel (taxol) neuropathy. *Ann Neurol*. 52:442-7.
- Watts, R.J., E.D. Hoopfer, and L. Luo. 2003. Axon pruning during *Drosophila* metamorphosis: evidence for local degeneration and requirement of the ubiquitin-proteasome system. *Neuron*. 38:871-85.
- Weber, U., N. Paricio, and M. Mlodzik. 2000. Jun mediates Frizzled-induced R3/R4 cell fate distinction and planar polarity determination in the *Drosophila* eye. *Development*. 127:3619-29.
- Wharton, K.A., J.M. Cook, S. Torres-Schumann, K. de Castro, E. Borod, and D.A. Phillips. 1999. Genetic analysis of the bone morphogenetic protein-related gene, *gbb*, identifies multiple requirements during *Drosophila* development. *Genetics*. 152:629-40.
- Wu, C., Y.P. Wairkar, C.A. Collins, and A. DiAntonio. 2005. Highwire function at the *Drosophila* neuromuscular junction: spatial, structural, and temporal requirements. *J Neurosci*. 25:9557-66.
- Zeitlinger, J., L. Kockel, F.A. Peverali, D.B. Jackson, M. Mlodzik, and D. Bohmann. 1997. Defective dorsal closure and loss of epidermal decapentaplegic expression in *Drosophila* fos mutants. *Embo J*. 16:7393-401.

Zhai, Q., J. Wang, A. Kim, Q. Liu, R. Watts, E. Hoopfer, T. Mitchison, L. Luo, and Z. He. 2003. Involvement of the ubiquitin-proteasome system in the early stages of wallerian degeneration. *Neuron*. 39:217-25.

Zhai, R.G., F. Zhang, P.R. Hiesinger, Y. Cao, C.M. Haueter, and H.J. Bellen. 2008. NAD synthase NMNAT acts as a chaperone to protect against neurodegeneration. *Nature*. 452:887-91.

**Publishing Agreement**

*It is the policy of the University to encourage the distribution of all theses, dissertations, and manuscripts. Copies of all UCSF theses, dissertations, and manuscripts will be routed to the library via the Graduate Division. The library will make all theses, dissertations, and manuscripts accessible to the public and will preserve these to the best of their abilities, in perpetuity.*

***Please sign the following statement:***

*I hereby grant permission to the Graduate Division of the University of California, San Francisco to release copies of my thesis, dissertation, or manuscript to the Campus Library to provide access and preservation, in whole or in part, in perpetuity.*

*Cathy Massaro*  
\_\_\_\_\_  
Author Signature

*12/16/09*  
\_\_\_\_\_  
Date